

ASSESSMENT OF LANDSLIDE SUSCEPTIBILITY AT  
CANADA HILL IN MIRI, SARAWAK

MARELYN TELUN DANIEL

FACULTY OF SCIENCE  
UNIVERSITI MALAYA  
KUALA LUMPUR

2020

**ASSESSMENT OF LANDSLIDE  
SUSCEPTIBILITY AT CANADA HILL IN MIRI,  
SARAWAK**

**MARELYN TELUN DANIEL**

**DISSERTATION SUBMITTED IN FULFILMENT  
OF THE REQUIREMENTS FOR THE DEGREE  
OF MASTER OF SCIENCE**

**DEPARTMENT OF GEOLOGY  
FACULTY OF SCIENCE  
UNIVERSITI MALAYA  
KUALA LUMPUR**

**2020**

**UNIVERSITI MALAYA**

**ORIGINAL LITERARY WORK DECLARATION**

Name of Candidate: **MARELYN TELUN DANIEL**

Matric No: **SGR150074**

Name of Degree: **MASTER OF SCIENCE**

Title of Project Paper/Research Report/Dissertation/Thesis ("this Work"): **ASSESSMENT OF LANDSLIDE SUSCEPTIBILITY AT CANADA HILL IN MIRI, SARAWAK**

Field of Study: **APPLIED GEOLOGY**

I do solemnly and sincerely declare that:

- (1) I am the sole author/writer of this Work;
- (2) This Work is original;
- (3) Any use of any work in which copyright exists was done by way of fair dealing and for permitted purposes and any excerpt or extract from, or reference to or reproduction of any copyright work has been disclosed expressly and sufficiently and the title of the Work and its authorship have been acknowledged in this Work;
- (4) I do not have any actual knowledge nor do I ought reasonably to know that the making of this work constitutes an infringement of any copyright work;
- (5) I hereby assign all and every rights in the copyright to this Work to the University of Malaya ("UM"), who henceforth shall be owner of the copyright in this Work and that any reproduction or use in any form or by any means whatsoever is prohibited without the written consent of UM having been first had and obtained;
- (6) I am fully aware that if in the course of making this Work I have infringed any copyright whether intentionally or otherwise, I may be subject to legal action or any other action as may be determined by UM.

Candidate's Signature

Date:

Subscribed and solemnly declared before,

Witness's Signature

Date:

Name:

Designation:

# ASSESSMENT OF LANDSLIDE SUSCEPTIBILITY AT CANADA HILL IN MIRI, SARAWAK

## ABSTRACT

Landslide occurrences have become a common sight in Miri, Sarawak due to the combination of unfavourable geological conditions, abundant rainfall and anthropogenic factors which leads to infrastructural damages following prolonged rainfall. Two of the major landslide events caused the demise of two lives and several damaged houses at *Kampung Lereng Bukit*. Events like this may recur if the landslide hazards are not effectively managed. Numerous studies on landslide susceptibility have been performed by researchers using different approaches. This study aims to evaluate the landslide susceptibility of Canada Hill area in Miri using a heuristic approach and bivariate statistical approach which could be helpful in future planning works. Nine landslide-controlling parameters consisting of planar failure susceptibility, slope gradient, geology, elevation, distance to lineament, slope curvature, normalized difference vegetation index (NDVI), slope aspect and cut and fill were analysed in this study, with the means of Geographic Information Systems (GIS). The susceptibility maps produced from the two methods were classified into five zones of susceptibility; very low, low, moderate, high and very high. The results of the susceptibility map produced using the heuristic approach showed a 74% success rate while this is 80.8% in the case of the bivariate statistical approach. The comparison of the two susceptibility while highlighting the major planar failures showed that the landslide susceptibility map produced by the heuristic approach showed a better agreement for all the types of failure occurrences, including the major planar failures while the landslide susceptibility map produced using the bivariate statistical approach showed a better agreement for the translational and shallow rotational failures.

**Keywords:** Landslide susceptibility, Miri, heuristic, bivariate statistics, planar failure.

# **PENILAIAN KERENTANAN TANAH RUNTUH DI BUKIT KANADA, MIRI, SARAWAK**

## **ABSTRAK**

Kekerapan kejadian tanah runtuh di Miri, Sarawak adalah disebabkan oleh gabungan keadaan geologi yang tidak bersesuaian, jumlah hujan yang tinggi dan faktor antropogenik. Ini mengakibatkan kerosakan infrastruktur terutamanya selepas hujan yang berpanjangan. Dua kejadian utama tanah runtuh telah mengorbankan dua nyawa serta kerosakan bangunan di Kampung Lereng Bukit. Pelbagai kajian kerentanan tanah runtuh menggunakan pendekatan yang berbeza telah dibuat oleh penyelidik-penyelidik lain. Kajian ini bertujuan untuk menilai kerentanan tanah runtuh di kawasan Bukit Kanada menggunakan pendekatan heuristik dan pendekatan statistik bivariat. Hasil kajian ini mampu membantu perancangan yang lebih teratur di masa hadapan. Sembilan faktor kecenderungan tanah runtuh telah dianalisa dalam Sistem Maklumat Geografi (GIS) iaitu kerentanan gelinciran planar, kecerunan, geologi, ketinggian, jarak ke lineamen, kelengkungan cerun, indeks vegetasi perbezaan normal (NDVI), aspek cerun serta potongan dan tambakan. Peta-peta kerentanan tanah runtuh yang dihasilkan telah diklasifikasikan kepada lima zon kerentanan; sangat rendah, rendah, sederhana, tinggi dan sangat tinggi. Peta kerentanan yang terhasil daripada pendekatan heuristik menunjukkan 74% kadar kejayaan manakala pendekatan bivariat statistik menunjukkan kadar kejayaan sebanyak 80.8%. Peta-peta kerentanan ini dibandingkan sambil memberi penekanan kepada kejadian gelinciran planar di Bukit Kanada. Peta kerentanan menggunakan pendekatan heuristik menunjukkan keselarasan yang lebih baik untuk semua jenis kejadian tanah runtuh, termasuk kegagalan planar manakala pendekatan bivariat statistik adalah lebih baik untuk gelinciran translasi dan gelinciran tanah yang kecil sahaja.

**Kata kunci:** Kerentanan tanah runtuh, Miri, heuristik, bivariat statistik, gelinciran planar.

## ACKNOWLEDGEMENTS

I would like to thank first and foremost, the Newton-Ungku Omar Fund for funding this project aside from providing workshops and conferences which gave various inputs that could be applied in this study. I am also grateful and would like to thank the Disaster Resilient Cities (DRR) project members that have been supportive in giving inputs for the betterment of this thesis.

My deepest gratitude goes to my supervisor, Associate Professor Dr. Ng Tham Fatt who have been a fully supportive, encouraging and patient mentor throughout the completion of this thesis.

I also owe my thanks to my co-supervisor, the late Dr. Mohamad Tarmizi Mohamad Zulkifley who gave thorough guidance within the short period of the time during the initial parts of this study.

I would also like to express my sincere gratitude to Mr. Roslan, Mr. Farid and Mr. Mizi from the Department of Mineral and Geoscience, Kuching for the assistance in the field and allowing access to the acquired LiDAR digital data. Sincere thanks are also due to the Malaysian Meteorological Department and Department of Irrigation and Drainage Malaysia for the provided data and the staffs of Department of Geology, UM for the access to physical maps, previous literatures and facilities.

I am also indebted to the guidance and encouragement given by my fellow friends. Special thanks to Elanni, Azlan, Aya and Galih for the joy we had working together.

Last but not least, my biggest thanks go to God and to my family, for being my rock until the end of this research.

## TABLE OF CONTENTS

<b>ABSTRACT .....</b>	<b>iii</b>
<b>ABSTRAK .....</b>	<b>iv</b>
<b>ACKNOWLEDGEMENTS.....</b>	<b>v</b>
<b>TABLE OF CONTENTS.....</b>	<b>vi</b>
<b>LIST OF FIGURES .....</b>	<b>xi</b>
<b>LIST OF TABLES .....</b>	<b>xvii</b>
<b>LIST OF SYMBOLS AND ABBREVIATIONS .....</b>	<b>xix</b>
<b>LIST OF APPENDICES .....</b>	<b>xx</b>
<b>CHAPTER 1 : INTRODUCTION .....</b>	<b>1</b>
1.1 Introduction .....	1
1.2 Problem Statement .....	2
1.3 Research Questions .....	4
1.4 Objective .....	4
1.5 Study Area.....	5
1.5.1 General Geology.....	6
1.5.2 Basis of Selection .....	8
1.5.3 Accessibility .....	9
1.5.4 Topography and Drainage .....	9
1.5.5 Climate .....	11
1.6 Research Significance .....	11
1.7 Organization of the Thesis .....	12

<b>CHAPTER 2 : LITERATURE REVIEW .....</b>	<b>15</b>
2.1 Introduction .....	15
2.2 Geology of Miri, Sarawak.....	15
2.2.1 Regional Geology.....	15
2.2.2 Geological Setting .....	17
2.3 Landslide .....	19
2.3.1 Definition and Concept.....	20
2.3.2 Causal Factors of Landslide .....	21
2.3.3 Failures in Rock Slope.....	21
2.3.4 Landslide Occurrences in Miri, Sarawak .....	22
2.4 Geographic Information System (GIS) .....	23
2.5 Landslide Susceptibility Assessment .....	24
2.5.1 Qualitative Approach.....	27
2.5.2 Quantitative Approach.....	28
 <b>CHAPTER 3 : METHODOLOGY .....</b>	 <b>32</b>
3.1 Introduction .....	32
3.2 Base Map and Landslide Inventory .....	32
3.3 Field Verification .....	33
3.3.1 Avenza Maps .....	34
3.3.2 Field Verification and Sampling .....	35
3.4 Preparation of Data.....	35
3.5 Landslide Susceptibility Assessment .....	36
3.5.1 Heuristic Approach.....	37



3.5.2	Bivariate Statistical Approach.....	40
3.5.3	Classification of the Landslide Susceptibility Classes .....	43
3.5.4	Success Rate Calculation of the Landslide Susceptibility Map .....	43
3.6	Limitation .....	44
<b>CHAPTER 4 : ENGINEERING GEOLOGY.....</b>		<b>46</b>
4.1	Introduction .....	46
4.2	Miri Formation and Seria Formation .....	46
4.2.1	Bedrock Characteristics.....	49
4.2.2	Weathering .....	52
4.3	Quaternary Deposits .....	55
4.4	Terrace Deposits (Miri Soil Series).....	56
4.5	Holocene Deposits.....	58
4.5.1	Peat (Anderson Soil Series).....	59
4.5.2	Beach Sand (Tatau Soil Series) .....	60
4.5.3	Sulfidic Marine Clay (Rajang Soil Series) .....	60
4.5.4	Organic Soil (Igan Soil Series).....	61
4.5.5	Artificial Deposits .....	61
4.6	Summary .....	62
<b>CHAPTER 5 : LANDSLIDE PARAMETERS .....</b>		<b>64</b>
5.1	Introduction .....	64
5.2	Landslide Occurrences .....	64
5.2.1	Landslide 1 (LS1).....	66
5.2.2	Landslide 2 (LS2).....	70

5.2.3	Landslide 3 (LS3) .....	74
5.2.4	Minor Landslide Occurrences .....	77
5.3	Planar Failure Susceptibility Assessment .....	79
5.3.1	Workflow of Planar Failure Susceptibility Assessment.....	80
5.3.2	Relationship Between Direction of Slope Face and Dip Direction of Bedding Plane .....	86
5.3.3	Relationship Between Slope Gradient and Dip Angle of Bedding Plane.....	92
5.3.4	Result.....	95
5.4	Slope Gradient.....	97
5.5	Geology .....	98
5.6	Distance to Lineament.....	101
5.7	Normalized Difference Vegetation Index .....	101
5.8	Elevation.....	104
5.9	Slope Curvature.....	104
5.10	Slope Aspect.....	107
5.11	Cut and Fill.....	107
5.12	Summary .....	107
<b>CHAPTER 6 : LANDSLIDE SUSCEPTIBILITY ASSESSMENT .....</b>		<b>112</b>
6.1	Introduction .....	112
6.2	Landslide Susceptibility Assessment Using the Heuristic Approach .....	112
6.3	Landslide Susceptibility Assessment Using the Bivariate Statistical Approach .....	116

6.4	Discussion .....	120
<b>CHAPTER 7 : CONCLUSION .....</b>		<b>124</b>
<b>REFERENCES.....</b>		<b>127</b>
<b>APPENDICES .....</b>		<b>139</b>

Universiti Malaya

## LIST OF FIGURES

Figure 1.1	:	Location of Miri and Canada Hill by Google, Maxar Technologies, 2020 (earth.google.com/web/). ....	5
Figure 1.2	:	Geological Map of Canada Hill prepared from information obtained in the present study. Extension and thrust faults, and naming of Miocene geological units after Wannier et al. (2011). ....	7
Figure 1.3	:	A geological cross section across A-A' in Figure 1.2. ....	8
Figure 1.4	:	Topography and drainage pattern of Canada Hill. ....	10
Figure 1.5	:	Mean Annual Rainfall from year 2007 to 2016 (Malaysian Meteorological Department, 2017). ....	11
Figure 1.6	:	Mean Monthly Rainfall from year 2007 to 2016 (Malaysian Meteorological Department, 2017) . ....	11
Figure 2.1	:	A vector and a raster file. ....	24
Figure 3.1	:	The interface of Avenza Maps application. ....	34
Figure 3.2	:	Workflow for the landslide susceptibility assessment using a heuristic approach. ....	38
Figure 3.3	:	Workflow of the landslide susceptibility assessment using a bivariate statistics approach. ....	40
Figure 4.1	:	a) Medium-grained sandstone from the Miri Formation, b) Fine-grained sandstone from the Miri Formation. ....	46
Figure 4.2	:	<i>Ophiomorpha</i> trace fossils in the Miri Formation. ....	47
Figure 4.3	:	(clockwise from top left) Facies B, E, I, L, K, J. ....	48
Figure 4.4	:	a) Gentle-dipping beds of Miri Formation, b) Subvertical beds of Miri Formation (Lopeng area). ....	49

Figure 4.5	:	Small reverse fault with the appearance of clay smears. ....	50
Figure 4.6	:	Four shale samples based on Muol (2009) located within the Clay region (CL) using the classification by Waltham (1994). ....	51
Figure 4.7	:	3D view of Canada Hill. ....	52
Figure 4.8	:	a) Grade 5 weathering, b) Grade 6 weathering.....	52
Figure 4.9	:	Results of XRD analysis on the minerals in the Nyalau Soil Series.....	53
Figure 4.10	:	Results of XRD analysis on the efflorescent sulfate salts. ....	54
Figure 4.11	:	a) Efflorescent sulfate salts on the surface of shale, b) Encrustations on sandstone surface. ....	55
Figure 4.12	:	XRD analysis on the sulfate mineral crusts.....	55
Figure 4.13	:	Podzolized layer in the terrace deposit overlying the Miri Formation. ....	56
Figure 4.14	:	Podzolized layer in the Miri Formation.....	57
Figure 4.15	:	Engineering geology map of the Canada Hill area.....	63
Figure 5.1	:	Location of landslide occurrences at Canada Hill. Naming of Miocene geological units after Wannier et al. (2011). ....	65
Figure 5.2	:	LS1 at <i>Kampung Lereng Bukit</i> . ....	66
Figure 5.3	:	Daily rainfall in January 2009 (Malaysian Meteorological Department, 2017) . ....	67
Figure 5.4	:	a) 3D view of LS1 by Google, Maxar Technologies, 2020 (earth.google.com/web/), b) Sketch of LS1 with its' inferred components. ....	67
Figure 5.5	:	Landslide Map of LS1. ....	68

Figure 5.6	:	Cross section of A-A' from Figure 5.5. ....	69
Figure 5.7	:	a) LS1 site in year 2013, b) Relief of LS1, c) LS1 site in year 2001 showing relict of an older landslide, d) LS1 site in year 2008 with a fair amount of vegetation growth. No signs of landslide activity. 5.7a, 5.7c and 5.7d were obtained from Google, Maxar Technologies, 2020 (earth.google.com/web/). ....	70
Figure 5.8	:	a) 3D view of LS2 by Google, Maxar Technologies, 2019 (earth.google.com/web/), b) Sketch of LS2 with its' inferred components. ....	71
Figure 5.9	:	a) Loose wedge cut by a north-south fault/joint located beneath the trees, which separates the wedge from the slope, b) Remnants of loose rocks on the slip surface of LS2. ....	71
Figure 5.10	:	Daily rainfall in January 2009 (Malaysian Meteorological Department, 2017). ....	72
Figure 5.11	:	a) LS2 site in year 2013, b) Relief of LS2, c) LS2 site in year 2001, d) LS2 site in year 2011. 5.11a, 5.11c and 5.11d were obtained from Google, Maxar Technologies, 2020 (earth.google.com/web/). ....	73
Figure 5.12	:	LS3 along the <i>Pujut Padang Kerbau</i> road, located at the Eastern side of Canada Hill. ....	74
Figure 5.13	:	Daily rainfall in January 2014 (Malaysian Meteorological Department, 2017). ....	75
Figure 5.14	:	a) LS3 site in year 2001 showing distinct relict landslide, b) Relief of LS3, c) LS3 site in year 2008, d) 2014 imagery of the LS3 area showing position slightly left of relict landslide. 5.14a, 5.14c and 5.14d were obtained from Google, Maxar Technologies, 2020 (earth.google.com/web/). ....	76
Figure 5.15	:	Domestic drains discharging water downslope. Direction of water flow is indicated by the yellow arrow. ....	77
Figure 5.16	:	LS4 along <i>Jalan Miri-Pujut</i> (opposite Bintang Megamall). The tension cracks on the upper slope is indicated by the red circle. ....	77

Figure 5.17	:	LS5 along the slopes adjacent to <i>Jalan Oil Well No. 1</i> .....	78
Figure 5.18	:	Landslide 6 .....	79
Figure 5.19	:	Landslide 7 .....	79
Figure 5.20	:	The 3 directional cosines of a vector in spatial form.....	80
Figure 5.21	:	Interpolated orientation of bedding overlain on Geology map.....	83
Figure 5.22	:	Interpolated dip direction of bedding overlain on dip angle map. ....	84
Figure 5.23	:	Workflow for the initial planar failure susceptibility assessment. The red-colored boxes indicate raster files and the blue-colored boxes indicate shapefiles.....	85
Figure 5.24	:	Map of the relationship between direction of slope face and dip direction of bedding plane.....	91
Figure 5.25	:	Map of the relationship between dip of slope and dip of bedding plane. ....	94
Figure 5.26	:	Planar failure susceptibility map of Canada Hill.....	96
Figure 5.27	:	Histogram of landslide occurrence and areal extent of the subclasses on the planar failure susceptibility map.....	96
Figure 5.28	:	Slope gradient map of Canada Hill.....	99
Figure 5.29	:	Histogram of landslide occurrences and areal extent of the subclasses on the slope gradient map.....	99
Figure 5.30	:	Geology map of Canada Hill. ....	100
Figure 5.31	:	Histogram of landslide occurrences and areal extent of the subclasses on the geology map. ....	100
Figure 5.32	:	Distance to lineament map of Canada Hill.....	102

Figure 5.33	:	Histogram of landslide occurrences and areal extent of the subclasses in the distance to lineament map. ....	102
Figure 5.34	:	NDVI map of Canada Hill. ....	103
Figure 5.35	:	Histogram of landslide occurrences and areal extent of the subclasses in the NDVI map. ....	103
Figure 5.36	:	Elevation map of Canada Hill. ....	105
Figure 5.37	:	Histogram of landslide occurrences and areal extent of the subclasses in the elevation map. ....	105
Figure 5.38	:	Slope curvature map of Canada Hill. ....	106
Figure 5.39	:	Histogram of landslide occurrences and areal extent of the subclasses in the slope curvature map. ....	106
Figure 5.40	:	Slope aspect map of Canada Hill. ....	108
Figure 5.41	:	Histogram of landslide occurrences and areal extent of the subclasses in the slope aspect map. ....	108
Figure 5.42	:	Cut and fill map of Canada Hill. ....	109
Figure 5.43	:	Histogram on landslide occurrences and areal extent of the subclasses in cut and fill map. ....	109
Figure 6.1	:	Landslide susceptibility map of Canada Hill produced through the heuristic approach. ....	115
Figure 6.2	:	Histogram of landslide distribution and areal extent of subclasses of landslide susceptibility in Canada Hill using the heuristic approach. ....	115
Figure 6.3	:	Landslide susceptibility map of Canada Hill produced through the bivariate statistics approach. ....	119
Figure 6.4	:	Histogram of landslide distribution and areal extent of subclasses of landslide susceptibility in Canada Hill using the bivariate statistics approach. ....	119



Figure 6.5	:	Comparison of the success rates obtained using the heuristic and bivariate statistics method. ....	121
------------	---	----------------------------------------------------------------------------------------------------	-----

Universiti Malaya

## LIST OF TABLES

Table 2.1	:	The classification of slope movements (after Varnes, 1984). ....	20
Table 2.2	:	Scale of analysis and applications after International Association of Engineering Geology (IAEG) (1976); Soeters & Van Westen (1996).....	26
Table 2.3	:	Basic input data sets for landslide susceptibility assessment and the update frequencies (after van Westen et al., 2008). ....	26
Table 3.1	:	Data generated for field verification. ....	33
Table 3.2	:	Application of Equation 3.1 for the calculation of the weightage of the parameter maps.....	39
Table 3.3	:	Application of Equation 3.3 for the calculation of the weightage of parameter maps.....	41
Table 3.4	:	Landslide susceptibility classifications.....	43
Table 4.1	:	Lithofacies of Miri FM and description of depositional environment after Abieda <i>et al.</i> (2005). ....	48
Table 4.2	:	Atterberg Limit test results for shale, after Muol (2009).....	51
Table 5.1	:	Relationship between signs of direction cosines and the quadrant of azimuth.....	82
Table 5.2	:	Relationship between direction of slope face and dip direction of bedding plane.....	86
Table 5.3	:	3D scenarios of four different relationships in Table 5.2. ....	87
Table 5.4	:	Relationship between the dip of slope face and the bedding plane. ....	93
Table 5.5	:	Planar failure susceptibility classification matrices. ....	95

Table 5.6	:	Planar failure susceptibility descriptors. ....	95
Table 5.7	:	List of landslide-controlling parameters applied in the heuristic and the bivariate statistics approach. ....	110
Table 6.1	:	The rank, contribution ratio and weightage of the parameters used in the overlay analysis of landslide susceptibility map. Weightages were calculated using Eq 3.1. ....	113
Table 6.2	:	The relationship of landslide-controlling parameters and landslide distribution. Weightages were calculated using Eq 3.3. ....	117

## **LIST OF SYMBOLS AND ABBREVIATIONS**

DEM	:	Digital Elevation Model
NDVI	:	Normalized Difference Vegetation Index
GIS	:	Geographic Information Systems
XRD	:	X-ray powder diffraction
SRTM	:	Shuttle Radar Topography Mission
LiDAR	:	Light Detection and Ranging

Universiti Malaya

## LIST OF APPENDICES

Appendix A	:	Newspaper report of erosion and landslide occurrences in Miri. ....	139
Appendix B	:	Landslide inventory of Canada Hill, Miri. ....	142

Universiti Malaya

## **CHAPTER 1 : INTRODUCTION**

### **1.1 Introduction**

Landslide is a common natural process in areas with topographic relief and can only be deemed as hazardous when people, property and livelihood is at stake (Crozier, 1986). The most common triggering factor of landslides is precipitation, followed by earthquake, volcanic activities and human activity. The increasing demands of resources, the trend of urbanization and the ignorance about the social, economic and political consequences of landslide processes have led to the exploitation of hillside areas which have contributed to the significant increase in the amount of people and property at risk for the past 100 years (Brabb, 1991; Crozier, 1986).

Annually, death tolls resulting from landslide incidences can reach up to thousands. In the period from January 2004 to December 2016, 55 997 people were killed in 4862 different landslide events, predominantly occurring in Asia (Froude & Petley, 2018). Malaysia receives an average of 2500mm rainfall a year and has a significant share to the reported number of casualties. A report by Brabb (1991) mentioned that 246 deaths in Malaysia from the year 1960 to 1980 was due to flow-slides in tin mine excavations. In a separate report by Haliza & Jabil (2017), 28 major landslides were reported in Malaysia from the year 1993 – 2011 which resulted in the loss of more than 100 lives coupled with an enormous economic loss.

Landslide occurrences cannot be prevented but are relatively predictable and can be mitigated to lessen the impacts on the society living near or at more landslide-susceptible areas. Mitigation efforts should be a joint effort between all levels of the government, non-governmental organizations (NGO's), academia, private sectors and local society and communities. International efforts to curb disaster-related-problems led to the implementation of Hyogo Framework for Action 2005 – 2015 (HFA) by the United

Nations International Strategy for Disaster Risk Reduction (UN-ISDR) which aims to build resilience and reduce the losses from natural disasters by 2015. The positive response and outcomes of HFA instigated the Sendai Framework for Disaster Risk Reduction 2015 - 2030 (SFDRR) as a continuance of the objectives from HFA alongside highlighting important issues that were identified. Malaysia does not shy away from realizing the goals of HFA which is shown through the Public Work's Department (PWD) comprehensive study of the National Slope Master Plan 2009 – 2023 (NSMP) which outlines the national policy, strategy and action plan for reducing risk from landslides on slopes nationwide during the period of 2009 – 2023 (United Nations Office for Disaster Risk Reduction (UNDRR)). Strategic mitigation programs at the national, state and local levels, both in the public and private sectors are discussed in this plan.

Landslide susceptibility assessment, which delineates areas with the probability of future landslide incidences has been adopted as one of the ways to ensure the way forward to a more sustainable development. The procedure of delineating landslide hazards involves the identification of external destabilization factors, terrain sensitivity and probability of landslide occurrence (Crozier, 1986). The advancement in geo-spatial technology prompted the integration of Geographical Information System (GIS) as a more efficient and inexpensive way to produce high-resolution landslide susceptibility maps. The widespread application of GIS has seen the utilization of different methods to generate landslide susceptibility maps based on the scale of study and available resources. The adaptation of a suitable assessment method ensures a smooth translation and transfer of information to decisionmakers for land use planning.

## **1.2 Problem Statement**

The rapid economic development has given a notable rise to the population growth of Miri, Sarawak its' declaration as a city in 2005. What started as an almost uninhabited fisherman village is now a city bustling with life. Miri became the pioneering site for oil

and gas in Malaysia since the first oil discovery in 1910. The pattern of urbanization focuses on the flat areas but the presence of a sole hill, known as Canada Hill or 'Miri Hill' in the middle of the city forces the exploitation of the lower slopes of the hill in addition to the already present villages scattered on top of the hill.

Landslides occurrences along the slopes of Canada Hill are common and the risks have escalated from the previous years as the lower slope areas are becoming more populated. Technical reports by *Jabatan Mineral dan Geosains* (JMG) mentioned Canada Hill's susceptibility to reactivation landslides based on interviews with the villagers residing on the hill who have observed landslides occurring on the same site every few years apart.

As the annual monsoon season approaches which lasts from October to March, Miri receives an abundant rainfall of 2500mm – 3500mm subsequently giving rise to hazards such as landslides and flood (The Star, 2009a, 2009d, 2009f, 2018a; Then, 2017a, 2018; Toyat, 2018). The most horrific landslide incidences occurred in January 2009 where two landslides resulted in the demise of 2 lives and damaged homes at *Kampung Lereng Bukit*, a village at the foot-slope of the west flank of Canada Hill (The Star, 2009e, 2009f). The jagged-like appearance and the distinct incised slopes of Canada Hill and the frequent need for road repairs indicate the hill's high susceptibility to erosion which also poses a threat to the public if suitable remedial actions are not taken. Cases like these are unfortunate as landslide events can be managed though admittedly it may be difficult with insufficient knowledge about endemic hazards, inappropriate adjustment mechanism and scarce resources to mitigate hazards (Crozier, 1986). This research will focus on the assessment of landslide susceptibility of Canada Hill and adjacent areas to facilitate the goal towards a more sustainable development in Miri. Another hazard in Miri is wildfires which generally occur during the dry months between March to October (Then, 2010, 2011).

The peculiarity of the landslides in Canada Hill lies in the low slope friction angle ( $\theta$ )



of below 30°. The west-dipping sandstone bed acted as the sliding plane for the failed debris to flow on following the infiltration of water through the joints and cracks in the rocks (Banda et al., 2009). This research aims to determine the possible causal factors of landslide in Canada Hill to provide a reliable landslide susceptibility map of Miri.

### **1.3 Research Questions**

The research questions this study is set out to answer are:

1. What is the extent of landslide occurrences in Miri?
2. What are the reliable parameters that can be used for the landslide susceptibility assessment?
3. Is the landslide inventory database for Miri enough for future use?
4. How can a landslide susceptibility assessment help in depicting landslide occurrences in Miri?

### **1.4 Objective**

The proposed research aims to assess the landslide susceptibility of Miri, Sarawak.

The main objectives of this research project are as follows:

1. To map the geological and geomorphological features and the landslide occurrences in Miri, Sarawak.
2. To identify the parameters to be used as contribution factors for susceptibility assessment.
3. To create a database in the Geographical Information System (GIS) from the information collected for integrating, storing, editing, analysing and for sharing purposes in the future.
4. To compare two analytical approaches of landslide susceptibility assessment to produce a reliable landslide susceptibility map for Miri.

## 1.5 Study Area



**Figure 1.1:** Location of Miri and Canada Hill by Google, Maxar Technologies, 2020 (earth.google.com/web/).

Canada Hill is a narrow northeast-southwest trending ridge located in Miri, which is situated at north-western Sarawak, adjacent to the neighbouring country of Brunei and Bintulu town of Sarawak (Figure 1.1). Canada Hill extends up to 8km from *Kampung Padang Kerbau* up to *Tanjung Lobang*. The famous Grand Old Lady (Miri Oil Well No. 1) was the first oil well drilled on this hill and what was once a quaint coastal town flourished to a main hub for oil and gas trade bustling with life. This hill is also well known to the locals as *Bukit Telaga Minyak* (Oil Well Hill). Canada Hill houses various settlements scattered on top and along it, as well as the Petroleum Museum and is also a popular spot for hiking.

### 1.5.1 General Geology

The Miri Zone is one of the three structural zones of Sarawak and is composed of Upper Eocene to Recent shallow marine rocks (Haile, 1974). Canada Hill is mainly underlain by middle Miocene-Pliocene (~10 Ma) Miri Formation, consisting of interbedded deltaic sandstone and shale. Miri Formation is divided into; the arenaceous Upper Miri Formation and the argillaceous Lower Miri Formation (Liechti *et al.*, 1960). Pleistocene Terrace Deposits are found on top of the hill while the adjacent areas of Canada Hill are comprised of Late Miocene Seria Formation and Quaternary alluvial deposits (Figure 1.2).

Canada Hill is part of the faulted Miri Anticlinical structure which extends to the sea in a westward direction and plunges towards the northeast (Wannier *et al.*, 2011). Canada Hill is bounded on both sides by reverse faults, attributed by the reactivation of Canada Hill tectonics. As a result of this young reactivation tectonics, an inferred Quaternary horizontal pressure in the NE-SW direction, coupled with strike-slip tectonics and overthrusting, triggered a diapiric remobilization of the underlying semi-liquid pillow Setap Shale in an upwards motion (Kessler & Jong, 2014) led to the uplift of the hill up to almost 90m above mean sea level above the Pleistocene peneplain as observed on this present day.

The flat top and the flanks of the plateau-like hill is underlain by loose and unconsolidated quartzitic sands of Terrace deposits which overlies the Miri Formation (Figure 1.3). Differences in facies on either side of the hill have been identified by von Schumacher (1941), in which he mentioned that the Miri Formation at the west of Canada Hill contains thicker and better developed sands, likely due to a strike-slip movement. The Miri Formation and the overlying Seria Formation are in perfect conformity and is almost alike in lithology. Seria Formation is comprised of laminated thin sandstone, sandy shale and shale with some lignite (Liechti *et al.*, 1960). These formations are severely

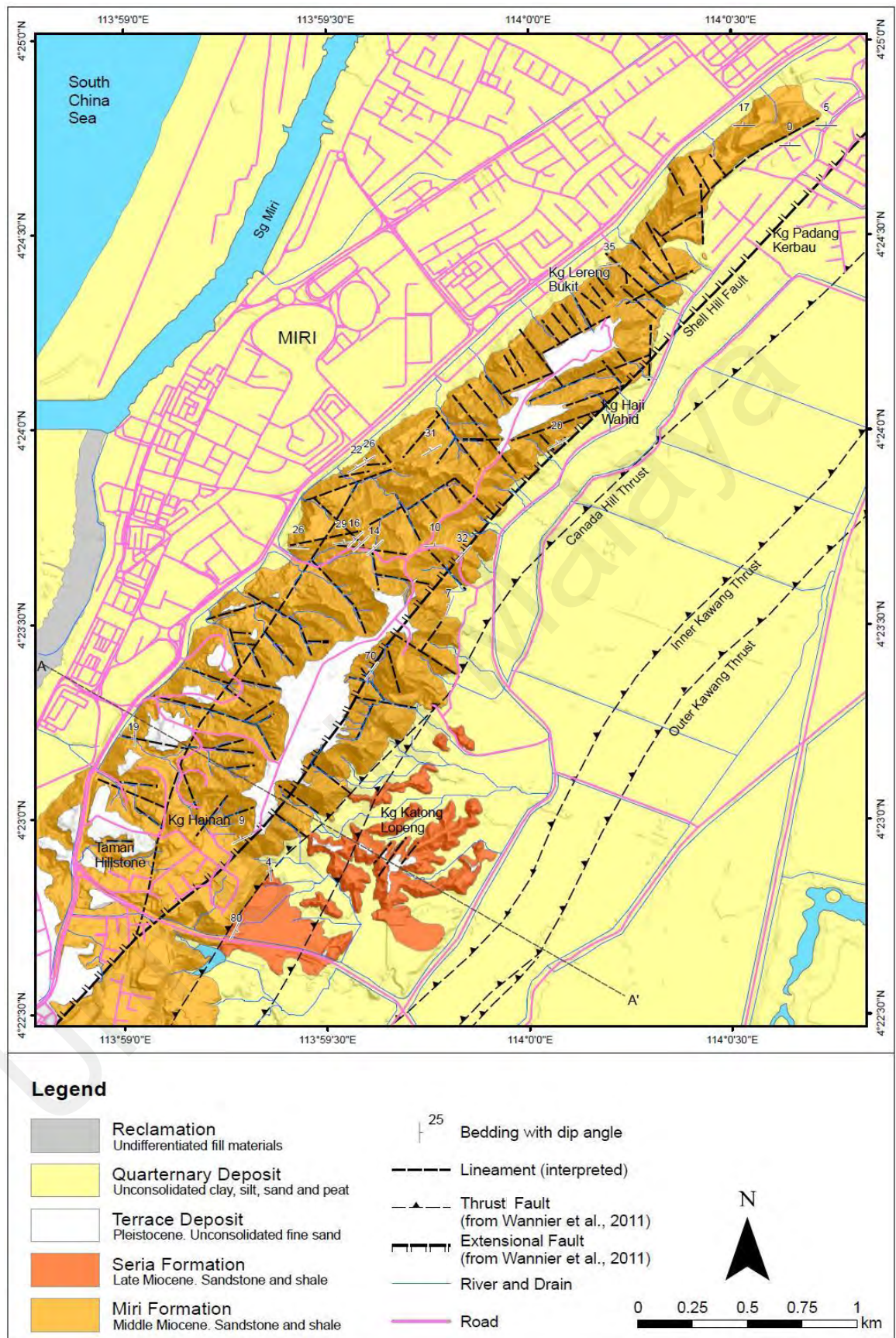


**Figure 1.2:** Geological Map of Canada Hill prepared from information obtained in the present study. Extension and thrust faults, and naming of Miocene geological units after Wannier et al. (2011).



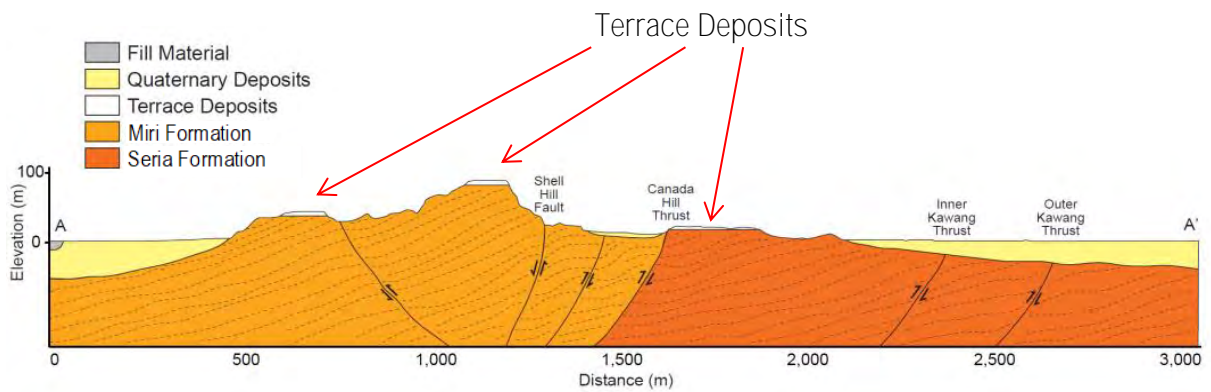


**Figure 1.3:** A geological cross section across A-A' in Figure 1.2.

eroded giving distinct incised slopes and jagged terrains due to the presence of many small-scale sharp ridges and narrow valleys especially within the Miri Formation. However, the relatively younger Seria Formation lies at a lower elevation, only present at the south-eastern flank of Canada Hill and appears to be folded and dips almost vertically. It is then inferred that the thrusting of the Miri structure superseded the deposition of the Seria Formation, which acted as footwall during the up-thrusting of the older Miri Formation during the Pleistocene (Wannier *et al.*, 2011). Holocene deposits occur above the marine sediments post-Pleistocene forming the low-lying flat plain around the hill.

The immense presence of major and minor faults at the vicinity of Canada Hill is attributed to the deposition manner of Miri Formation and its' strike slip tectonic regime. Shell Hill Fault and Canada Hill Thrust is an apparent conjugated pair of faults, both reactivated at the same time (Kessler & Jong, 2014). The presence of growth normal faults, a syn-depositional deformation within the Miri Formation was a result of the accumulating sands exerting pressure on the underlying water-rich, ductile Setap Shale and subsequently, inducing flow of the shales (Wannier *et al.*, 2011).

### 1.5.2 Basis of Selection

Landslides are a common occurrence in the vicinity of Canada Hill especially during the annual monsoon season which lasts from October to March. The relatively young hill

is undergoing erosion at a reasonably fast rate making it prone to landslides. For the past decade (2009 – 2019), 4 major landslides occurred at Canada Hill, impacting the livelihood of the population directly and indirectly. 2 lives were lost to the landslides and several properties were damaged. The landslides are attributed to the geological, human and rainfall pattern factor. Engineering geological survey showed tension cracks and relicts of previous landslides near the failed slopes. Closely spaced faults were also observed in the vicinity of the failed hill slope areas at *Kampung Lereng Bukit*, a village at the foot slope of Canada Hill. Banda et al. (2009) stated that water seeped through cracks in the sandstone beds, dipping 20-25° and 25-28° northwest which then acted as a sliding plane for the failed loose debris to slide upon.

This study aims to determine as much causal factors as possible from field investigation and laboratory analysis which in turn will generate a reliable landslide susceptibility map of Miri. This research hopes to aid in future planning purposes and landslide managements in Miri, Sarawak.

### **1.5.3 Accessibility**

Miri City is located at the coast of Northwest Sarawak. The major cities in Sarawak are interconnected by the Pan Borneo Highway. The nearest cities from Miri are Brunei (56km NE) and Bintulu (197km SW) both of which are highly accessible. Miri is accessible from outside Sarawak by flights from most national airlines. The navigation around Miri is easy using the main roads except for some less developed or abandoned areas where it is only accessible by motorcycles and by foot.

### **1.5.4 Topography and Drainage**

The study area focused in this research is generally a flat low-lying area with only Canada Hill as the highest elevation (Figure 1.4). The feature of Canada Hill resembles a plateau with a flat top and gentle to steep incised slopes surrounded by a flat plain overlain by Quaternary sediments. The Southeast of Canada Hill is dominated by a hill of lower

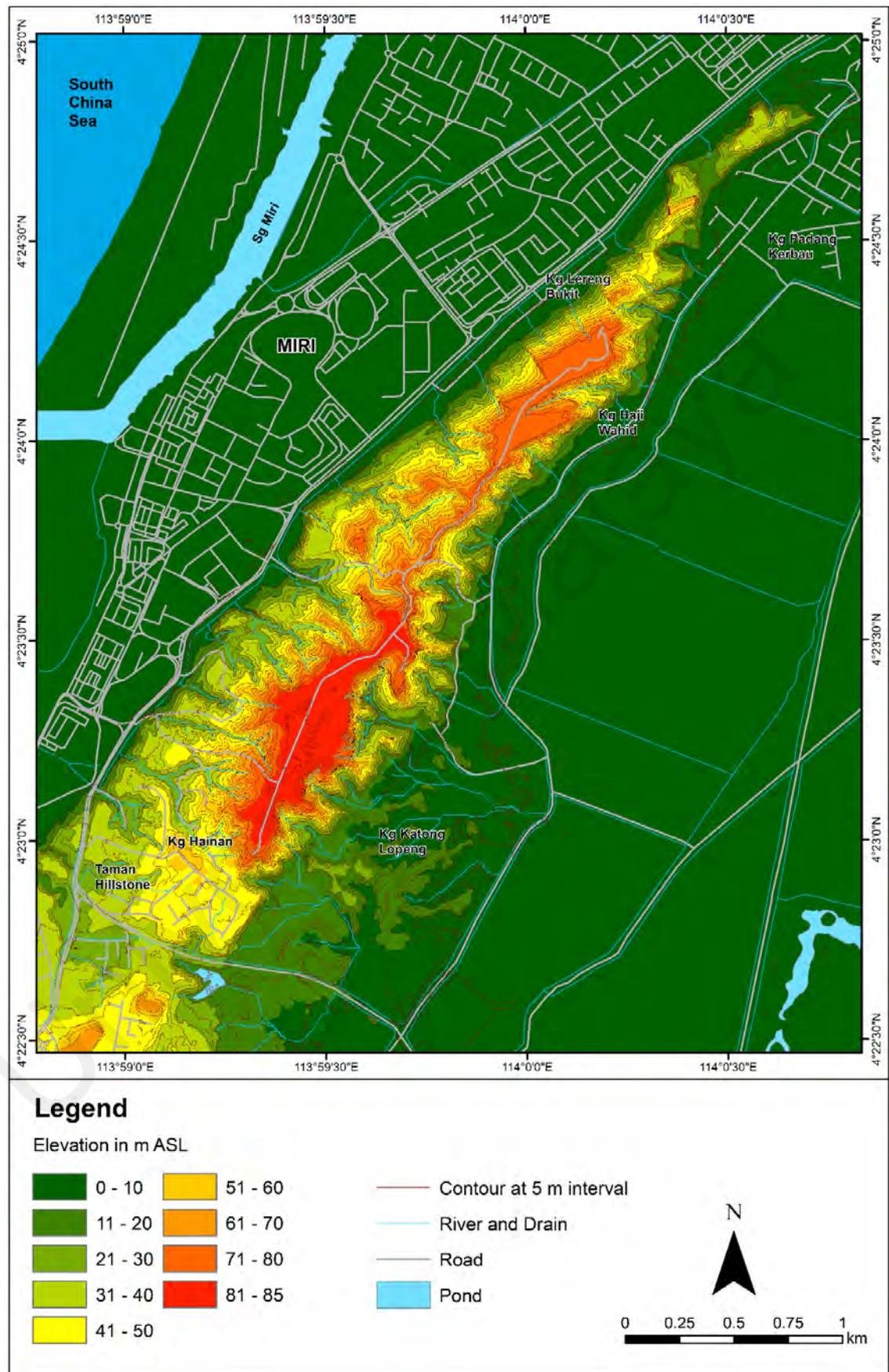


**Figure 1.4:** Topography and drainage pattern of Canada Hill.

elevation with relatively smooth undulating slopes. The topmost part of the hill, including the lower elevated ones are overlain by loose white leached sand which resembles beach sands. The main river, Sungai Miri meets the sea at the Southwest which was previously redirected to make way for the Marina Park project. The smaller drainages in the area are either natural seasonal rivers along the slopes of Canada Hill and artificial drainages at the low-lying areas.

### 1.5.5 Climate

Miri has a tropical rainforest climate associated with its' position in the equatorial region. This allows an annual high rainfall average of 4325.5mm from 2007 to 2016 (Figure 1.5). Miri is also affected by two monsoon seasons every year; the Northeast Monsoon and the Southwest Monsoon. The former lasts from October to March while the latter lasts from April to September. The mean monthly rainfall ranges from 191.22mm to 825.75mm (Figure 1.6) with the lowest in June and the highest in December. The mean rainfall amount in January and December makes up 35.5% of the mean annual rainfall.

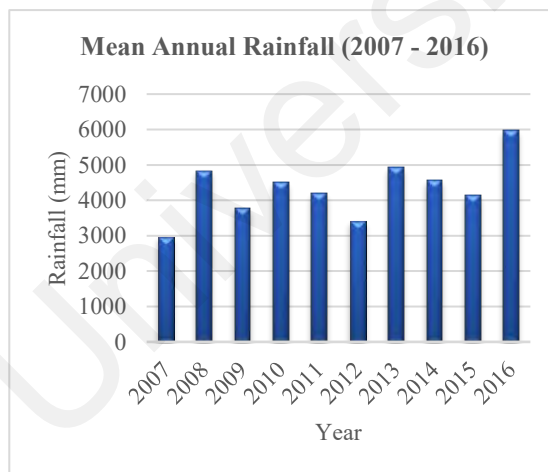


**Figure 1.5:** Mean Annual Rainfall from year 2007 to 2016 (Malaysian Meteorological Department, 2017).

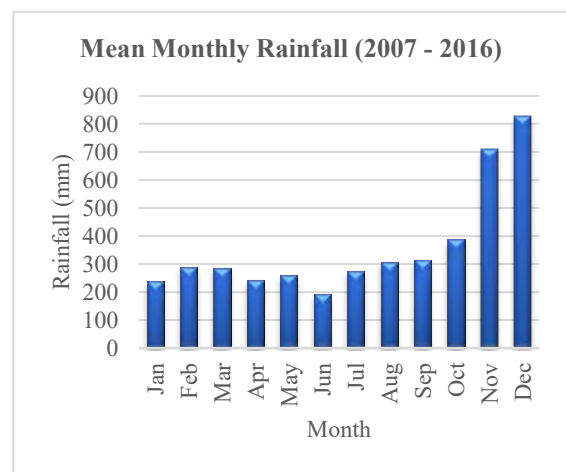


**Figure 1.6:** Mean Monthly Rainfall from year 2007 to 2016 (Malaysian Meteorological Department, 2017) .

## 1.6 Research Significance

Prior to the development of an area, land use planners are often the key person involved in decision-making. Planners need to be well-formed in the effective management of areas



with landslide potential to make a sound decision on land development. Hence, a reliable landslide susceptibility map will be able assist in identifying a sustainable solution with regards to land exploitation to ensure lower costs in construction and maintenance of engineering structures.

The landslides in Canada Hill are geologically controlled, accelerated by the high levels of rainfall during the monsoon season and the geomorphological features of the hill. This research will determine the most plausible factors of landslide occurrences and to focus on the relationship between the bedding and slope.

Landslide susceptibility assessment is a well-known approach to delineate potential areas with landslide. However, the literature review on Canada Hill shows a lack of a fitting assessment of its' landslide potential, considering the tendency of these occurrences. This research is an effort to identify a reasonable method for the landslide susceptibility assessment of Canada Hill.

## **1.7 Organization of the Thesis**

Chapter 1 introduces this research and contains subchapters that describe the problem statement, research questions, objectives, study area and the research significance. The problems arising regarding the landslide occurrences in Canada Hill, Miri have instigated a research on landslide susceptibility assessment on the study area. Research questions and objects stemmed from this problem which became a main guideline for this research. The research significance was also described in this chapter.

Chapter 2 contains the literature review which summarized the viewpoints, definitions and concepts used in the context of this study. The general geology of Miri was described in detail regionally and locally in the first subchapter followed by the second subchapter reviewing landslides of its definition, concepts and the terminologies used. The causal factors of landslides were also described in this subchapter, following a detailed review

on failure occurrences in a rock slope and lastly, a review of the past landslide occurrences in Miri. The next subchapter describes the geographic information systems (GIS) and the application of this system in spatial analysis for the subsequent landslide susceptibility assessment. The last subchapter describes the landslide susceptibility assessment and the available methods which is divided into a qualitative approach and a quantitative approach.

Chapter 3 gives a summary of the methodologies used in this study. The chapter starts off with the preparation of a base map and landslide inventory. Field verification methods are described in the next subchapter, followed by the preparation of data for the landslide susceptibility assessment. The next subchapter describes the different approaches applied to perform the landslide susceptibility assessment of the study area. This chapter ends with the summary of the limitations faced in this study.

Chapter 4 focuses on the engineering geology of the Canada Hill area. The sequence of the subchapter in this chapter are arranged according to the age of deposition of the formations in the study area from the oldest to the youngest. The Miri Formation and Seria Formation is combined in the first subchapter owing to exhibiting similar characteristics. The minor differences between these two formations are also described in this subchapter. It is further divided into the bedrock characteristics and weathering tendencies of the formations. The next subchapter describes the quaternary deposits in the study area followed by the terrace deposits in the next subchapter. Holocene deposits are described in another subchapter and is divided into four soil series, describing the engineering implications of the different soil series. The last subchapter mentions briefly on the artificial deposits in Miri.

Chapter 5 describes the findings of the investigation of the three major landslides in Canada Hill in details along with minor landslide occurrences in the first subchapter. This investigation is the first step of the selection of the landslide-controlling parameter which

is described in the subsequent subchapters in the following order; planar failure susceptibility, slope gradient, geology, distance to lineament, normalized difference vegetation index (NDVI), elevation, slope curvature, slope aspect and cut and fill. Each of the subchapters describe the relationship of the landslide occurrence to the areal extent of the subclasses delineated for the respective parameters. A summary of chapter 5 is included at the end of this chapter which links to the next chapter.

Chapter 6 highlights the findings, in two subchapters, of the landslide susceptibility assessment which used the qualitative approach (heuristic) and the quantitative approach (bivariate statistics). The comparison of the application of the two methods, which includes the advantages and disadvantages are described in the discussion at the end of this chapter.

Chapter 7 summarizes the findings in this study and concludes the landslide susceptibility assessment based on the applied methods. This chapter also mentions the suggestions for future work.

## **CHAPTER 2 : LITERATURE REVIEW**

### **2.1 Introduction**

This chapter will describe the regional geology of the study area, geological setting, definitions, terminologies and concepts used in this research. This research focuses on landslide and landslide susceptibility assessments and will also be further explained in the following subtopics. The landslide subtopic will be further divided into the causal factors and occurrences in Miri, Sarawak while the landslide susceptibility assessment will be subdivided into qualitative and quantitative methods and each will be described of their definitions, applications, advantages and disadvantages.

### **2.2 Geology of Miri, Sarawak**

This study area being researched is situated in Miri, northwest of Sarawak. The area is underlain by mid-Miocene Miri Formation, late-Miocene Seria Formation, Pleistocene Terrace deposits and Holocene deposits. The following subchapters will include descriptions for the regional geology and geological setting of the study area. The general geology will later be described in detail in Chapter 4.

#### **2.2.1 Regional Geology**

Sarawak lies at the intersection of three major plates, the Eurasian at the north, Indo-Australian at the south and Philippines at the east (Tongkul, 1996) and the movement of these plates relative to each other have brought an episodic tectonic convergence in Sarawak which led to the uplifting of the Rajang mountains (Wannier *et al.*, 2011).

Prior to getting into detail about the regional geologic history, Haile (1974) divided Sarawak into three main structural zones separated by suture zones, which also young in this sequence; Kuching zone, Sibu zone and Miri zone. The youngest division in the north, the Miri Zone is characterized by post-Eocene shallow marine (miogeosynclinal) deposits, molasse strata deposited on older continental crust and deltaic sediments

(Hutchison, 2005; Wannier *et al.*, 2011). The boundary that separates Miri Zone and Sibul Zone is the Tatau-Mersing Line (Hutchison, 1989). The Sibul Zone consists of a Late Cretaceous to Eocene thick deep-water Rajang Group mainly deposited in a eugeosynclinal flysch (Hutchison, 2005), overlain by Oligocene-Miocene clastic sediments with coal deposits at the base (Nyalau Formation) (Wannier *et al.*, 2011). This zone is separated from the Kuching Zone by the Lupar Line (Tan, 1979). Kuching Zone is composed of basement complex, Jurassic-Cretaceous schists and phyllites overlain by Mesozoic volcanics and sedimentary rocks and Tertiary clastics (Wannier *et al.*, 2011). 'Post-basement intrusions' are a distinct character of this zone.

The evolution of the Sarawak Basin in the Cenozoic times is owed by the development of the Rajang subduction zone of the Paleocene age, along the Lupar Line which resulted in the continental collision of the Luconia block (rifted from the south-eastern margin of the Eurasian Plate) with the West Borneo Basement, part of the Asian Sundaland, consisting of Cretaceous volcanic and plutonic rocks (Hutchison, 2005). Northern Sarawak was once part of a deep marine basin, with a continuous deposition of shales, sandstones and conglomerates that make up the Mulu Formation, part of the Rajang Group and an initial Late Eocene "soft collision" in an oblique manner from the northwest to northeast and the later Mid-Miocene "hard collision" against the crust of central Borneo consequently halted deep marine sedimentation, closed the Rajang Sea that once separated Luconia and the West Borneo continental blocks, which then later formed the arcuate Rajang-Fold-Thrust belt (Madon, 1999), present as a mountain range in the Sibul Zone. A major strike-slip fault zone, the West Baram Line may also have become active due to the collision. Further subsidence from terrane accretion produced the northwest Borneo geosyncline which extends from the vicinity of Lupar Valley in Sarawak to up to Mount Kinabalu in Sabah, Malaysia. It is characterized by a large-scale subsidence owed by the deposition of very thick Upper Cretaceous and Tertiary sediments partly in flysch

facies (Liechti *et al.*, 1960) contributed by stream erosions sourced from the Rajang mountains, resulting in wide coastal plains and large deltas (Champion and Baram Delta) which later on prograde seaward throughout the Paleogene and Neogene times, accordingly migrating the axis of the geosyncline. This supplied a wedge of clastic sediments up to 15km thick (Wannier *et al.*, 2011) which included the formation of isolated Neogene coastal basins, later infilled with late Miocene and Pliocene sediments with a thickness of up to 8.5km that include the Belait, Lambir, Miri and Seria Formations. Sedimentation of this sort can still be seen up to this present day, inferred to be a continuation since the late Cretaceous, evidenced by progressing tilting of the shelf in recent offshore basins in South China Sea which in due time, accumulation of sufficient sediments may trigger another folding and uplifting phase, attributing to the migration of the geosyncline axis further seawards (Liechti *et al.*, 1960).

Subduction along the North Borneo Trough combined with transpression generated from strike slip motions in the Indo-China Block across the South China Sea to Sarawak have probably resulted in the Pliocene compressional deformation within the sedimentary sequences producing syn-sedimentary growth faults and folds (Wannier *et al.*, 2011). This compression also probably led to inversion tectonics, causing the reactivation of the previous normal faults as reverse faults and folds (Morley *et al.*, 2003) and the Pleistocene uplift of Canada Hill and also Lambir Hills, located at the south of Miri.. A distinct feature resulting from this process is the Miri anticlinal structure which is bounded by thrust faults parallel to the hill and adjacent to normal faults which are possibly growth faults.

### **2.2.2 Geological Setting**

The geology of Miri has been researched extensively by natural history explorers as early as the year 1845, subsequently by Shell geologists that led the exploration of natural and mineral resources in 1909. Miri is located at the northwest coast of Borneo and is comprised mainly of interbedded deltaic sandstone and shale, a resulting deposition of

the eroded sandstones of the Rajang Formation dating back to 14 – 9 Ma ago. The highest elevation of Miri of up to 85m is at Canada Hill. This hill is a 8km long NE-SW trending, less than 2km wide ridge comprised of the Mid Miocene Miri Formation, Late Miocene Seria Formation and Pleistocene Terrace Deposits on the hill and Quaternary alluvial deposits on the flat-lying vicinity (Figure 1.2).

Canada Hill is part of the faulted Miri Anticlinical structure which extends to the sea in a westward direction and plunges towards the northeast (Wannier *et al.*, 2011). Canada Hill is bounded on both sides by reverse faults, attributed by the reactivation of Canada Hill tectonics. As a result, this young reactivation tectonics generated an inferred Quaternary horizontal pressure in the NE-SW direction, coupled with strike-slip tectonics and overthrusting which triggered a diapiric remobilization of the underlying semi-liquid pillow Setap Shale in an upwards motion (Kessler & Jong, 2014). This has led to the uplift of the hill, part of the Miri Formation up to almost 300 feet above mean sea level above the Pleistocene peneplain.

The flat top and the flanks of the plateau-like hill is underlain by loose and unconsolidated quartzitic sands of Terrace deposits which overlies the Miri Formation (Figure 1.3). The Miri Formation, an interbedded sandstone shale succession is what makes most of Canada Hill. Differences in facies on either side of the hill have been identified by von Schumacher (1941), in which he mentioned that the Miri Formation at the west of Canada Hill contains thicker and better developed sands, likely due to a strike-slip movement. The Miri Formation and the overlying Seria Formation are in perfect conformity and is almost alike in lithology. Seria Formation is comprised of laminated thin sandstone, sandy shale and shale with some lignite (Liechti *et al.*, 1960). These formations are severely eroded giving distinct incised slopes and jagged terrains due to the presence of many small-scale sharp ridges and narrow valleys especially within the Miri Formation. However, the relatively younger Seria Formation lies at a lower

elevation, only present at the southeastern flank of Canada Hill and appears to be folded and dips almost vertically. It is then inferred that the thrusting of the Miri structure superseded the deposition of the Seria Formation, which acted as footwall during the up-thrusting of the older Miri Formation during the Pleistocene (Wannier *et al.*, 2011). Holocene deposits occur above the marine sediments post-Pleistocene forming the low-lying flat plain around the hill.

The immense presence of major and minor faults at the vicinity of Canada Hill is attributed to the deposition manner of Miri Formation and its' strike slip tectonic regime. Shell Hill Fault and Canada Hill Thrust is an apparent conjugated pair of faults, both reactivated at the same time (Kessler & Jong, 2014). The presence of growth normal faults, a syn-depositional deformation within the Miri Formation was a result of the accumulating sands exerting pressure on the underlying water-rich, ductile Setap Shale and subsequently, inducing flow of the shales (Wannier *et al.*, 2011).

### **2.3 Landslide**

Landslide is a geologic hazard, categorized side by side with earthquakes, major floods, hurricanes and other natural catastrophes which cause major loss of lives and properties globally and annually. It has a significant role in landscape evolution but is also a danger to the population in many parts of the world (Petley, 2012). Landslide hazards are not as costly as other major hazards but are more widespread and linked closely to earthquakes and intense storms as a consequent occurrence of these hazards, which can cause more property damage and loss of lives (Varnes, 1984). Landslides can be generated either naturally as land surface processes or through human disturbances. Either way, when the balance of layers of a surface is disrupted, a weak plane will act as a failure plane which leads to the topmost layer of the land slipping away. The common factor is rainfall or when gravity overcomes the frictional forces which keeps the layers intact on a slope. Lack of knowledge or an oblivion to the surface processes that can cause



landslides may lead to more damage in the future, which puts the population especially near mountainous terrains at a higher risk. The definitions and concepts of landslide, causal factors of landslide and landslide occurrences in Miri, Sarawak will be discussed in the following subchapters.

### 2.3.1 Definition and Concept

The definition of landslide varies across studies by different authors. Varnes (1984) defined landslide as all the varieties of mass movements on slopes including those which involve little or no true sliding while Highland & Bobrowsky (2008) defined landslide as the downslope movement of soil, rock, and organic materials under the effects of gravity and also the landform that results from such movement. National Research Council (U.S.) Transportation Research *et al.* (1978) defined landslide as a constitution of a group of slope movements wherein shear failure occurs along a specific surface or combination of surfaces. A landslide mass is composed of either rock or soil. The soil will be termed as ‘earth’ if it composes of sand-sized particles and ‘debris’ if coarser fragments dominate (Highland & Bobrowsky, 2008). The classification of landslides depends on the materials and the mechanics involved. The landslides can be classified as falls, topples, slide, lateral

**Table 2.1:** The classification of slope movements (after Varnes, 1984).

Type of Movement		Type of Material		
		Bedrock	Engineering Soils	
			Predominantly Coarse	Predominantly Fine
	FALLS	Rock fall	Debris fall	Earth fall
	TOPPLES	Rock topple	Debris slide	Earth slide
SLIDES	ROTATIONAL	Rock slide	Debris slide	Earth slide
	TRANSLATIONAL			
	LATERAL SPREADS	Rock flow (deep creep)	Debris flow (soil creep)	Earth flow (soil creep)
	FLOWS			
		COMPLEX	Combination of two or more principal types of movement	

spread and flow (National Research Council (U.S.) Transportation Research *et al.*, 1978; Varnes, 1984) as shown in Table 2.1. A complex failure with more than one type of movements may also be encountered in landslides.

### **2.3.2 Causal Factors of Landslide**

Landslide occurrences are attributed by a combination of intrinsic and extrinsic factors. The former is also referred to as preparatory variables and the latter as triggering variables (Ramachandra *et al.*, 2012).

Intrinsic factors (preparatory variables) include geology, slope gradient, slope aspect, elevation, normalized differential vegetation index (NDVI), terrain roughness, slope roughness, total slope height, distance from road, distance from fault, distance from river and other factors that directly reduces the shearing strength of the rocks and soil (Wu & Chen, 2013).

Extrinsic factors (triggering variables) are events or processes that disrupt the stability of a slope, in relation to its' stress conditions and strength of material (Varnes, 1984). These factors can either be natural, human-induced or both. Natural factors include heavy rainfall, seismic activity, volcanic activity and glacier outbursts, among others while human-induced-factors usually involves construction of a susceptible area.

### **2.3.3 Failures in Rock Slope**

Slope instabilities occurring on rock slope varies distinctively with soil slopes in which sliding can only occur in rock slope a result of movement towards the free face created by excavation. The varying types of block failures in rock slopes are associated with different geological structures and the identification of these different mode of slope instabilities can be carried out by kinematic analysis, among many other conventional and numerical methods. The four types of failures are plane failure, wedge failure, toppling failure and circular failure in rock fill. The plane failure mode will be focused in this

research as the major landslide occurrences in the study area inhibits a planar failure characteristic. The structural geology conditions that likely caused plane failure in rock is the presence of persistent joints dipping out of the slope face and striking parallel to the face (Wyllie & Mah, 2004).

Plane failures are prone to occur if the basal plane daylight on the slope and the extent of the occurrence depends on two factors, namely the relationship between the dip direction of the bedding plane and the direction of slope face and the relationship between the dip angle of the plane and the dip angle of slope face. The basal discontinuity must dip at a sufficiently steep angle to overcome friction and the discontinuity also must be suitable oriented to allow detachment of the slipped rock mass and for its forward movement out of the slope (Lisle & Leyshon, 2004).

#### **2.3.4 Landslide Occurrences in Miri, Sarawak**

The knowledge of landslides in Miri and its' processes during this present-day was extracted from various reports from the Mineral and Geoscience Department, Malaysia. Additional archive research of the landslides recorded a total of 58 landslides in the area. Newspaper reports on landslide occurrences and soil erosion around Miri is shown in Appendix 1. The major and minor landslides in Miri occurred in the Miri Formation. The landslides that need critical attention are described in detail in Chapter 5.

The landslides in Miri are concentrated at Canada Hill due to rate of erosion this hill is subjected to, which makes it very prone to landslide occurrence. There are three major landslides that occurred from 2009 – 2014 which involved the demise of two lives and several houses. The probable causes of landslides in the vicinity was delineated in several reports by Banda *et al.* (2009), Luqman (2009), Mohd (2014), Muol (2009) and Zaid (2009). The cracks in the sandstone beds dipping Northwest allowed for water seepages which then allowed the bed to act as a sliding plane for the failed loose debris to slide upon (Banda *et al.*, 2009). This led to the conclusion that slope failures for Canada Hill

are a result of the combination of geological, human and rainfall pattern factors. Another major landslide in in *Kampung Padang Kerbau* in 2014 was also attributed to the heavy rainfall and surface water runoff from the adjacent *Kampung Haji Wahid* which is located near the crown of the landslide, in which water seeped between the joints causing a weakening in the structure and leading to failure (Mohd, 2014).

## **2.4 Geographic Information System (GIS)**

Geographic Information System (GIS) was pioneered by Roger Tomlinson in 1962 and has greatly evolved the world of mapping and geospatial technologies throughout the years. Through its' widespread use among government agencies, planners, science communities utilizing geospatial data and many others, the way around in terms of problem solving revolving spatial analysis has been paved.

GIS is a computer-based system of hardware and software capable of capturing, storing, analysing and displaying geographically reference data (Montana, 2008). Geospatial and mapping technologies have taken a leap with the presence of Geographic Information System (GIS) predominantly in the wake of the digital era, as a turnaround from the notoriously difficult paper map analysis.

Geological data is stored in a spatially referenced GIS database, which can be presented spatially as a map, or in a graphical or tabular form as attribute tables. For instance, landslide points displayed on a map can be attached with attributes such as location, type, length and depth. These attributes can be viewed and edited in tabular form in ArcGIS. Objects presented on a map can also be reclassified, based on different attributes to be presented in map form, showing patterns and relationships that are not always obvious in tabular form or the original geological map (Mason, 2013).

Data in GIS are either represented in vector or raster forms. Vector geographic data consists of either point, lines or polygons while raster forms are represented in continu-

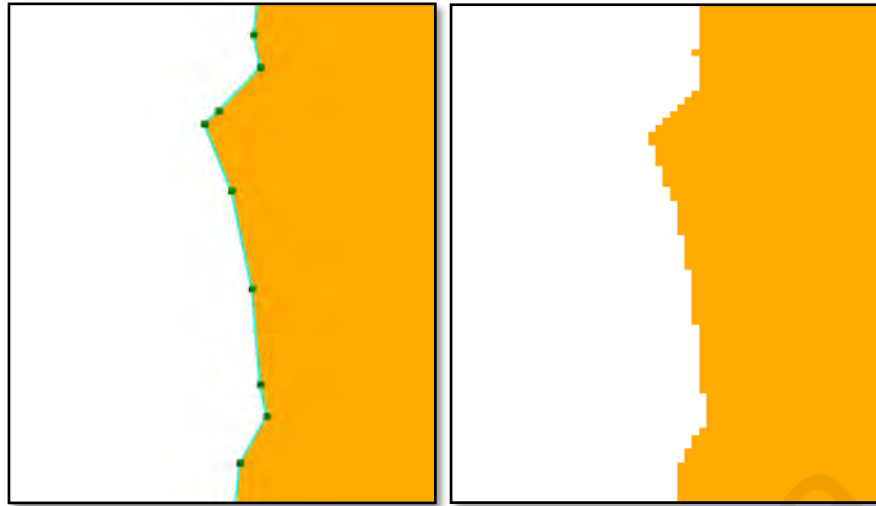


**Figure 2.1:** A vector and a raster file

ous grid cells or in pixel cells (Figure 2.1). Raster forms are highly favoured due to its' simplicity and smaller size. However, the points, lines and polygons in vector forms are infinitely thin, giving a more accurate representation of a spatial data (Goodchild, 2015).

GIS has paved the way to a seamless exchange of information, analysis and solution in a more inexpensive and time savvy manner. The various means of GIS data collection are either through Global Positioning System (GPS), remote sensing or digitizing existing hard copy maps. The utilization of GIS allows for a more accurate spatial analysis through the concept of combining layers of varying variables from a common geographic location. For example, an end user may combine layers of soil type, vegetation cover type, elevation, slope to visualize the geographic reality of an area.

## **2.5 Landslide Susceptibility Assessment**

Landslide susceptibility assessment displays the tendency of a terrain to produce slope failure and is usually expressed in forms of maps (Yalcin, 2008). It is also known as landslide hazard zonation (LHZ) in some literatures (Soeters & Van Westen, 1996; van Westen *et al.*, 2005). The term “susceptibility” and “hazard” bring different concepts, often mistakenly used and treated as synonyms. The term “susceptibility” in this study is in accordance to the United Nations Office for Disaster Risk Reduction (UNDRR), which

defines susceptibility as the spatial probability of a landslide event in which the temporal frequency of an event is not considered. Meanwhile, landslide hazard will include the spatial, temporal and the magnitude of landslide events in addition to the spatial probability (Guzzetti *et al.*, 2006).

Landslide susceptibility assessment (LSA) visualizes the spatial distribution of landslide probability classes and has become a more sought-after assessment method throughout the years. Landslide susceptibility maps represent the spatial distribution of landslide-prone areas from the correlation of factors that contribute to landslides with the historical distribution of slope failures (Brabb, 1985). This map is often useful for planners who wish to develop an area as means to reduce construction and maintenance cost. Landslide susceptibility can be assessed by different methodologies that have been developed to suit given parameters (Wu & Chen, 2009). The application of these methodologies depends on the input data, procedures, scale of study and the final output (Corominas *et al.*, 2013).

The scale of analysis of study relies on the user's objectives of study and possibilities of data collection (Soeters & Van Westen, 1996). A brief outline of the different scales of analysis and applications can be seen in Table 2.2. The selection of input data depends on the scale of analysis, characteristics of the study area, the landslide type and the failure mechanisms (Crozier & Glade, 2005). The input data can be subdivided into data that are relatively static and dynamic data that needs to be updated regularly as shown in Table 2.3. Static data sets comprise of those related to geology, soil types, geomorphology and morphography (van Westen *et al.*, 2008). Meanwhile, dynamic data comprises of those such as meteorological data, landslides, landuse and elements at risk which needs continuous update with a time frame ranging from hours to days (meteorological data and its effect on slope hydrology), to months and years (land use and population data, landslide information).

**Table 2.2:** Scale of analysis and applications after International Association of Engineering Geology (IAEG) (1976); Soeters & Van Westen (1996).

No	Category	Scale	Significance
1	National scale	< 1:1,000,000	<ul style="list-style-type: none"> <li>• Inventory-based</li> <li>• Public awareness and public support</li> </ul>
2	Regional scale	1:100,000 – 1:500,000	<ul style="list-style-type: none"> <li>• For reconnaissance phases for planning projects prior to a development.</li> </ul>
3	Medium scale	1:25,000 – 1:50,000	<ul style="list-style-type: none"> <li>• For land use planning and construction of infrastructural works, environmental impact assessment and municipal planning</li> </ul>
4	Large scale	1:5,000 – 1:15,000	<ul style="list-style-type: none"> <li>• For risk assessment and detailed planning</li> </ul>
5	Site investigation	> 1:5,000	<ul style="list-style-type: none"> <li>• Detailed risk assessment and design of slope stabilization work.</li> </ul>

**Table 2.3:** Basic input data sets for landslide susceptibility assessment and the update frequencies (after van Westen et al., 2008).

No	Data		Update Frequency (Years)
	Main Type	Data Layer	10 ..... 1..... 0.002 (day)
1	Landslide Inventory	Landslide Inventory	←————→
2	Environmental Factors	DEM	←————→
		Slope Angle/Aspects etc.	←————→
		Lithology	—→
		Structure	—→
		Faults	—→
		Soil Types	—→
		Soil Depth	—→
3	Triggering Factors	Rainfall	←

The assessment can be approached qualitatively which relies on expert knowledge or opinions (Ayalew & Yamagishi, 2005) or quantitatively which is based on numerical expressions of the relationships between controlling factors and landslides (Aleotti & Chowdhury, 1999). Alternatively, the approach to landslide susceptibility assessment

can be carried out semi-quantitatively, combining both approaches depending on the user. Generally, the proposed methods can be categorised into five main categories; i) field geomorphological mapping, (ii) analysis of landslide inventories, (iii) heuristic or index-based approaches, (iv) process-based methods, and (v) statistically-based modelling methods (Reichenbach *et al.*, 2018). The different approaches to landslide susceptibility assessment is described in detail in the next subchapters.

### **2.5.1 Qualitative Approach**

The qualitative approach relies on expert knowledge and opinions. Yalcin (2008) stated that the most common types of this approach involve simply using the landslide inventories to identify sites of similar geological and geomorphological properties that are susceptible to failure. Ayalew & Yamagishi (2005) mentioned that some approaches used a more semi-quantitative approach which is the ranking and weighting concept. An example of this approach is the use of the Analytical Hierarchy Process (AHP) (Barredo *et al.*, 2000; Saaty, 1980) and the weighted linear combination (WLC) (Ayalew *et al.*, 2004). The basis of this approach is: decomposition, comparative judgement and synthesis of priorities (Malczweski, 1999) which consequently produce subjective results depending on the knowledge of experts. Hence, qualitative or semi quantitative methods are often useful for regional studies (Guzetti *et al.*, 1999; Soeters & Van Westen, 1996).

Field geomorphological analyses involve having an earth scientist to assess and map the potential slope instability conditions directly in the field based on previous experiences in the same geological conditions. This allows a rapid assessment of stability in an area. However, in this case, the result of this method relies heavily on the ability and experience of the earth scientist and the complexity of the study area (Reichenbach *et al.*, 2005). The main limitations of this method include the difficulty of comparing landslide susceptibility maps among different experts and updating the assessment maps as new data becomes readily available.



Analyses of landslide inventories use the distribution of past and present landslides in terms of landslide density maps to estimate the future occurrences of landslides. The entirety and the quality of the landslide inventory data will determine the effectiveness of this method.

The heuristic or index-based approach involves combination of parameter maps that were selected and weighted by the experts based on the assumed or expected relative contribution to landslide occurrence. The advantages of this method are that it greatly reduces the problem of hidden rules, enables automation of maps in the GIS and the standardization of data management techniques from acquisition to final analysis can be easily done (Aleotti & Chowdhury, 1999). The limitations of the heuristic method include the subjectivity of the different parameter, the lengthy operations of the methods especially in large areas and the difficulty of model extrapolation between a specific area with other sites or zones (Carrara, 1983).

The physical-based methods rely upon simplified, physically-based landslide modelling schemes to analyse the stability/instability conditions using simple limit equilibrium models, such as the “infinite slope stability” model or other more complex approaches (Montgomery & Dietrich, 1994).

### **2.5.2 Quantitative Approach**

The quantitative approach is based on numerical expressions of the relationship between controlling factors and landslides. This approach can be classified into statistical analysis, geotechnical engineering approaches and neural network analysis (Aleotti & Chowdhury, 1999).

A statistical method involves the analysis of the historical links between known or inferred landslide-controlling factors and the past and present distribution of landslides by comparing each individual factor map with the landslide distribution map (Guzetti *et*

*al.*, 1999). This method can be divided into a multivariate statistical method and a bivariate statistical method.

The usage of multivariate statistical method involves the analysis of all the landslide-causing parameters with multiple regression techniques which then correlates the landslide distribution map and the parameters to determine the stable and unstable areas through discriminant analysis (van Westen *et al.*, 1997). This method is data-driven and highly objective with the requisition of only using small first-order catchments and morphological terrain units which can be differentiated automatically by using a detailed terrain model. The use of natural units produced from the detailed terrain model are more favourable compared to grid cells due to homogeneity.

The bivariate statistical method can be differentiated from the multivariate statistical method by the assignation of new values to the terrain units or grid cells. These new values represent the degree of probability, certainty, belief or plausibility the terrain units or grid cells may have or subject to landslide occurrences (van Westen *et al.*, 1997). This semi-quantitative method combines the subjective professionally handled direct mapping and the objective data-driven analysis capabilities of a GIS which enables the introduction of expert opinion into the process. The determination of parameters or parameter combinations used in the assessment is determined by the professional who executes the analysis.

The limitations of any statistical methods include the assumption of conditional independence which can be avoided with the evaluation of the data and combining the dependence parameters maps into a new map independent with the rest with respect to the probability for the occurrence of landslides (van Westen *et al.*, 1997). Another limitation would be the accuracy of the prediction of the resulting landslide susceptibility maps which can be prevented by comparing it with the existing landslides in the area. Multitemporal landslide maps can be used by the user to avoid circular reasoning which

means the models should be constructed using a landslide map of a previous period preferably a decade ago and the resulting map should be verified by present landslides. Lastly, the biggest challenge of a statistical approach is to gather data of a large area economically. Naranjo *et al.* (1994) evaluated the use of training areas and prediction (target) areas in a bivariate statistical analysis which involved a delineation of a small area within the overall study area that represents the variability of the whole area. The established decision rules are then extrapolated over the whole study area after detailed analysis of the landslide occurrences in relation with terrain conditions in the training area with careful confrontation of the hazard prediction with the “real world” and adaptation of decision rules. Nevertheless, the prediction of landslides in terms of the real world and the adaptation of the decision rules should be carefully considered (van Westen *et al.*, 1997).

The deterministic method involves the engineering principles of slope instability expressed in terms of Factor of Safety (FOS). It is suitable for calculating the stability of homogenous and non-homogenous individual slopes (Aleotti & Chowdhury, 1999). This can also be used to run scenarios with the effect of slope modifications (van Westen *et al.*, 1997). Exhaustive sets of data from individual slopes are utilized such as shear strength data and pore water pressure, making it effective for mapping site-specific areas (Guzetti *et al.*, 1999). Safety factors can be used significantly by engineers, consulting firms or local planning agencies for the detailed planning of infrastructural work or mitigation. The emergence of Geographic Information System (GIS) have led to the extensive application of slope stability models in landslide assessment and mapping in larger areas as opposed to only site-specific areas. The first deterministic approach application in GIS was done by van Westen & Terlien (1996) for Manizales, Colombia by using a one-dimensional deterministic slope stability model (infinite slope model) to calculate the average safety factors and failure probabilities and later used a two-

dimensional hydrological model to estimate groundwater level conditions in relation to rainfall events. This approach was also applied in Kota Kinabalu, Sabah, Malaysia by Roslee *et al.* (2017) based on two-dimensional slope stability (infinite slope model) (DESSISM). Armas, *et al.* (2013) used a one-dimension infinite slope stability model and later combined it with a raster-based GIS (ILWIS) to create landslide susceptibility maps for Breaza town, Romania.

The limitations of a deterministic approach include the high degree of uncertainty of the input data, resulting in calculated values that cannot be taken as absolute values of landslide occurrence. Considerable parametrization is also needed as some parameters may be difficult to measure, such as estimated soil depth (van Westen, 2004). In cases where the development of complex landslides with a complex hydrological system is concerned, a deterministic approach may also not be suitable (Van Asch *et al.*, 1999). Another challenge to producing a susceptibility map using the deterministic approach at a larger scale is the amount of time to collect data, especially when heterogeneous variables are considered. Hence, this approach may be relatively more applicable for homogeneous areas at a large scale (1 : 10 000) (van Westen & Terlien, 1996).

## CHAPTER 3 : METHODOLOGY

### 3.1 Introduction

This chapter will elaborate on the methodologies used throughout the process of data collection and analysis. The outlined subchapters include base map and landslide inventory, field verification, preparation of data and landslide susceptibility assessment. The limitations will also be discussed at the end of this chapter.

### 3.2 Base Map and Landslide Inventory

In order to produce a landslide susceptibility map, several landslide influencing or conditioning parameters are imperative for analysis along with landslide inventory. A collection and review of data from previous studies from articles, journals, books, geological bulletins and unpublished materials were used to facilitate this process. The selection of landslide parameters depended on the analyses of literatures and data availability. A spatial database is also needed to be constructed to extract relevant factors attributing to landslide occurrences.

The digitization of the base map of Canada Hill utilized remote sensing data comprised of Shuttle Radar Topography Mission (SRTM) data, Light Detection and Ranging (LiDAR) data and satellite imageries. SRTM was obtained freely through a public domain run by United States Geological Survey (USGS) (<https://earthexplorer.usgs.gov/>) while the contour map of 1m spacing produced from LiDAR data was obtained from the Department on Minerals and Geoscience Malaysia. The obtained remote sensing data was used to generate the Digital Elevation Model (DEM) also known as a shaded relief map with a 1m contour spacing which was later combined with high resolution satellite imageries from Google Earth to aid in the base map digitization and early identification of spatial locations of past landslides. The digitization was also supported by referring to the geological map by Wannier *et al.* (2011) and existing 1:50 000 scale topographical

map obtained from the Survey and Mapping Department. The base map that were produced prior to fieldwork is shown in Table 3.1. Despite having different formats during the pre-processing time of the maps, a conversion into GeoTIFF format was necessary in order to be used in the “Avenza Maps” application explained in the further subchapter.

The landslide inventory was prepared through interpretation of aerial photographs, satellite imageries, DEM and referring to records from existing reports and literature. This step is necessary to obtain an overview of the type and subtype of landslides as well as the degree of activity or size. Malaysia’s tropic climate promotes erosion and overgrowth of vegetation which can easily wipe out the evidence of slope movements in a few years. This highlights the importance of sequential aerial photograph coverages (van Westen *et al.*, 1997). Imageries from different years ranging from 5 to 7 years difference were interpreted and compared to obtain the best sense of slope movement, possible influence changes of land use and other human activities on the stability of the slopes to be recorded in the landslide inventory.

**Table 3.1:** Data generated for field verification.

No	Data Attribute	Source
1	Slope	DEM – JMG
2	Relief	DEM – JMG
3	Geology	DEM, Topographical Map, Book Review
4	Engineering Geology	Geology Map, Soil Map, Field Observation (Cut and Fill), Book Review
5	Landslide	DEM, Google Earth Satellite Imageries, JMG Reports (1: 5000)
6	Soil Map	Book Review

### 3.3 Field Verification

The relevant prepared base maps were transferred and accessed through an iOS application called “Avenza Maps” prior to fieldwork. This application uses real- time

GPS while accessing the maps offline for verification and updating purposes in the field. Additional data, readings or observations of the present landforms were marked and recorded in the maps through the application. Field mapping, facies identification and sample collections were also done in the field.

### 3.3.1 Avenza Maps

Avenza Maps (Figure 3.1) is one of the many applications in the market used for the purposes of offline map viewing. This application can be used in any supported mobile or tablet devices and was used in this research to carry out field verification. Additional information that were not captured through remote sensing data were updated in the map to be further updated in GIS after fieldwork.

Pre-processed maps can be loaded into the application as a geospatial PDF, GeoPDF or GeoTIFF. Although taking up more disk space, GeoTIFF was the preferred file format to be used in this research due to a faster import duration making the transfer of maps more seamless while maintaining the map resolution. GeoTIFF is a TIFF (Tagged Image File Format) with spatial information embedded into the file (Avenza Systems Incorporated, 2017).

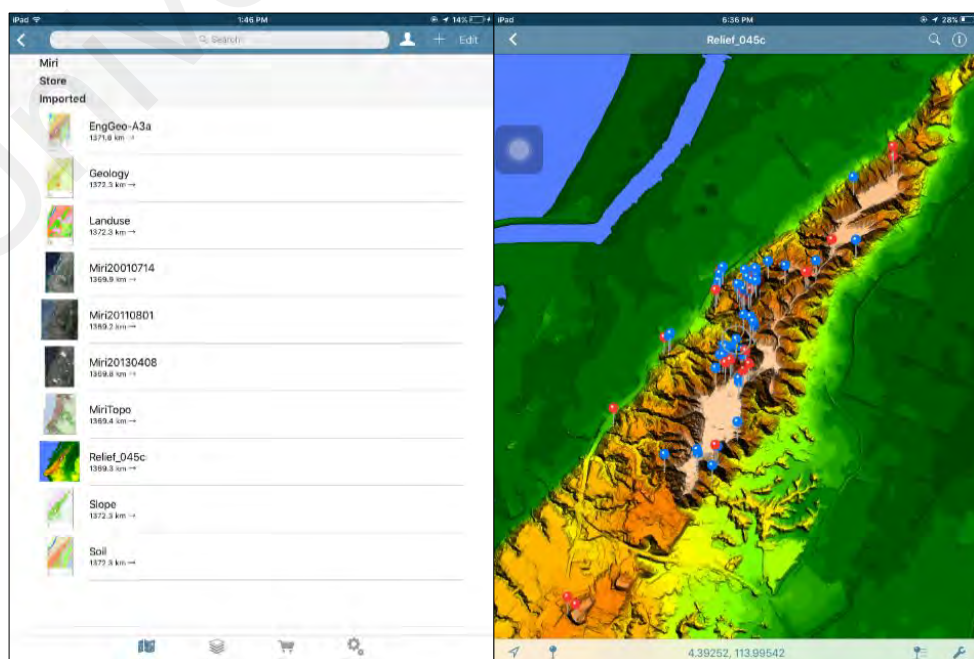


**Figure 3.1:** The interface of Avenza Maps application.

### **3.3.2 Field Verification and Sampling**

Outcrops with exposed rocks and soils were examined to obtain records of rock types and their bedding orientation. This was updated in the geological base map. The observed minor and major landslides were marked and described and additional features analogous to potential lineaments were matched in the map. The landslide inventory was utilized in this verification. The slope gradient map was also verified in the field. 9 representative samples of soil, sandstone, shale and salt encrustation samples were taken from landslide areas and outcrops for further laboratory tests which will be further explained the next chapter.

Subsequently after fieldwork, the additional information in the updated base maps during field verification were transferred into GIS to be enhanced for further analysis which will be further explained the next subchapter.

### **3.4 Preparation of Data**

The landslide parameter maps were processed using ArcGIS 10.5, a popular commercial Geographic Information System (GIS) software developed by ESRI to aid geospatial data-related processes. GIS was used in this study as a database to store spatial data of the study area to be processed and compiled as the subsequent landslide susceptibility map.

The various spatial data or landslide parameter maps are stored as vector files or raster files. Vector files can be produced through the digitization of a map and raster files are image files containing grids or pixels. The conversion from vector files (shapefiles) to raster files can be done through the Conversion Tools in ArcGIS. Shapefiles are more visually accurate while mathematical and overlay operations are easier to perform in raster files. The process of generating the final landslide susceptibility map will require only raster files and therefore, prompting conversion of all the map layers into raster files.



A map with cell size of 1m by 1m is also ensured to maintain the scale of the resulting map.

The geological map was produced through digitization based on the interpretation of the DEM and a 1:50 000 topographical map, as well as information from the geological map in Wannier *et al.* (2011). Subsequently, the distance of lineament can be produced from the lineament data in the geological map by using the Analysis tools in ArcGIS. The slope gradient, elevation and slope curvature map were derived from the DEM and was produced using the Spatial Analyst extension in ArcGIS. The NDVI map was derived from the LANDSAT 8 imagery and the cut and fill map was prepared based on observations in the field. The planar failure susceptibility map is a combination of the slope aspect map, dip and dip direction map. The slope aspect map was derived from the DEM while the dip and dip direction map were produced by the interpolation of points containing bedding orientation using circular statistics.

### **3.5 Landslide Susceptibility Assessment**

The past few decades have seen the increase in significance of landslide susceptibility assessments, ascribed to the need for landslide disaster risk reduction in developed areas. Prior to carrying out landslide susceptibility assessments, a few assumptions should be highlighted. The first among these assumptions or principles is that slope failures leave recognizable morphological features which can be identified and mapped through field observations or remote sensing (Dikau *et al.*, 1996; Hansen, 1984; Hutchinson, 1988; Rib & Liang, 1978; Varnes, 1978). The second assumption is the past is a guide to the future, as adapted from the uniformitarianism principle, indicating that slope failures will likely occur under the same conditions that led to instabilities in the past and present (Guzetti *et al.*, 1999; Varnes, 1984). However, the absence of the landslide-causing conditions does not necessarily imply that landslides will not occur which leads to the third assumption.

The identification, understanding and collection of the conditioning factors directly or indirectly linked to landslide occurrence is imperative to be able to build predictive models (Dietrich *et al.*, 1995). The basic conditioning factors of a landslide occurrence can be recognized to be rated or weighed and some can be mapped and correlated with each other and past failures (Varnes, 1984). The fourth assumption is the degree of potential hazard can be summarized by zoning a territory into different susceptibility classes, based on the number of landslide-conditioning factors, their severity and relationship. These conditioning factors can often be estimated of their relative contributions to landslide occurrences and analysed qualitatively, statistically or through physical models (Guzetti *et al.*, 1999; Varnes, 1984). It is noteworthy that these assumptions are the essence of minimizing the limit of the relevance of any landslide susceptibility assessments, regardless of the imposed methodologies or approach. However, some exception must be taken into consideration such as when the source of landslide is consumed by earlier landslide occurrences (Fell *et al.*, 2008).

Several methods and techniques to evaluate landslide susceptibility have been proposed and tested. The methods can generally be divided into qualitative or quantitative and direct or indirect. The indexing (heuristic) approach and bivariate statistical approach to landslide susceptibility assessment were employed in this study and will be described in the following subchapter.

### **3.5.1 Heuristic Approach**

The heuristic or index-based approach involves the combination of parameter maps that were selected and weighted by the experts based on the assumed or expected relative contribution to landslide occurrence. The advantages of this method are that it greatly reduces the problem of hidden rules, enables automation of maps in the GIS and the standardization of data management techniques from acquisition to final analysis can be easily done (Aleotti & Chowdhury, 1999). The limitations of the heuristic method

include the subjectivity of the different parameter, the lengthy operations of the methods especially in large areas and the difficulty of model extrapolation between a specific area with other sites or zones (Carrara, 1983).

The heuristic approach incorporates a direct or semi-direct mapping method by comparing the occurrences directly to the causative factors. It is suitable for small-scale regional surveys ranging from 1:100 000 to 1:250 000. The workflow using this approach is shown in the Figure 3.2. The parameters to be analysed using this approach are slope direction; geology; elevation; slope curvature; planar failure susceptibility; and distance to lineament. This method was approached by translating a heuristic estimation (very low, low, medium, high, very high) into numerical digits.

The weightages of parameters were obtained through a two-step iterative method. These parameters were evaluated in the field at all places where landslides are encountered prior to making preliminary conclusions on the causative factors. Detailed analysis on the different landslide parameters is described in the next chapter. These

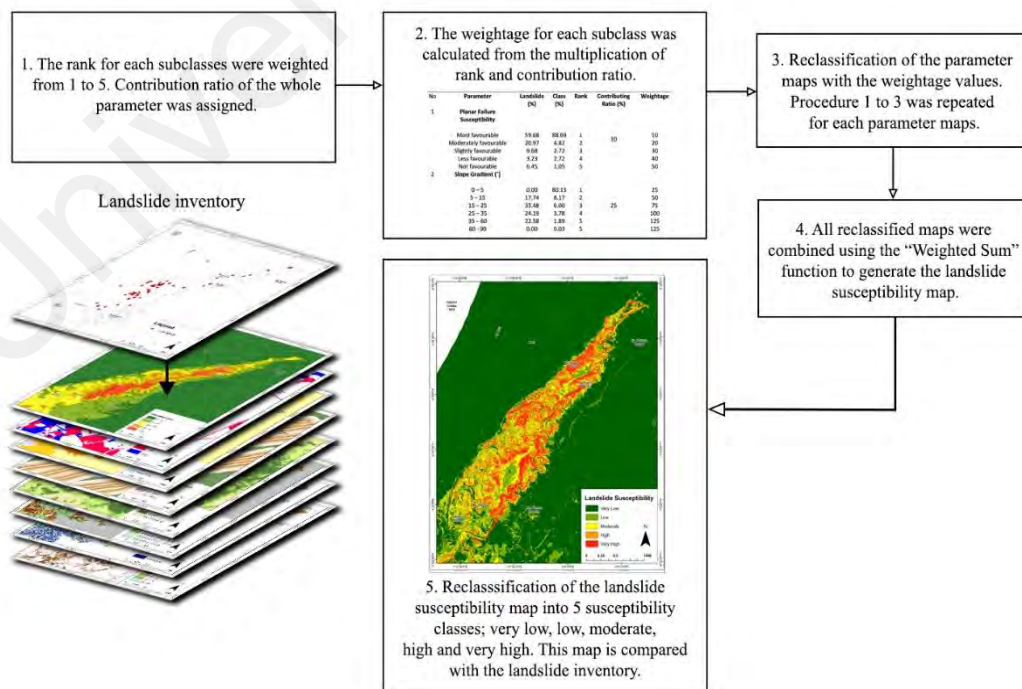


**Figure 3.2:** Workflow for the landslide susceptibility assessment using a heuristic approach.

parameters are then analysed individually through the comparison with landslide occurrences to obtain the rank of the subclasses, which were ranked from 1 to 5 to denote areas with very low to very high susceptibility.

The second step was the assignation of the contributing ratio (%) of the parameter layers through expert opinion and comparison of the respective results to landslide inventory. The sum of the contributing ratio (%) would add up to a 100%. The acquisition of the rank and contributing ratio (%) now enables the calculation for weightage (Table 3.2) and landslide susceptibility of each cell of the study area in ArcGIS by applying the Eq 3.1 and 3.2.

$$\text{Weightage} = \text{Rank} \times \text{Contributing Ratio} \quad (3.1)$$

$$\text{Landslide Susceptibility} = W_{Sl} + W_{Geo} + W_{Dl} + W_{El} + W_{Cf} + W_{Cu} + W_S + W_N \quad (3.2)$$

Above is the equation for landslide susceptibility where  $W_{Sl}$  is the weight of slope gradient,  $W_{Geo}$  is the weight of geology,  $W_{Dl}$  is the weight of distance to lineament,  $W_{El}$

**Table 3.2:** Application of Equation 3.1 for the calculation of the weightage of the parameter maps.

No	Parameter	Rank	Contributing Ratio (%)	Weightage
1	<b>Slope Gradient (°)</b>			
	0 – 5	1	25	25
	5 – 15	2		50
	15 – 25	3		75
	25 – 35	4		100
	35 – 60	5		125
	60 - 90	5		125
2	<b>Elevation (m)</b>			
	0 – 5	1	10	10
	5 – 25	2		20
	25 – 50	3		30
	50 – 75	4		40
	> 75	5		50
3	<b>Planar Failure Susceptibility</b>			
	Most favorable	1	25	25
	Moderately favorable	2		50
	Slightly favorable	3		75
	Less favorable	4		100
	Not favorable	5		125

is the weight of elevation,  $W_{Cf}$  is the weight of cut and fill,  $W_{Cu}$  is the weight of slope curvature,  $W_S$  is the weight of stability in relation to planar failure susceptibility and  $W_N$  is the weight of normalized difference vegetation index (NDVI).

### 3.5.2 Bivariate Statistical Approach

The prior identification of the landslide parameters for the purpose of the bivariate statistical analysis were also done based on the decision of a professional expert and literature reviews, akin to the heuristic approach. However, the chosen parameters to be analysed using this approach slightly differs which are slope direction, slope aspect, geology, elevation, slope curvature, distance to lineament, cut and fill, and normalized difference vegetation index (NDVI). The workflow of using this approach is shown in Figure 3.3.

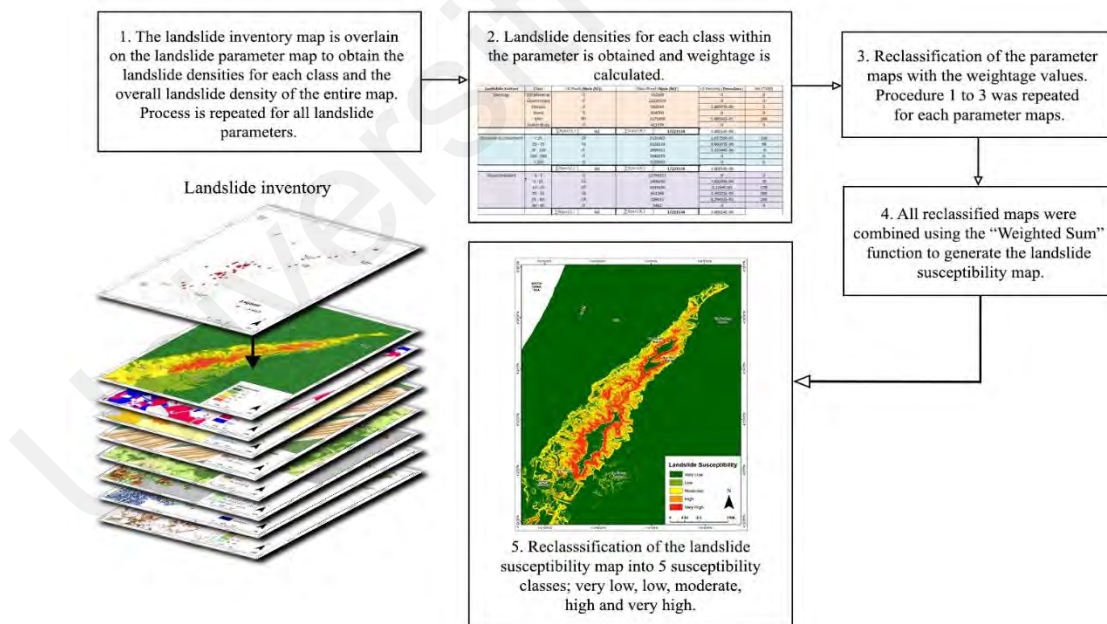


**Figure 3.3:** Workflow of the landslide susceptibility assessment using a bivariate statistics approach.

The importance of each landslide-controlling parameters is analysed individually by comparing the map of the parameter with the landslide distribution map. Landslide

densities were calculated for each parameter maps to obtain the weightage of a certain parameter. In other words, landslide densities are equivalent to the number of landslides over the area occupied by the parameter.

$$W_i = \ln\left(\frac{Densclass}{Densmap}\right) = \ln\left(\frac{\frac{Npix(S_i)}{Npix(N_i)}}{\frac{\sum Npix(S_i)}{\sum Npix(N_i)}}\right) \quad (3.3)$$

Equation 3.3, proposed by van Westen (1993) was utilized in the bivariate statistical analysis where  $W_i$  is the weight given to a certain parameter class (e.g. a rock type, or a slope class), *Densclass* is the landslide density within the parameter class, *Densmap* is the landslide density within the entire map,  $Npix(S_i)$  is the number of pixels, which contain landslides, in certain parameter classes and  $Npix(N_i)$  is the total number of pixels in a certain parameter class.

Negative weights will be obtained if the landslide density is lower than normal, positive weights will be obtained if the landslide density is higher than normal and a zero weight will be obtained if there are no landslide occurrences in a certain parameter class (van Westen, 1997).

This analysis utilizes the pixel cells in a map and therefore, raster maps were used. Maps that were initially in a shapefile format would need to be converted into a raster format using the Conversion tools in ArcGIS which are then analysed using the Zonal Statistics tool to obtain the number of pixels for landslide densities of individual parameters. For example, polygon shapefiles would need to be transformed using the “Polygon to Raster” function in the Spatial Analyst toolset. The number of pixels were then used to apply Equation 3.3 in a Microsoft Excel spreadsheet. An example of the calculation of the weightage for geology, distance to lineament and slope gradient is shown in

. Integer values are required for a simpler further analysis in GIS. Hence, the calculated weightage value was normalized by multiplying it by 100. The seven landslide parameter maps are then reclassified with the obtained weight values for each parameter class, using the Spatial Analyst extension in GIS.

Parameter	Class	LS Pixel ( <i>Npix</i> ( <i>S<sub>i</sub></i> ))		Class Pixel ( <i>Npix</i> ( <i>N<sub>i</sub></i> ))		Densclass	Wi (*100)
Geology	Fill Material	0		142589		0	0
	Quaternary	0		12528329		0	0
	Terrace	2		542039		3.6898E-06	2
	Seria	0		424700		0	0
	Miri	60		3171898		1.8916E-05	166
	Water Body	0		411979		0	0
		$\sum Npix(S_i)$	62	$\sum Npix(N_i)$	2E+07	3.6001E-06	
Distance to Lineament	< 25	22		2120302		1.0376E-05	106
	25 - 75	31		3228133		9.6031E-06	98
	75 - 150	9		2699911		3.3334E-06	-8
	150 - 250	0		1944255		0	0
	> 250	0		7228933		0	0
		$\sum Npix(S_i)$	62	$\sum Npix(N_i)$	2E+07	3.6001E-06	
Slope Gradient	0 - 5	0		13799323		0	0
	5 - 15	11		1406292		7.822E-06	78
	15 - 25	22		1033156		2.1294E-05	178
	25 - 35	15		651266		2.3032E-05	186
	35 - 60	14		326035		4.294E-05	248
	60 - 90	0		5462		0	0
		$\sum Npix(S_i)$	62	$\sum Npix(N_i)$	2E+07	3.6001E-06	

**Table 3.3:** Application of Equation 3.3 for the calculation of the weightage of parameter maps.

The final landslide susceptibility map (LSM) is a result of the addition of the reclassified parameter maps as shown in Eq 3.4 where  $W_i Sl$  is the weight of slope gradient,  $W_i Asp$  is the weight of slope aspect,  $W_i Geo$  is the weight of geology,  $W_i El$  is the weight of elevation,  $W_i Cu$  is the weight of slope curvature,  $W_i Dl$  is the weight of distance to lineament,  $W_i Cf$  is weight of cut and fill and  $W_i N$  is the weight of normalized difference vegetation index (NDVI).

$$LSM = W_i Sl + W_i Asp + W_i Geo + W_i El + W_i Cu + W_i Dl + W_i Cf + W_i N \quad (3.4)$$

The LSM will yield a continuous value and should be normalized, if necessary, for subsequent reclassification into five classes to denote areas of very low, low, moderate, high and very high susceptibility to landslide occurrences.

### 3.5.3 Classification of the Landslide Susceptibility Classes

The resulting landslide susceptibility map generated from the combination of the landslide parameter maps is made up of a continuous value. Therefore, the values will need to be classified according to the different susceptibility descriptors. The susceptibility classes will need to correspond to the proportion of the area being susceptible to landslides and the classification used in this study was adapted from Fell *et al.* (2008). The different susceptibility classes are described in Table 3.4

**Table 3.4:** Landslide susceptibility classifications.

Level	Landslide Susceptibility	Description
1	Very Low	Slope failure is very unlikely to occur in the area but consideration to potential problems of the adjacent areas must be considered.
2	Low	Slope failure problems are not likely to happen but consideration to potential problems of the adjacent areas must be considered.
3	Moderate	Slope failure problems of small to moderate scale may exist or possible to happen after major changes in ground conditions and triggering factors are present.
4	High	Slope failure in moderate to large scale probably exist in the past and could reoccur if the combination of contributing factors exists in the adverse event of an intense or continuous rainfall period.
5	Very High	Slope failure in moderate to large scale have occurred in the past and may be active if the combination of contributing factors exists in the adverse event of an intense or continuous rainfall period.

### 3.5.4 Success Rate Calculation of the Landslide Susceptibility Map

The subsequent landslide susceptibility maps produced from the two approaches were compared and validated to determine the success rates or also known as the sensitivity of these models. A validation curve, or also known as receiver operating characteristic



(ROC) curve was plotted using the obtained cumulative percentage of landslide occurrences (y-axis) and the percentage of landslide susceptibility classes (x-axis). A totally random prediction would yield a hypothetical validation “curve” coinciding with a diagonal from 0 to 1 and the position of the validation curve resulting from the landslide data of a study area relative to the hypothetical “curve” would determine the model’s predictive value and capability (Remondo *et al.*, 2003). The quantitative assessment of the success rates were possible by calculating the area under the ROC curve (AUC) (Sameen *et al.*, 2019) which can be easily analysed in Microsoft Excel.

### **3.6 Limitation**

Landslide studies require an exhaustive ground data for an in-depth comprehension of the ground conditions. The analysis of the potential landslide parameters and the validation of the predictive power of the landslide susceptibility maps would benefit from these data. One of the limitations faced in this study was the lack of data such as rainfall data and a detailed landslide inventory. The four current rainfall stations are in concordance to the shoreline, which data points prove difficult for interpolation into a rainfall map. Recent landslide data from the interpretation of satellite imageries, DEM and field verification was used for the analysis. However, unreported past landslides lack additional data such as date of occurrence. The obtained landslide data in Canada Hill are also mostly clustered in the centre of the hill where it was relatively more accessible and has less developments. Insufficient landslide data for this study did not allow for data partitioning as mentioned in Chung & Fabbri (2003) for the further validation of the landslide susceptibility map. Comparison of the generated landslide susceptibility map with an area with similar geology and geomorphology would be an encounter to the previous method but was also not possible due to unavailable published literatures.

The bivariate statistical approach utilizes logarithmic normalization in weightage calculation for parameters. The overlapping of landslide inventory over the landslide

parameter maps returned a “no pixel data” or 0  $N_{pix}(Si)$  value for certain subclasses due to no landslide occurrences in the certain subclass. This problem led to errors in calculation for certain subclasses’ weightages as the calculation involving a 0  $N_{pix}(Si)$  value would approach infinitesimal. Therefore, an initiative to quantitatively assign a relatively lower value as the weightage was done although this would not exactly show the information value of the area (Oliveira *et al.*, 2015). Future works to improve the weightage calculation for the Canada Hill area would be applying the Modified Information Value Method (MIVF) adapted from Mandal & Mondal (2019).

Limitations were also faced in the field such as weathered, excavated outcrops for development purposes and subsequent deposition. Hence, fieldwork was done at any adjacent areas with available outcrops and any data gaps were filled with references from previous literatures. There was also an issue of inaccessibility to private lands in addition to difficult interpretation of satellite imageries caused by heavy vegetation growth.

## CHAPTER 4 : ENGINEERING GEOLOGY

### 4.1 Introduction

This chapter will describe the findings for the geology of Canada Hill while giving highlights to the engineering geology and the implications. The outline subchapters include; Miri Formation and Seria Formation, superficial deposits, artificial deposits and geological structures.

### 4.2 Miri Formation and Seria Formation

The main components of Canada Hill are the Miri Formation and Seria Formation, with a respective age of Mid-Miocene and Late Miocene. Miri Formation is comprised of sandstones with alternation of shales, carbonaceous shales, siltstones and clayey shales. The sandstones in the Miri Formation are generally medium-grained to fine-grained sandstones with subangular to well-rounded grains as shown in Figure 4.1, and is mainly made up of quartz, chert, rock fragments, feldspars, mica, iron oxide, clay matrix and a small amount of siltstone clasts and fragments of molluscs. Liechti *et al.* (1960) mentioned that the formation can be further divided into the Upper Miri Formation and the Lower Miri Formation. He also mentioned that the Seria Formation overlies the Miri Formation. Some authors have mapped the Seria Formation as Liang formation but the terminology by Wannier *et al.* (2011) to classify the Seria Formation is used in this study.

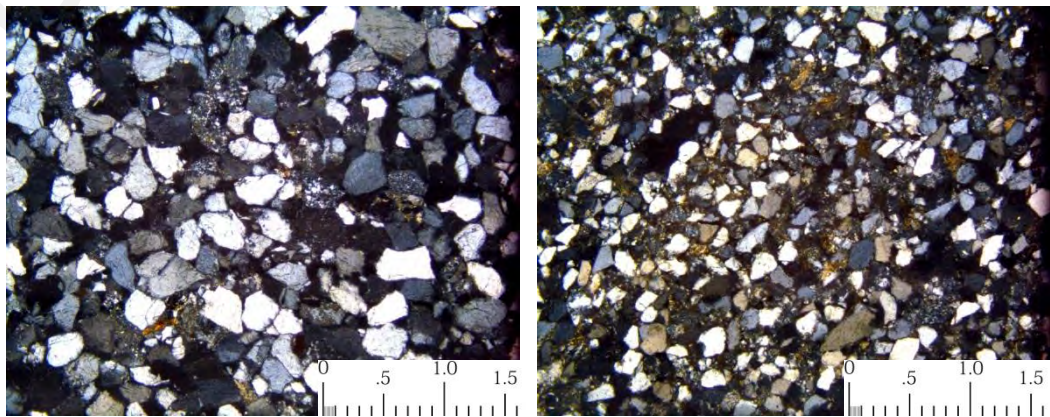


**Figure 4.1:** a) Medium-grained sandstone from the Miri Formation, b) Fine-grained sandstone from the Miri Formation.

The Seria Formation consists of relatively poor sediment sorting of a general composition of sandy shale or laminated thin sandstone and shale with a presence of lignite. The Miri and Seria Formation are mostly similar stratigraphically, mainly comprised of interbedded sandstone and shale.

Various sedimentary structures present in both the formations include flaser beddings, hummocky stratifications, bioturbations, lamination and soft sediment deformations. The sedimentary beds are mostly bioturbated with trace fossils namely *Ophiomorpha nodosa*, *Ophiomorpha labuanensis*, *Teichichnus* and *Gyrolithes* (Wannier *et al.*, 2011), indicating a shallow marine environment (Figure 4.2). Miri Formation was deposited in a littoral to inner neritic shallow marine environment and the environment stayed uniformly marine throughout the deposition. The fluvial environment was characterized by braided-streams and meander-belt system of upper deltaic plain while the marine environment consists of a delta fringe. The transitions between these two environments were; a deltaic environment comprised of mangrove swamps, floodplain basin and marsh; and a coastal environment which comprised of beaches, barrier bars and lagoons (Dundang, 1983). Six lithofacies were identified in the Miri Formation based on the classification by Abieda *et al.* (2005) as shown in Figure 4.3 and described in Table 4.1. The environment of deposition for Seria Formation was relatively less marine and deposited at a shallower



**Figure 4.2:** *Ophiomorpha* trace fossils in the Miri Formation.





**Figure 4.3:** (clockwise from top left) Facies B, E, I, L, K, J.

sea level as indicated by the reworking of the strata and the alternation of bands rich in marine micro faunas with less fossiliferous strata (Liechti *et al.*, 1960).

**Table 4.1:** Lithofacies of Miri FM and description of depositional environment after Abieda *et al.* (2005).

No	Facies	Depositional process	Depositional environment
1	B: Parallel stratified sandstone with mud drapes	<ul style="list-style-type: none"> <li>Tidal currents</li> </ul>	Upper flow sand flat, occupies the head portion of an estuarine channel
2	E: Lenticular bedding	<ul style="list-style-type: none"> <li>Dominant periods of quiescence</li> <li>Fine sediments settle down with periodic current activities depositing sand</li> </ul>	Mud tidal flat, fringing the estuary margin
3	I: Fine grained bioturbated sandstone	<ul style="list-style-type: none"> <li>Low intensive and frequent storm action</li> <li>High organisms' activity</li> </ul>	Lower shoreface
4	J: Interbedded to bioturbated siltstone and fine sandstone	<ul style="list-style-type: none"> <li>Waning storm action</li> <li>Fair-weather condition</li> </ul>	Distal lower shoreface

**Table 4.1, continued.**

5	K: Bioturbated siltstone	<ul style="list-style-type: none"><li>• Low energy environment</li><li>• Fallout of silt particles with intense animal activities</li></ul>	Upper offshore transition
6	L: Fine grained parallel stratified and hummocky cross-stratified sandstone and mudstone inter-bedding	<ul style="list-style-type: none"><li>• Alternative fair-weather conditions</li><li>• Combined or pure oscillatory flows</li></ul>	Offshore transition

#### **4.2.1 Bedrock Characteristics**

The vicinity of Canada Hill is entirely overlain with sedimentary rocks comprising of sandstone interbedded with shale. The strengths of the bedrock in Miri and Seria formations are not homogenous, though exhibiting an almost similar geology, due to the presence of lithofacies, varying grain sizes, consolidation, minerals and structures.

The beds on the flanks on both sides of Canada Hill are gently-dipping. The dip of the bedding ranges from  $4^{\circ}$  -  $83^{\circ}$  with an average of  $27^{\circ}$  towards NW trending towards NNE-NE, with an exception to the Northwest flank which dips toward the direction of N to NNW. Subvertical beds are present due to drag folding by thrust faults, localized at the Hospital area and the Lopeng area adjacent to the faults (Figure 4.4).

Faults, joints and lineaments are also distinct characteristics of this hill. Previous reports by the Shell/Royal Dutch Group in 1960 revealed 4 major faults within this area



**Figure 4.4:** a) Gentle-dipping beds of Miri Formation, b) Subvertical beds of Miri Formation (Lopeng area).

through the interpretation from rock cores, seismic sections and well logs. The Shell Hill Fault is a normal fault while Canada Hill Thrust, Inner and Outer Kawang Thrusts are thrust faults (Wannier *et al.*, 2011). These major faults are not visible in the outcrop during this present day. However, several faulting features have been observed in the field. Small reverse faults may make up to what might be splays related to the Canada Hill Thrust. Continuous clay smear features were observed on the faults (van der Zee & Urai, 2005) and are most prominent along the relatively ductile shale layers (Figure 4.5).



**Figure 4.5:** Small reverse fault with the appearance of clay smears.

Joints are commonly seen cutting the sandstones with trending E-W, NW-SE and NS with varying distance of spacing. The joints observed in the study area have an average strike of  $054^{\circ}$  and are steeply dipping. Lineaments can be seen trending perpendicular to the NW-SE trending major faults, cutting across the hill. There are three sets of lineaments trending NW-SE, NE-SW and E-W with the NW-SE trending set being most prominent. The NE-SW lineaments may also be related to the major faults.

The shale layers in the formation are relatively weaker and more prone to weathering and erosion which causes stair-stepping erosion within the interbedded layers. Some shale layers show bifurcation to many layers along a few centimetres which then merge again (Dundang, 1983) producing lenticular sandstone or shale. Based on the shale plasticity index by Muol (2009) (Table 4.2) and the classification by Waltham (1994) (Figure 4.6),



the shale in the Canada Hill can be classified as clay of medium plasticity (CL), which is an indicative of the shale behaviour to change from plastic to liquid with a small addition of water.

**Table 4.2:** Atterberg Limit test results for shale, after Muol (2009).

Sample Label	Lab Reference No.	Liquid Limit (LL)	Plastic Limit (PL)	Plasticity Index (PI)
LSD MY 1	2009 003 001	34	19	15
LSD MY 2	2009 003 002	38	20	18
AU 2	2009 003 003	39	22	17
AU 3	2009 003 004	39	23	16

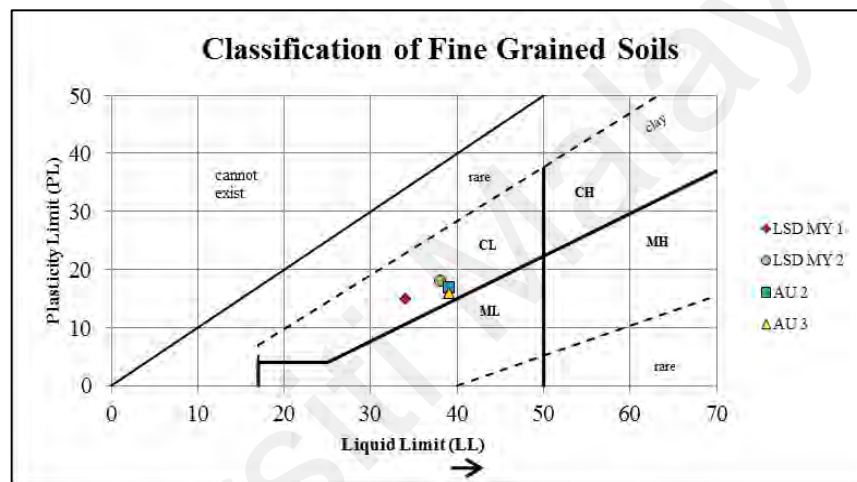


**Figure 4.6:** Four shale samples based on Muol (2009) located within the Clay region (CL) using the classification by Waltham (1994).

Moderately sloping ground condition is an essential attribute of the Miri and Seria Formation. Miri formation stands at a higher elevation, has steeper and more incised terrains and sharp ridges while Seria Formation is characterized as a more low-lying with a relatively gentle sloping feature (Figure 4.7). Construction activities especially along sharper ridges or narrow valleys at the Miri Formation is not advisable as significant cut and fill will be needed, which may lead to stability issues on high cut slopes and embankments.



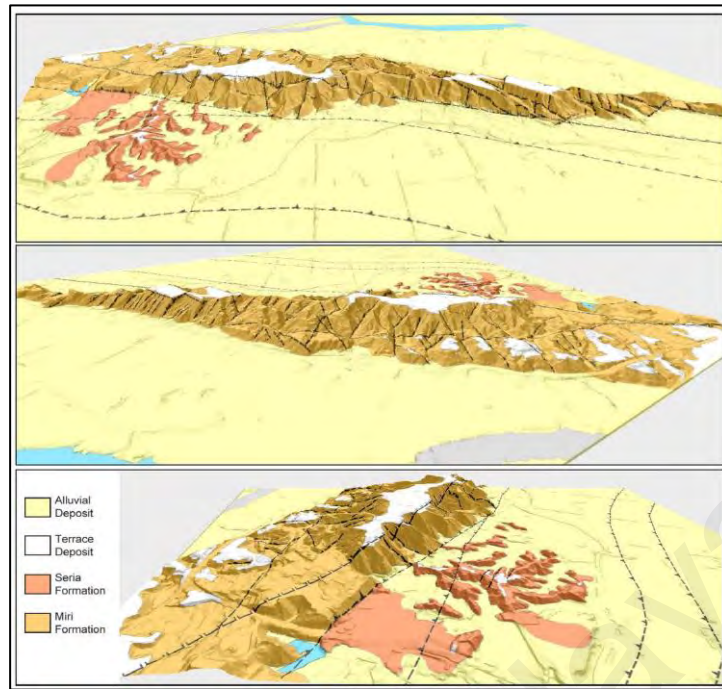


**Figure 4.7:** 3D view of Canada Hill.

#### 4.2.2 Weathering

The data used in this study revealed that Miri receives a high annual rainfall average of 4325.5mm and a mean monthly rainfall of up to 825.75mm. The highest amount of rainfall happens essentially during the Northeast Monsoon period. This has led to the extensive weathering in the formations due to the intense rainfall coupled with high humidity on top of attributing relatively young sedimentary rocks. Based on established weathering grade systems (Geotechnical Control Office (GCO), 2017; International Association of Engineering Geology (IAEG), 1981; International Society for Rock



**Figure 4.8:** a) Grade 5 weathering, b) Grade 6 weathering.

Mechanics (ISRM), 2007), weathering zones of grade 5 and grade 6 were observed at the outcrops at the vicinity of Seria Formation, showing a soil horizon with mottles of relict fabric and a homogenized soil structure with no relict fabric, respectively (Figure 4.8).

The sandstones and shales are weathered into soils that make up the Nyalau Soil Series on the slopes of Canada Hill. Nyalau Soil Series is a brownish yellow to yellow sandy loam in an argillic horizon, has a well-drained profile and high erodibility (Paramanathan *et al.*, 2000). The fine sandy soil grains have a high tendency to be transported in an event of high rainfalls over a short period. The soils from this series are mainly clayey silt with low plasticity (Muol, 2009) though isolated cases of sandy and non-plastic soils can be present and consist of mainly quartz, kaolinite and illite (Figure 4.9).

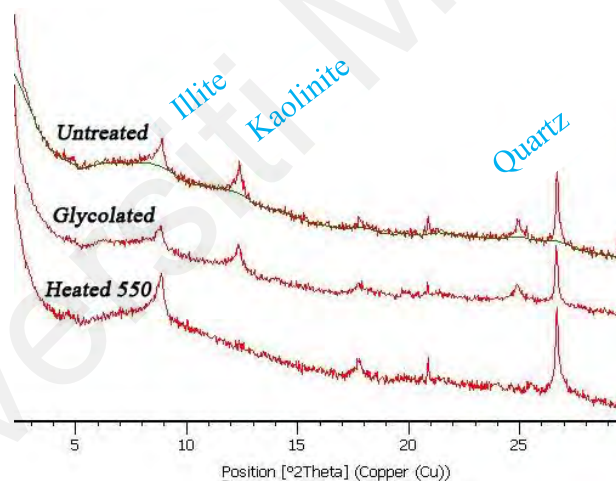
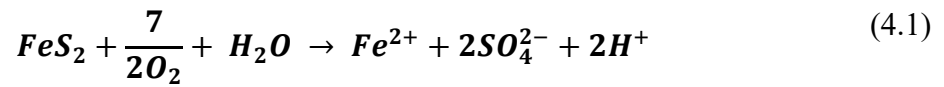


**Figure 4.9:** Results of XRD analysis on the minerals in the Nyalau Soil Series.

Chemical weathering features were observed in the outcrops of Canada Hill, which exhibit surficial mineral crusts on the sandstones and efflorescent sulfate salts “blooms” on the shale surface and are common for areas with prolonged dry periods after a rainfall. The weathering of pyrite ( $\text{FeS}_2$ ) in pyrite-bearing shales is a plausible cause of the efflorescence and is driven by shallow groundwater discharge by evaporation and recharge by precipitation. Pyrite oxidation leads to the formation of acid-sulfate soil and acidic waters especially at coastal plains (Joeckel *et al.*, 2005). The oxidation of pyrite by

molecular oxygen yields ferrous iron and sulfate (Rimstidt & Vaughan, 2003) as shown by the reaction shown in Eq 4.1.



The mobilization of Al, Fe and Si is also facilitated by chelation. XRD analysis shows the presence of jarosite and gypsum in the efflorescence (Figure 4.10). may be due to the dissolution of calcite from the calcareous bedrocks of Miri Formation and Seria

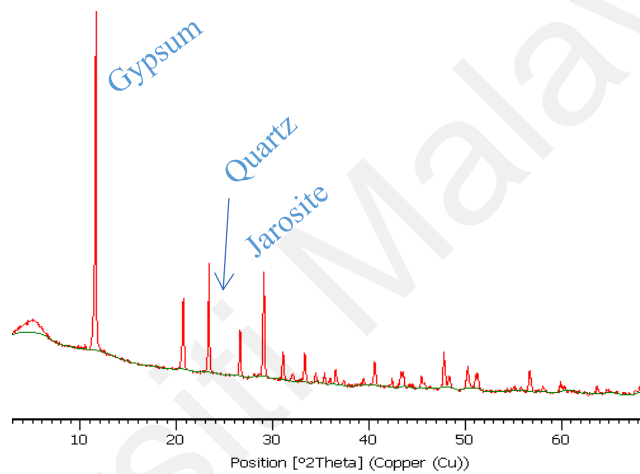


**Figure 4.10:** Results of XRD analysis on the efflorescent sulfate salts.

Formation. The efflorescence sulfate salts (Figure 4.11a) are prominent in outcrops that lies under overhangs, which prevents direct exposure to rainfall. The presence of gypsum or any sulfate minerals within bedrock layers may have implications in engineering geology due to high swelling–shrinking movements of the sandstone and shale during intensive wetting–drying cycles (Joeckel *et al.*, 2005; Siedel *et al.*, 2010). This accelerates the physical weathering of the outcrop, directly contributing to the difficulty of long-term maintenance of slopes, control of erosion as well as maintaining the stability of road grades. Joeckel *et al.* (2005) also mentioned that gypsum can readily grow in cracks in shallow subsoil materials after pyrite weathering. This poses a threat to any adjacent developments.



**Figure 4.11:** a) Efflorescent sulfate salts on the surface of shale, b) Encrustations on sandstone surface.

Encrustations on the sandstone surfaces are characterized as the yellowish to dark brown Fe- and Al-sulfate crusts (Figure 4.11b). These crusts are the result of a later stage in the pyrite oxidation, with fresh sulfate material forming underneath sandstone shale layer and subsequently pushes them away from the outcrop surface. 4-6 weeks of dry weather is an essential condition for oxidation processes to form a mature, thick, brittle, porous crust that is cohesive enough to be pried off the outcrop in irregular sheets (Joeckel *et al.*, 2005). XRD analysis on the crusts show presence of jarosite (Figure 4.12).

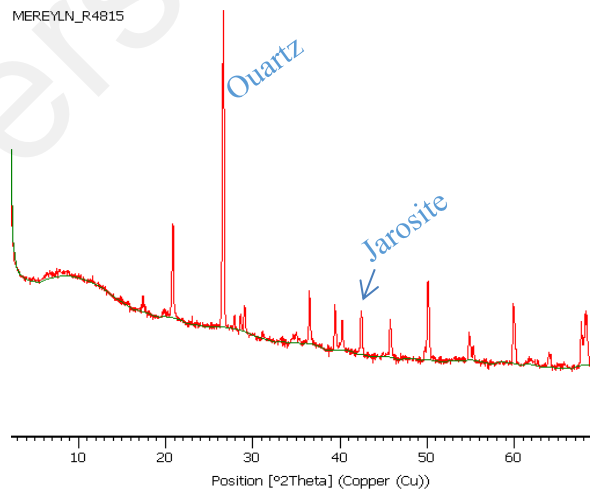


**Figure 4.12:** XRD analysis on the sulfate mineral crusts.

### 4.3 Quaternary Deposits

This subchapter will describe the layers deposited from the Quaternary and onwards which make up Canada hill. Terrace Deposits, Holocene deposits and its' subclasses will be described in detail.



#### 4.4 Terrace Deposits (Miri Soil Series)

Terrace deposits are loose, fine-grained, unconsolidated and well-sorted sands overlying the Seria Formation and Miri Formation (Figure 4.13). These Pleistocene deposits started to overlie the two formations after a hiatus in sedimentation after uplift and erosion. It can be observed as an extensive white sand layer above the Terrace Unconformity. The Terrace Deposits were divided into two based on colour, namely the Upper and Lower Terrace Deposits and were inferred to be deposited at two different times (Dundang, 1983; Kessler & Jong, 2014).



**Figure 4.13:** Podzolized layer in the terrace deposit overlying the Miri Formation.

However, they may belong to the same sequence with the latter being an organic-rich layer as a result of podzolization after the Terrace deposits were uplifted by post-Pleistocene faults. Podzolization causes downward migration of fine organic matter together with other elements such as Fe and Al, producing leached pure white sands at the top and a dark organic-rich and variably cemented spodic (harder from the top) layer near the bottom.

Podzolization is a common occurrence in Canada Hill especially in the permeable sand layer of the terrace deposits which later formed hydromorphic tropical podzols, enabling lateral water flow accelerating further hydrolysis of clay. This process lies on the assumption that aluminium is residual and does not mobilize readily in the profile and it

starts with loss of clay, biodegradation and migration of chelates. The reduction of iron and its migration as  $\text{Fe}^{2+}$  would increase the proportion of highly dispersable, iron-free kaolinite that could migrate over long distances, leaving a sandy residual material (Thomas, 1995). This may also leave behind a hard-cemented spodic layer at the bottom of the hydromorphic podzols, though the process of downward migration of Al and Fe ions which subsequently precipitates to form an “iron pan” due to changes in Eh and pH condition, commonly known as the illuviation of organic matter. The podzol layer as shown in Figure 4.14, is the leached podzol layer, with decreased cohesion and more prone to erosion once subjected to an intense rainfall, encouraging throughflow.



**Figure 4.14:** Podzolized layer in the Miri Formation.

These deposits are also present at 20m, 40m and 80m above the mean sea level with observations on the plateau at the northwest end of the Canada Hill and on top of the low-lying hills of Seria Formation as opposed to previous geological maps that mentions the locality at only on top of the hill. The Terrace Deposits are likely to have deposited at the same level during the Pleistocene, and the difference in elevation is probably caused by post-Pleistocene faults that have uplifted the adjacent blocks to the present elevations. The reactivation of the post-Pleistocene faults may have also caused the further uplifting of the Miri Formation.

The Miri Series developed from the Pleistocene Terrace Deposits is characterized by fine grained, loose, well sorted and unconsolidated sands that occur on flat plateau above the current drainage level. Paramanathan *et al.* (2000) recognized this series by the presence of an albic horizon and a thick spodic horizon located 50cm-100cm from the surface of the soil. It is also mentioned that Miri Series was developed over older Alluvial terraces. Wannier *et al.* (2011) and Dundang (1983) initially inferred this deposits as beach deposits.

The spodic horizon in this series is a strongly cemented layer, impervious to both water and roots, which leaves highly impoverished soils (loose leached white sand) above the spodic layer. A layer of organic-rich sand is also observed at the top of the spodic horizon. This cemented layer produced a perched water table which will impose several implications.

During rainy seasons, the perfectly drained sandy soils above the spodic layer have a flooding potential especially if the spodic horizons are shallow. Meanwhile, during the dry seasons, these soils suffer from moisture stress due to extensive drying of soils. The poor vegetative cover consisting of *Imperata* (alang-alang), shrubs and grasses coupled with high soil surface temperatures cause the areas to be susceptible to fires (Paramanathan *et al.*, 2000). The loose characteristic of the sandy soils also makes it fragile, unstable and very prone to soil erosion. Observation at the study area indicates that strong winds are also capable of eroding the soils. Other implications include collapsing and silting of drains in developed areas.

#### **4.5 Holocene Deposits**

The Holocene deposits that were deposited until the present day is described in this subchapter and will be divided into four subchapters describing the different soil series overlying this study area.

#### 4.5.1 Peat (Anderson Soil Series)

This series is a deep organic soil (more than 150cm thick) formed at coastal swamps, with fibric materials as a dominant material (Paramanathan *et al.*, 2000). This series locally has a high groundwater conditions and is often associated with water-logged areas namely wetlands, ponds and margins of shallow lakes.

Unless artificially drained, peat deposits are poorly drained and have a high water-bearing capacity. This minimizes flooding during rainy seasons by absorbing a lot of water. During wet seasons, this deposit acts as a water catchment while during dry seasons, prolonged droughts may cause the peat to burn which causes haze and air pollution (Paramanathan, 2008). The high carbon content in peat encourages the fire to last longer. In the context of the study area, the whole of Miri City will be affected by haze.

The internal structure of peat either fibrous or granular is an important factor in determining the capability of retaining and releasing water which has an influence on strength and performance of the peat in later engineering projects. This series has a very low strength but very high compressibility. Settlement, stability of earth fill embankments, support for bridge foundations and locating culverts are implications on a peat-related development (Waltham, 1994).

Any development done on peat deposits will eventually cause considerable shrinkage of about more than 50% as it releases water upon compaction. This is an irreversible action as the original volume and moisture content could not be obtained after rewetting the peat. In an extent when peat is dried and is under a good enough condition for oxidation, it will disappear. Strength of peat increases with consolidation and lower moisture and therefore, deeper peat layers have higher strengths. Secondary compressions are large for this series, which is why careful considerations should be practiced, preventing any long-term settlement.



Other problems related to development over peat are acidic water that can corrode steel and concrete, and the potential of methane generation (Bell *et al.*, 2009). Depending on the thickness and distribution of peat, it can be removed and replaced with soil fill.

#### **4.5.2 Beach Sand (Tatau Soil Series)**

Tatau Series occurs along the coast of Miri and the Sungai Miri estuary and is characterized as sand deposited on beach ridges and swales, similar to Miri Series or Terrace Deposits. However, this series has no cemented horizon (podzol) and a perched water table. This deposit is located on a generally levelled ground close to the coastline and groundwater levels are low. Thin layer of organic matter is common on top of the sand.

The sandy soils of this series are highly erodible, loose and unconsolidated. Engineering projects should be given high precautions and alternative measures in order to proceed with the development especially involving deep excavation due to the potential collapse of the excavated wall/slope and flooding of the pit. This difference of these sands with the terrace sands are the terrace sands have limited thickness and underlain by sandstone and shale bedrock. The Terrace Deposit ranges from 2m to 3m depending on locality and is generally thicker at the higher elevation. The beach sands are much thicker than the terrace deposit and are probably underlain by marine clay deposits.

#### **4.5.3 Sulfidic Marine Clay (Rajang Soil Series)**

Rajang Series is deep, poorly drained clays (clay >35%) inundated by sea water and potentially acid sulfate soils. It was developed over sulfidic marine clay (Paramanathan, 2011). The soil is dark grey, sticky and has tiny grains of orange-brown jarosite on dried samples. Similar to the peat of the Anderson Soil Series, this series exhibits high groundwater conditions and is often associated with water-logged areas.

The soft clay of this series can lead to settlement problem. The water content in clays is released upon stress application. In time, the soils shrink and lose volume which leads to cracking of brittle drains and cracking of house walls. The pore water in the soils is highly acidic ( $\text{pH} < 4$ ) and saline ( $> 4 \text{ dSm}^{-1}$ ), and the soil produces sulphate upon exposure (Paramanathan & Pupathy, 2012). Both these factors can be the cause of dissolution and cracking in concrete structures built on top of this series, and failure of turfing or ground cover on this soil. The remedies include avoid loading on these clays or wait until settlement is complete (Waltham, 1994) and to use sulphate resistant cement in concrete.

#### **4.5.4 Organic Soil (Igan Soil Series)**

Igan series is composed of very poorly drained organic soils found at lowland swamps close to the coast, especially between beach ridges. It is underlain by marine sand. In this study, it is located at the eastern side of Canada Hill. This series has a high-water table unless artificially drained. Fibric organic soil materials are dominant in the subsurface tier and are permanently underwater (Paramanathan *et al.*, 2000).

Problems related to engineering work include settlement of the soft organic clay, shallow acidic groundwater and low permeability. If this problem persists without proper effective mitigation, flooding is prone to occur.

#### **4.5.5 Artificial Deposits**

Fill materials were used to reclaim part of Sg. Miri towards the Southwest diverting the flow towards the west. Fill materials were also used for developments on hillslopes particularly on the slopes on Canada Hill as seen at the Petroleum Museum area. These fill materials were indicated by the presence of various grain sizes and orientations embedded in soil.

The engineering properties of the fill materials depend on the composition of the material, the method of emplacement (end-tipping vs compacted fill) and any subsequent

geotechnical treatment (Bell *et al.*, 2009). The fill materials require it to be compacted to reach peak strength prior to development to prevent settlement problems. Otherwise, development should not be continued, or the settlement should be done prior to building on top of the materials.

#### **4.6 Summary**

The engineering geology map of the study area (Figure 4.15) was produced as a complement to this chapter. This map shows the spatial location of the described soil series as well as other features which may be useful for the understanding of the geological and anthropogenic factors that may lead to instabilities.

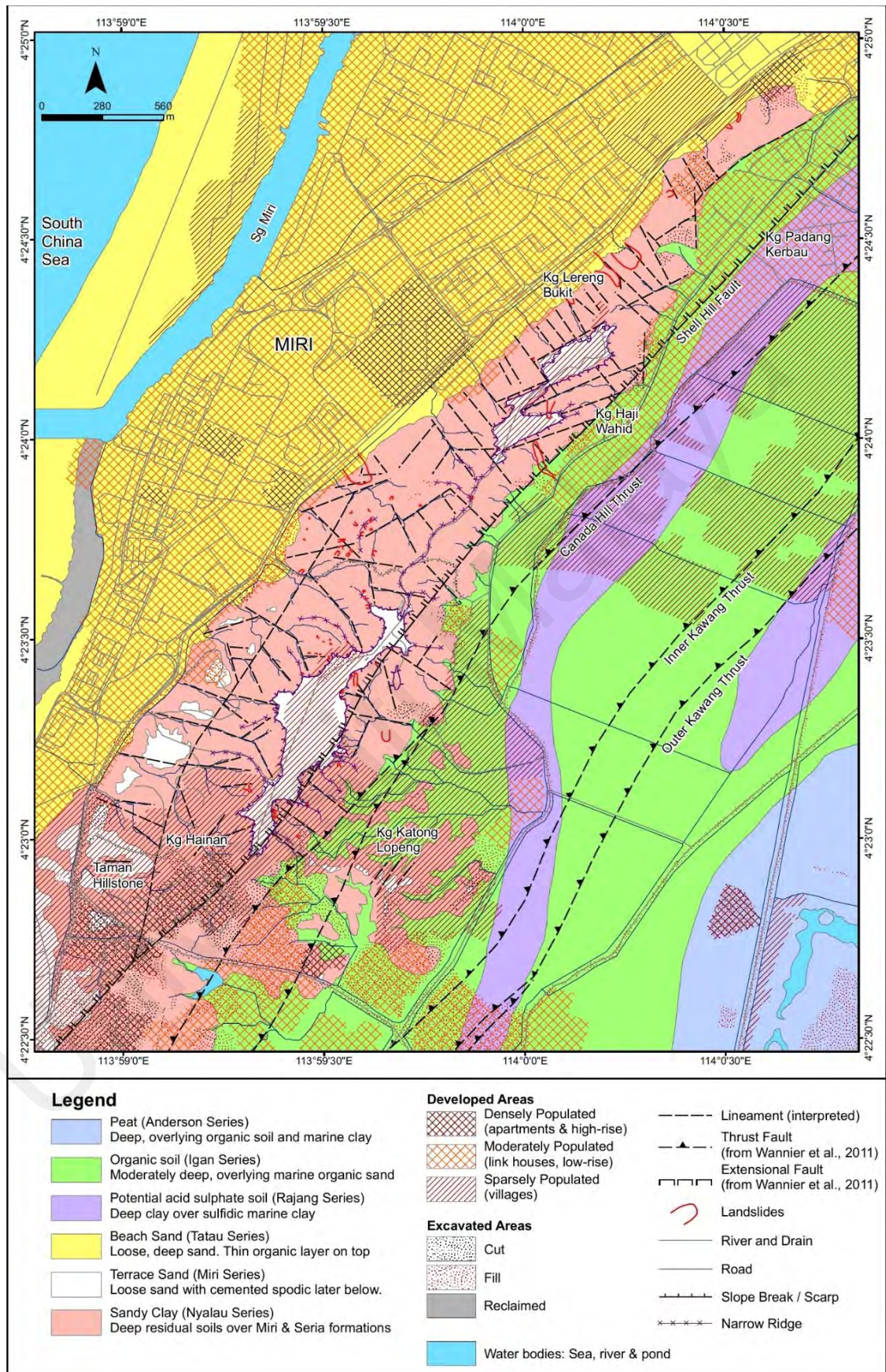


**Figure 4.15:** Engineering geology map of the Canada Hill area.



## CHAPTER 5 : LANDSLIDE PARAMETERS

### 5.1 Introduction

This chapter will describe the findings for the highlighted major and minor landslide occurrences followed by the landslide-controlling parameters used in the landslide susceptibility assessment. The basis of selection of these causal factors will also be described in this chapter. Landslide parameters were analysed and visually shown as maps in ArcGIS.

The occurrence of landslides in Canada Hill are controlled by a combination of terrain conditions. The factors of landslide occurrence can be divided into intrinsic (predisposing), factors that contribute to the instability of a slope and extrinsic (triggering), factors that trigger the landslide event (Corominas *et al.*, 2013). However, only the intrinsic factors are discussed in this research due to the lack of data for the triggering factors.

### 5.2 Landslide Occurrences

The inventory of landslides done in this study accounts for a total of 61 landslides, obtained from field observation, interpretation of satellite imageries and DEM. The distribution of landslides spans over the Miri Formation, concentrated at higher elevations and were classified into major failures (LS1, LS2 and LS3) and minor failures (Figure 5.1). The major landslides consist of reactivated planar failures and a translational failure while the minor failures are composed of smaller translational failures and circular failures in soil. The major landslides and some minor landslides where care needs to be exercised are described in detail in the following subchapters. The relationship of each landslide parameters with landslide occurrences will also be discussed in this chapter.

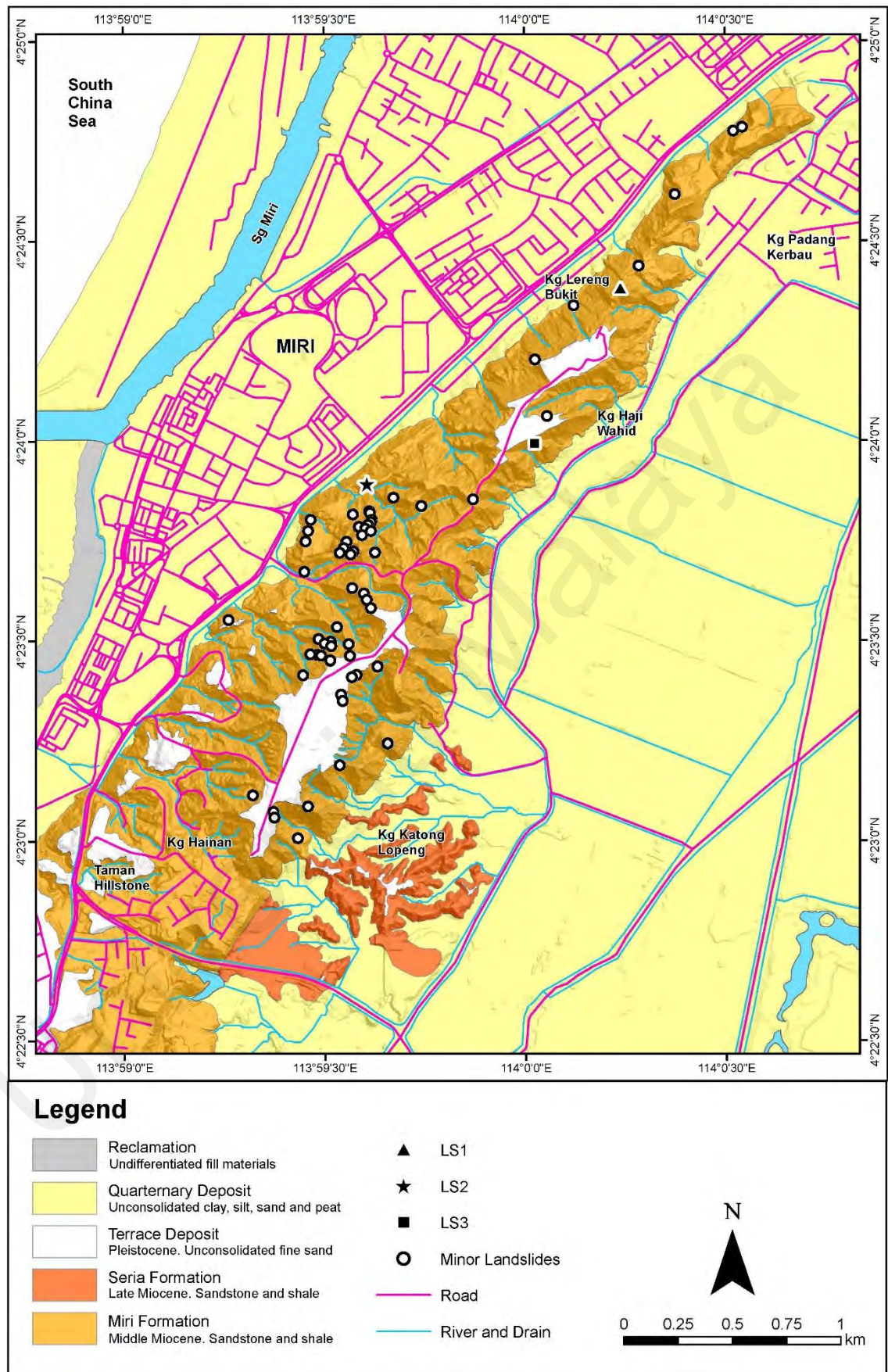


**Figure 5.1:** Location of landslide occurrences at Canada Hill. Naming of Miocene geological units after Wannier et al. (2011).

### 5.2.1 Landslide 1 (LS1)

LS1 is one of the major landslides that occurred at the Northwest of Canada Hill, particularly at *Kampung Lereng Bukit* (N 4.40662; E 114.00632) as shown in Figure 5.2. This landslide was controlled by a prominent lineament adjacent to the landslide, which acted as a release plane for the slope to fail. The lineament was interpreted from satellite imageries and shorter sets of joints were observed in the field. Two sets of joints observed above the failure near to the crown are the possible scarp of the landslide. First set of joints had a reading of  $175^{\circ}/75^{\circ}$  WSW (J1) while the second set of joints had a reading of  $112^{\circ}/67^{\circ}$  ESE. The beddings in this slope had a reading of  $262^{\circ}/35^{\circ}$  W. The slip surface is an almost planar bedding and with average slope gradient of  $23^{\circ}$ . Although planar failure can occur along the bedding, the slope is not a typical “day-lighting” slope. The landslide occurred on the 30th of January 2009. The rainy season during the Northeast Monsoon may have a significant role LS1 occurrence. Data obtained from the Malaysian Meteorological Department shows that the 3-day cumulative rainfall prior the LS1 event is 199.2mm (Figure 5.3). The total rainfall in January 2009 contributed 10.9% of the rainfall in 2009.

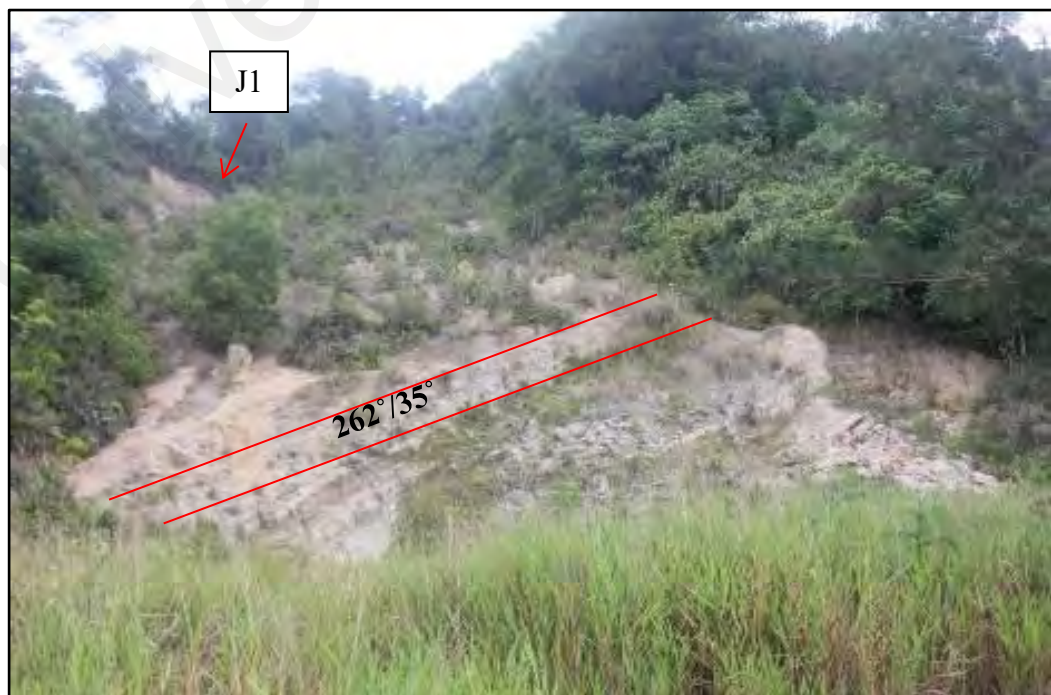


**Figure 5.2:** LS1 at *Kampung Lereng Bukit*.



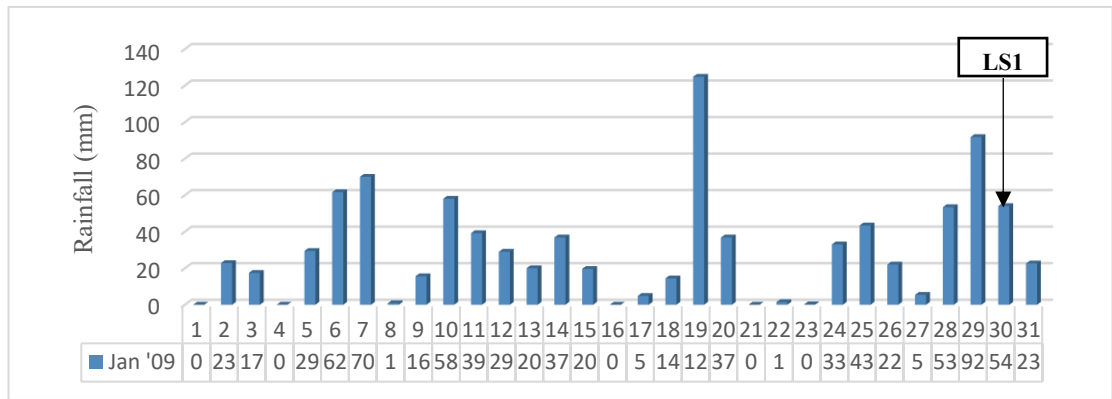


**Figure 5.3:** Daily rainfall in January 2009 (Malaysian Meteorological Department, 2017).

Following the LS1 occurrence, the slip surface was an intact sandstone-shale bedrock dipping  $262^{\circ}/35^{\circ}$  N underneath the supposed failed debris. Previous study by Banda *et al.* (2009) also stated that the sandstone bed acted as a sliding plane as the slope failed. The scarp that developed along the  $130^{\circ}/67^{\circ}$  SW fault and the crest is along a N-S joint (Figure 5.4b). These indicate that the landslide is partly controlled by geological structure, where the fault acted as a release plane. The landslide debris consisted of large, angular and relatively fresh sandstone blocks, indicating that the sandstone was probably intact before the landslide occurrence. The sliding probably involved a sequence of interbedded sandstone-shale and soil, failing en masse and produced a subsequent debris flow. Figure 5.5 shows that the development of debris flow is common from the failed rock and soil materials after initial displacement (Waltham, 1994). The cross section of A-A' is shown in Figure 5.6.

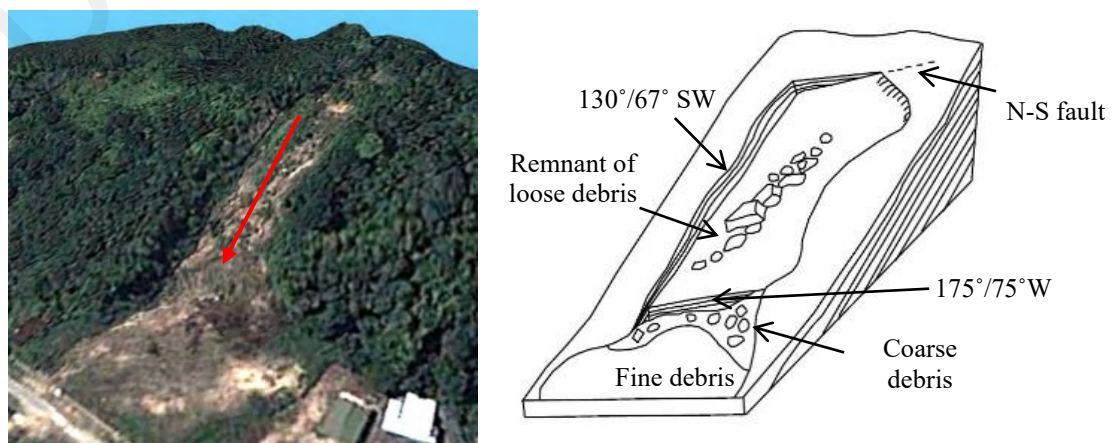


**Figure 5.4:** a) 3D view of LS1 by Google, Maxar Technologies, 2020 (earth.google.com/web/), b) Sketch of LS1 with its' inferred components.



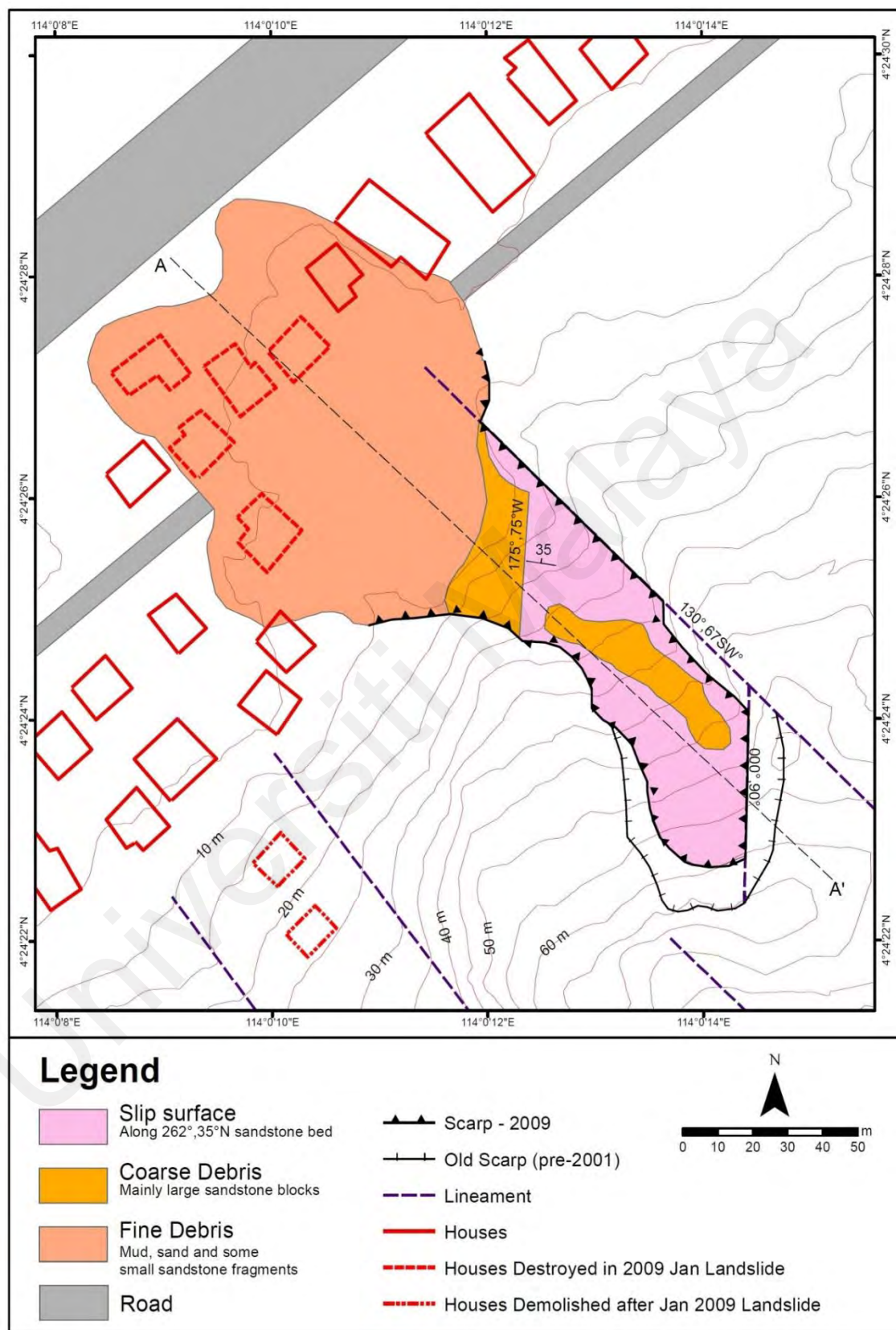


**Figure 5.5:** Landslide Map of LS1.

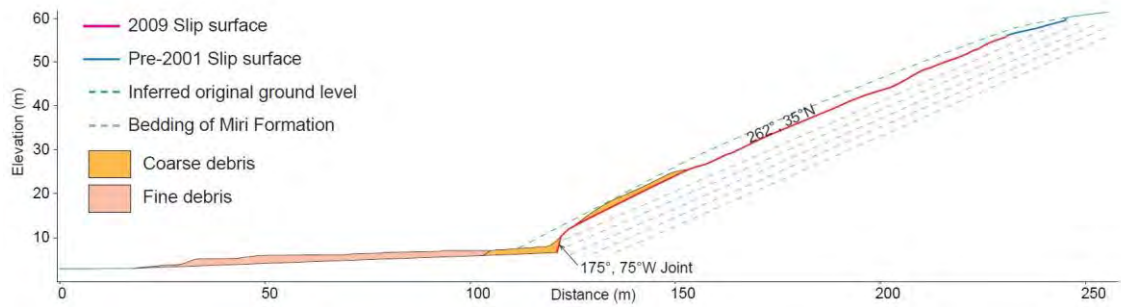


**Figure 5.6:** Cross section of A-A' from Figure 5.5.

The surrounding areas of LS1 has a moderate vegetation cover. The low fertility and water-holding capacity, sandy loam textures of the soil and the nature of the slope allows only the growth of generally poor forests (Paramanathan *et al.*, 2000). The foot slopes of Canada Hill are occupied by houses and minor developments belonging to the village community residing in *Kampung Lereng Bukit*. Some houses are also located above the slopes which can be accessed by man-made pathway and stairs up the slopes.

The sequence analysis (Figure 5.7) of the satellite imageries of LS1 led to the discovery of a prior landslide occurrence. The 2001 satellite imagery of the LS1 area showed a relict landslide structure, which led to the inference that a landslide had occurred at the same location sometime before 2001. Though occurring in the same location, the crown of the pre-2001 landslide was slightly higher than the 2009 landslide. The 2008 satellite imagery portrayed a fair amount of vegetation growth at the landslide area, indicating that there was no growth at the landslide area, indicating that there was no reactivation of this landslide since 2001 until the 2009 event.

LS1 was concluded to be a reactivation failure of the pre-2001 landslide. The landslide was inferred to be due to the saturation of shale beds above the sandstone slip surface and being at the intersection of two sets of joints. The slope may also be subjected to an increased rate of weathering between the cracks and joints from rainfall or possible domestic water flow from the neighbourhood living above the slope, in addition to the development pressure around the vicinity.

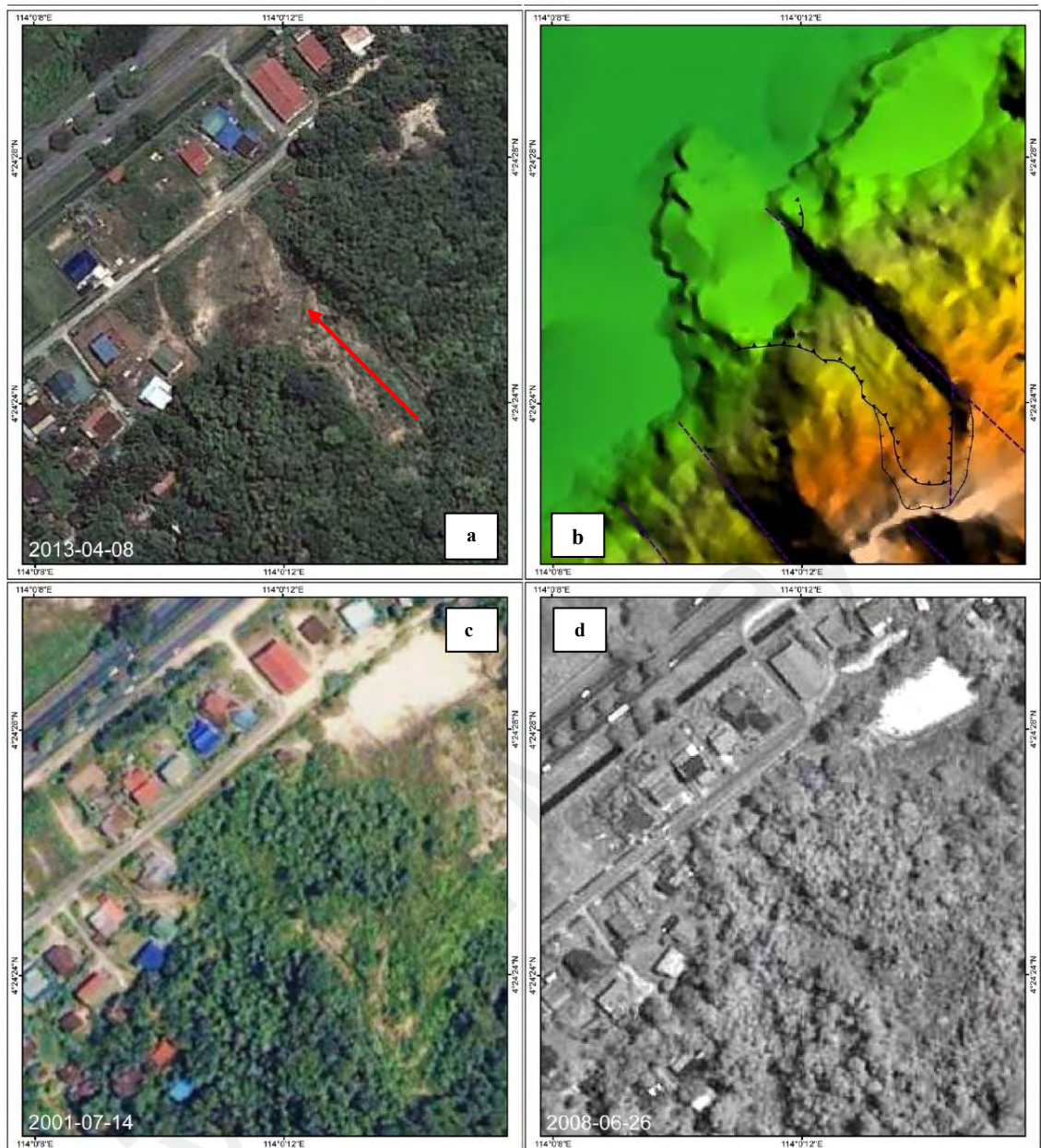


**Figure 5.7:** a) LS1 site in year 2013, b) Relief of LS1, c) LS1 site in year 2001 showing relict of an older landslide, d) LS1 site in year 2008 with a fair amount of vegetation growth. No signs of landslide activity. 5.7a, 5.7c and 5.7d were obtained from Google, Maxar Technologies, 2020 (earth.google.com/web/).

### 5.2.2 Landslide 2 (LS2)

LS2 occurred on the 16th of January 2009, which is only a few days prior to the occurrence of LS1. Located 3km Southwest of LS1, both landslides occurred on the west flank of Canada Hill. Figure 5.8 shows the area of LS2 (N 4.39776; E 113.99604) which has already been cleared of displaced loose debris for the construction of a gas station. The beds at this slope have an average reading of 238°/26° NE while the joint at the loose wedge on the slope showed a reading of 195°/81° N.



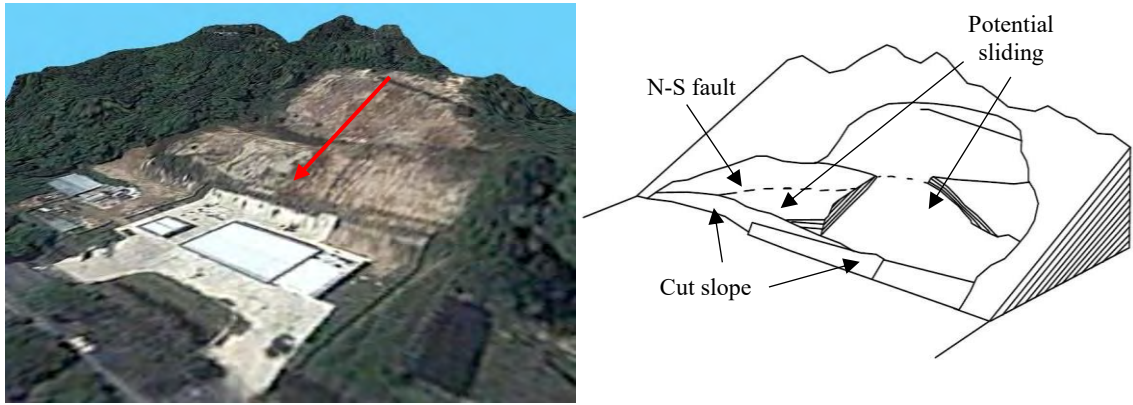


**Figure 5.8:** a) 3D view of LS2 by Google, Maxar Technologies, 2019 (earth.google.com/web/), b) Sketch of LS2 with its' inferred components.

The interpretation extent of this failure is only based on the observation after removal of the loose debris post-landslide. Previous report by Luqman (2009) stated that a 6-meter block at the foot slope was moved 8 meters further away from the slope. Remnants of loose rocks and a loose wedge cut by a north-south fault/joint can still be seen on the slope (Figure 5.9). The slope may pose some instability issues due to the presence of loose debris constituting of rocks and soil on the slope. A distinct line of vegetation was also observed in the gap between the joints along the wedge, near the foot slope.

LS2 is surrounded by moderately high vegetative cover and occasional shrubs on the slope. The effect of vegetation toward stability depends on the intensity of the rainfall, humidity, temperature and wind conditions. Moderate rainfalls during a wet season will increase infiltration to reduce surface runoffs and decrease soil moisture by



**Figure 5.9:** a) Loose wedge cut by a north-south fault/joint located beneath the trees, which separates the wedge from the slope, b) Remnants of loose rocks on the slip surface of LS2.

evapotranspiration while intense rainfalls can cause a build-up in pore-water pressures to a level exceeding the limit and an increase in throughflow through piping along root channels which will then increase the downslope drag (Thomas, 1995). Figure 5.10 shows

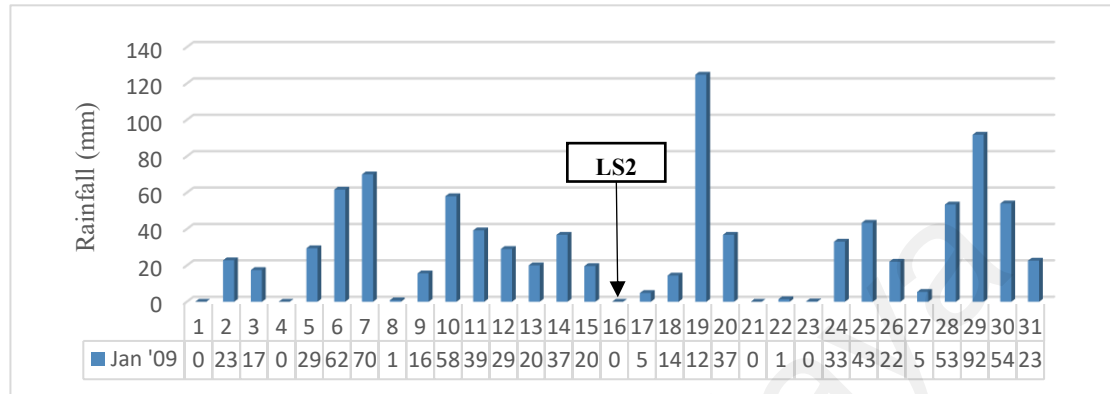


**Figure 5.10:** Daily rainfall in January 2009 (Malaysian Meteorological Department, 2017).

that no rainfall occurred on the day of landslide occurrence. However, the 3-day cumulative rainfall totalled to 56.4mm rainfall, which may be a more useful reference as the landslide occurred early in the morning before dawn. The Nyalau Series is prone to have desiccation cracks during the dry season which promotes water entry into soil during the next wet season which may consequently aggravates the problem. Bigger trees that anchor their roots into the bedrock layers will have more weight subjected on the slope, affecting the normal and downhill components of force subjected to the slope. Bigger trees also have bigger swaying effects during windy days which can widen the existing fractures.

The 2001 satellite imagery of the LS2 area shows a crescent-shape pattern due to a change in tree line is observed in Figure 5.11c. This change in tree line could be associated with small downslope displacement of rock and soil, tension cracks or scarps of an older failure. The crescent-shape pattern also roughly coincides with the 2009 landslide scarp (Figure 5.11a).

The nature of LS2 was a planar failure and subsequent flow after displacement may

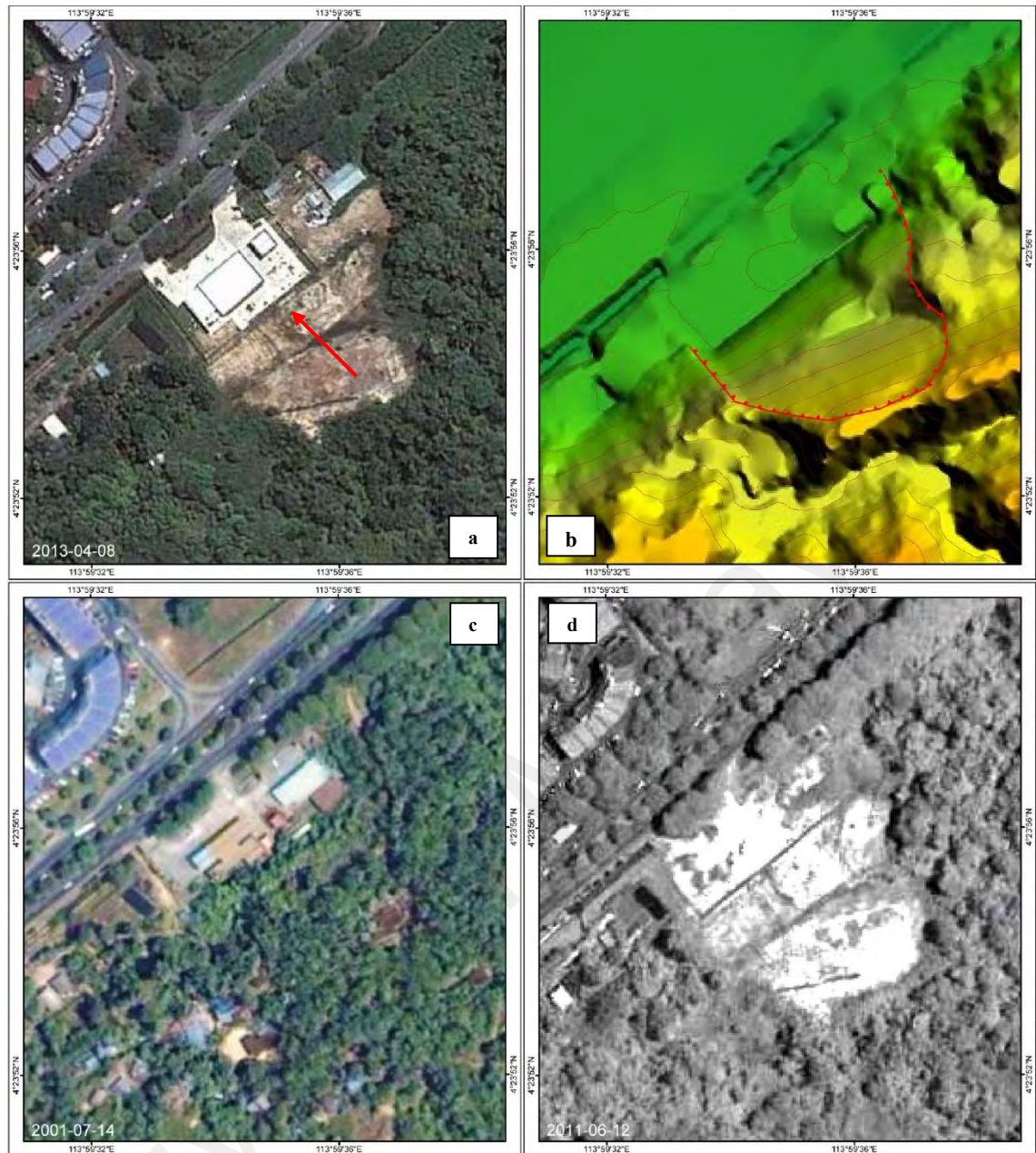


**Figure 5.11:** a) LS2 site in year 2013, b) Relief of LS2, c) LS2 site in year 2001, d) LS2 site in year 2011. 5.11a, 5.11c and 5.11d were obtained from Google, Maxar Technologies, 2020 (earth.google.com/web/).

also occur, like LS1. Saturation of shale beds and having sandstone beds as a slip surface is another similarity LS2 have with LS1. This failure may also be induced by the excavation at the toe of slope to allow for the construction of the previous gas station. The N-S lineament cutting the loose wedge has a potential of being a release plane which can cause the failure of the block. The loose wedge will need to be given extra care and precaution during windy days or storm events due to the presence of trees in the lineament feature. Care also needs to be exercised for the loose debris on top of the slope as rainfall



will increase surface runoff on the slope. Concrete drainages to trap any sediments flowing downslope is one of the preventive measures taken by the authorities. The loose debris on the slope was also nailed into the beds to keep it intact.

### 5.2.3 Landslide 3 (LS3)

LS3 happened in the morning of 22nd January 2014. It is the third major landslide being studied in this research and is located along the *Pujut Padang Kerbau* road (N 4.39819; E 114.00374) (Figure 5.12). The geology of this area is of the interbedded sandstone-shale, attributing to Miri Formation. Loose debris that failed along this slope extended more than 70m away from the slope, affecting the main road and a house at the foot slope. The failed materials were composed of sand, clayey sand and sandstone blocks and appeared to be detached from a subvertical joint with a reading of  $237^{\circ}/58^{\circ}$  NE. Slope inclination near the crown averaged to  $45^{\circ}$ ,  $25^{\circ}$  at the lower scarp and between  $6^{\circ}$  and  $15^{\circ}$  at the footslope. The average measurement of the beds taken adjacent to the failure is  $234^{\circ}/10^{\circ}$  NE. Cultivation activity is present at the footslope while the top of the slope has a moderate vegetation cover.



**Figure 5.12:** LS3 along the *Pujut Padang Kerbau* road, located at the Eastern side of Canada Hill.

LS3 occurred during the rainy Northeast monsoon, which can be accepted as a common factor attributing to landslides at unstable slopes near Canada Hill. The amount of rainfall on the day of failure recorded an amount of 70mm while the 3-day cumulative was 226.8mm, giving the highest 3-day cumulative for January 2014 (Figure 5.13).

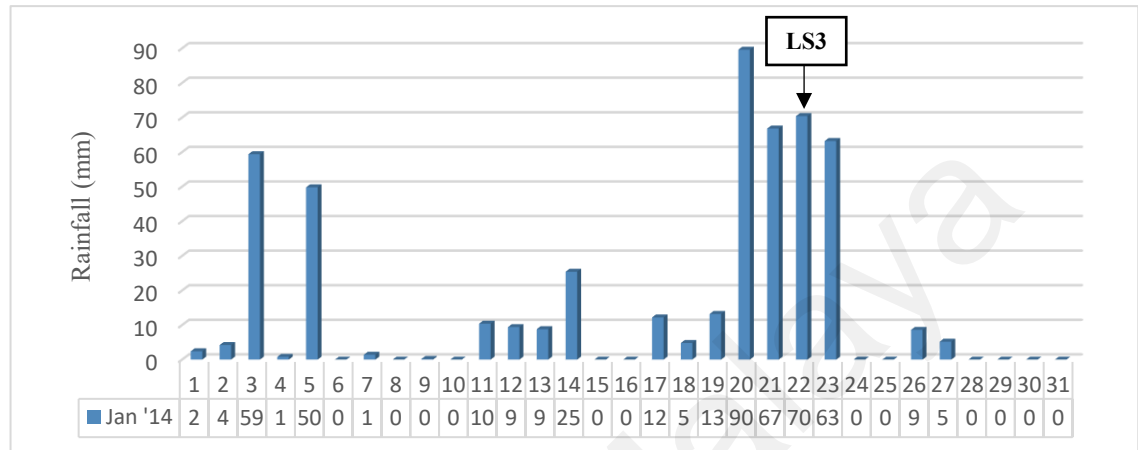


**Figure 5.13:** Daily rainfall in January 2014 (Malaysian Meteorological Department, 2017).

A week after the occurrence of LS3, a seasonal river flowing from both sides of the scarp was observed, which later merges near the foot slope, retaining moisture in the debris which has not failed completely. The debris was observed at the higher part of the landslide, nearest to the escarpment and has a potential to flow upon the next rainfall. The mechanism of LS3 could relate to this observation. Initial landslide may have already occurred at the crown, blocking the water channel of the seasonal river. The slow accumulation of loose debris due to oversaturation may have already occurred for some time. Prolonged rainfall prior to the occurrence probably prompted the flow of the debris accumulation, which caused LS3 to fail along the subvertical joints.

Distinct relict landslide features can be observed in the 2001 satellite imagery (Figure 5.14a), indicating a landslide occurrence prior to the 2014 event, indicating a reactivation of a previous landslide. The 2008 imagery showed no signs of reactivation (Figure 5.14c) and the 2014 imagery showed the position of the new landslide slightly left to the relict landslide (Figure 5.14d).



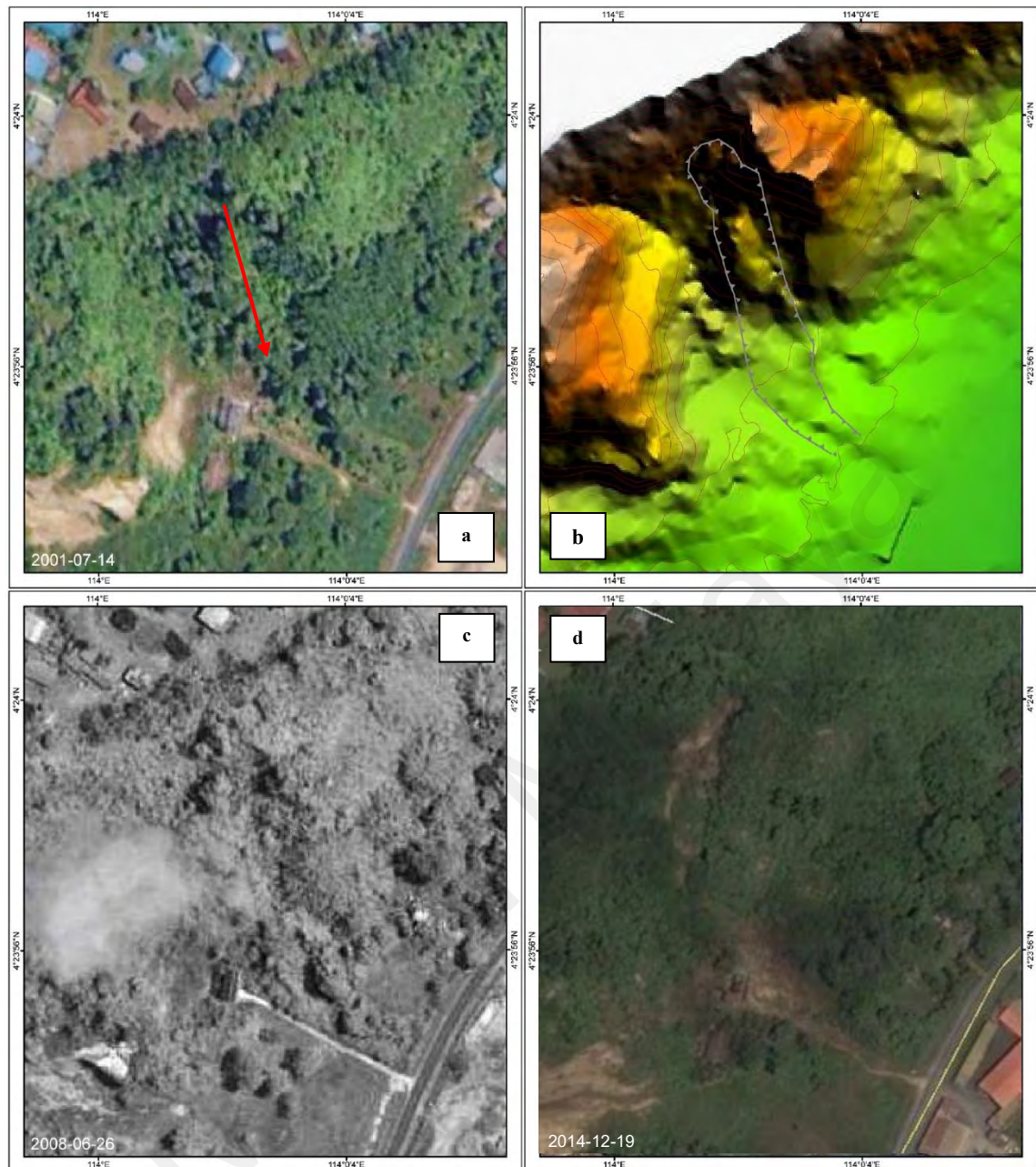


**Figure 5.14:** a) LS3 site in year 2001 showing distinct relict landslide, b) Relief of LS3, c) LS3 site in year 2008, d) 2014 imagery of the LS3 area showing position slightly left of relict landslide. 5.14a, 5.14c and 5.14d were obtained from Google, Maxar Technologies, 2020 (earth.google.com/web/).

Additional factor to note in relation to the occurrence of LS3 is the location of *Kampung Wahid* above the slope. The houses in *Kampung Wahid* faces inadequate drainage facilities for the discharge of waste water and therefore, the discharge of waste water is directed downslope using PVC pipes (Figure 5.15). This could increase the aggravation of surface runoff down the slope, in addition to being subjected to heavy rainfall.



**Figure 5.15:** Domestic drains discharging water downslope. Direction of water flow is indicated by the yellow arrow.

#### 5.2.4 Minor Landslide Occurrences

LS4 occurred at the western side of the Canada Hill flank, 200 meters south from LS2 (N 4.39633; E 113.99447) as shown in Figure 5.16. Displaced loose debris at the foot slope indicates the occurrence of a previous landslide. The slope is a slope cut that have been subjected to the aggravating effects of weathering. This site is prone to bushfires during the dry season, stripping the vegetation cover which will increase the chance of landslide occurrence during periods of heavy rainfall on the next rain season. The expansion and contraction of rocks because of bushfires may also pose a considerable threat to the stability of this slope, in addition to having a higher slope angle than the bedding plane. Tension cracks of about 1m – 3m length and leaning trees below the



**Figure 5.16:** LS4 along *Jalan Miri-Pujut* (opposite Bintang Megamall). The tension cracks on the upper slope is indicated by the red circle.



tension cracks were also observed at upper slope. Care should be exercised during extreme events as reactivation of LS4 or landslide occurrence at adjacent areas may occur.

LS5 is located on the slope adjacent to *Jln Oil Well No. 1* (Figure 5.17), also located the western part of Canada Hill (N 4.39435; E 113.99588). The failed materials consist of loose debris and rocks. The failed loose debris at the foot slope have been cleared prior to fieldwork. However, the remnants of loose debris on the upper slope that were not displaced completely during the landslide event were observed. The landslide left a circular relict structure, which indicates a rotational failure.



**Figure 5.17:** LS5 along the slopes adjacent to *Jalan Oil Well No. 1*.

LS6 is a rock fall, which occurred at a subvertical slope which faces SE towards *Kg. Katong Lopeng* (N 4.38351; E 113.99273) as shown in Figure 5.18. Failed loose debris were observed at the foot slope. The rock fall may be ascribed to a possible previous sandstone-shale overhang that failed upon prolonged exposure to weathering and surface runoff.

LS7 is located at the slope of Canada Hill at the Petroleum Museum (N 4.39009; E 113.99504) as shown in Figure 5.19. The slope is facing West. The landslide is a shallow rotational slide with failed debris comprised of soil. The presence of the fallen concrete

chairs as part of the walkway behind the museum indicates that the landslide happened post-dating the completion of the Museum.



**Figure 5.18: Landslide 6**



**Figure 5.19: Landslide 7**

### **5.3 Planar Failure Susceptibility Assessment**

The relationship between the orientation slopes with the present sets of discontinuities greatly determines the type of failure a rock and soil slope get subjected to. The different types of failure include planar failure, rotational failure, wedge failure and toppling. The focus of this study would be on planar failures, which occurs as a result of the strike of discontinuities such as bedding plane, fault plane or preferred orientations of a joint set being parallel to the slope and the dip of the discontinuities being steep enough to overcome friction, but not steeper than the slope itself. It is a common failure mode for areas with stratified sedimentary rock formations such as Canada Hill, Miri with observed blocks of rock sliding down a plane dipping out of the slope face. Most of the landslides in Miri, including the major ones (LS1 and LS2) are contributed by planar failure which prompted an assessment of planar failures in the area. The process of this assessment will take the concordance of slope aspect, dip and direction into consideration by extracting the direction cosines of the planar features in the study area to create speculative 3D

predictions and visualizations of varying geometric scenarios with respect to the field observation (De Kemp, 1998). This is a prior step to the GIS analysis of landslide-controlling parameters by creating an initial susceptibility map (Amadesi & Vianello, 1978) combining the slope aspect, dip and dip direction of bedding, which will later be refined by overlaying it with other landslide-controlling parameters to form the final landslide susceptibility map. It is also noteworthy to mention that regardless of its' importance, this initial susceptibility map was only utilized for the heuristic approach in this study due to the difficulty in performing statistical analysis on the combination of the factor maps.

### 5.3.1 Workflow of Planar Failure Susceptibility Assessment

In order to perform planar failure susceptibility analysis, for the whole study area, interpolation needs to be carried out to estimate the orientation of the bedding for areas where bedding is unknown by interpolation of known bedding from adjacent areas using circular statistical analysis. Direction cosines which represent the orientation of the unit vector ( $\bar{a}$ ) parallel to a plane in three dimensions (Groshong, 2006) can be extracted from the known bedding orientations (strike and dip) to be interpolated in Surfer 8 and ArcGIS, consequently producing a planar failure susceptibility map. Angle  $\alpha$ ,  $\beta$ , and  $\gamma$  are angles between the feature and the x-axis, y-axis and z-axis respectively (Figure 5.20). The direction cosine for these angles are  $\cos \alpha$ ,  $\cos \beta$ , and  $\cos \gamma$ .

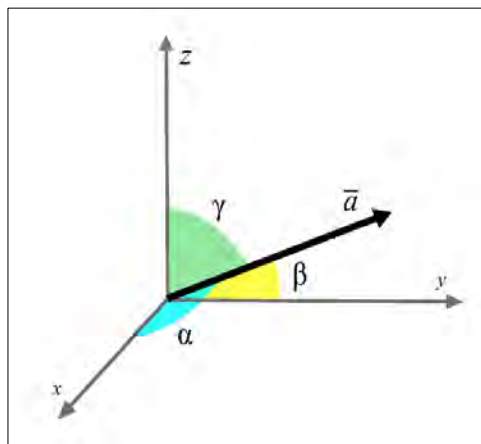


**Figure 5.20:** The 3 directional cosines of a vector in spatial form.

The azimuth (strike) and dip which were initially obtained from the field and literature reviews, recorded in maps and stored in the GIS database were extracted into an excel sheet for the calculation of  $\cos \alpha$ , and  $\cos \beta$ ,  $\cos \gamma$  as shown in the equation 5.1 – 5.3.

$$\cos \alpha = \cos(dip/57.2958) \times \sin(azimuth /57.2958) \quad (5.1)$$

$$\cos \beta = \cos(dip/57.2958) \times \cos(azimuth /57.2958) \quad (5.2)$$

$$\cos \gamma = \sin(dip /57.2958) \quad (5.3)$$

The obtained vales for  $\cos \alpha$ , and  $\cos \beta$ ,  $\cos \gamma$  were then analysed in Surfer 8 for the purpose of interpolation into 3 separate grid files. These grid files underwent a conversion from grid files into point shapefiles in ArcGIS, to be merged into as a single shapefile containing the attributes of  $\cos \alpha$ , and  $\cos \beta$ ,  $\cos \gamma$ . This procedure now needs to be reversed to find the azimuth and dip to obtain the angle of  $\alpha'$ ,  $\beta'$ , and  $\gamma'$  for the interpolated points using the following formula.

$$\gamma' = \arcsin(\cos \gamma) \times 57.2958 \quad (5.4)$$

$$\alpha' = \arcsin\left(\frac{\cos \alpha}{\cos \frac{\gamma'}{57.2958}}\right) \times 57.2958 \quad (5.5)$$

$$\beta' = \arccos\left(\frac{\cos \alpha}{\cos \frac{\gamma'}{57.2958}}\right) \times 57.2958 \quad (5.6)$$

The value  $\alpha'$  and  $\beta'$  returned by Eq 5.5 and Eq 5.6 will be in the range of  $\pm 90^\circ$  and must be corrected to give the true azimuth over a range of  $0^\circ$  to  $360^\circ$ . This is because direction cosines are a form of directed vectors. The true azimuth- $\alpha$  and azimuth- $\beta$  can be determined from the signs of  $\cos \alpha$  and  $\cos \beta$  as shown in Table 5.1. Consequently, after

obtaining the azimuth values, dip direction can be calculated too. These calculations can be done in ArcGIS using the Field Calculator tool with the application of conditioning formulas where necessary. The interpolated azimuth and dip direction of bedding can be seen in Figure 5.21 and Figure 5.22 respectively.

**Table 5.1:** Relationship between signs of direction cosines and the quadrant of azimuth.

<b>Azimuth quadrant</b>	<b><math>\cos \alpha</math></b>	<b><math>\cos \beta</math></b>	<b><math>\alpha</math></b>	<b><math>\beta</math></b>
000 to 090	+	+	$\alpha'$	$90 - \beta'$
090 to 180	+	-	$180 - \alpha'$	$90 + \beta'$
180 to 270	-	-	$180 - \alpha'$	$90 + \beta'$
270 to 360	-	+	$360 + \alpha'$	$450 - \beta'$



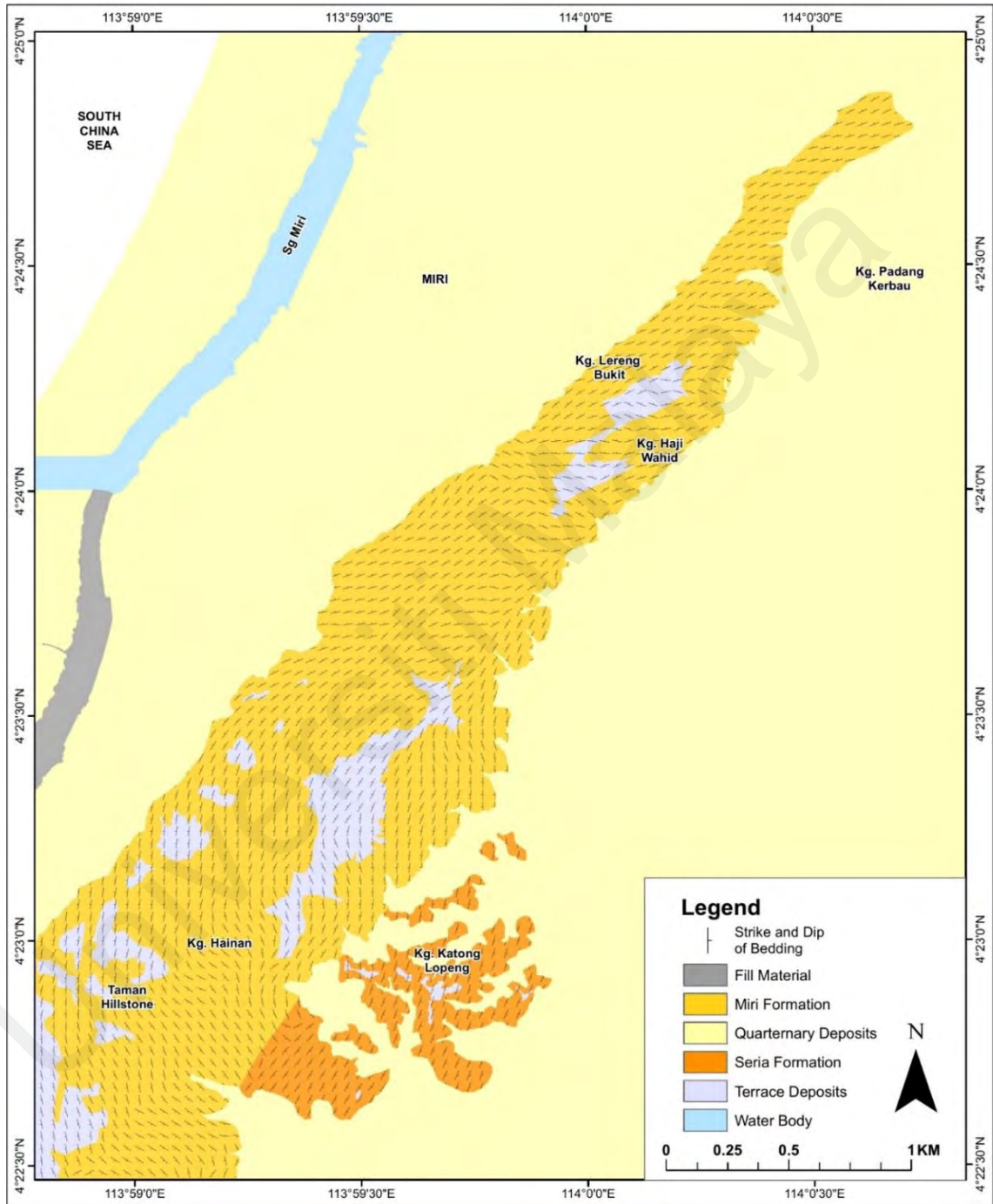


**Figure 5.21:** Interpolated orientation of bedding overlain on Geology map.



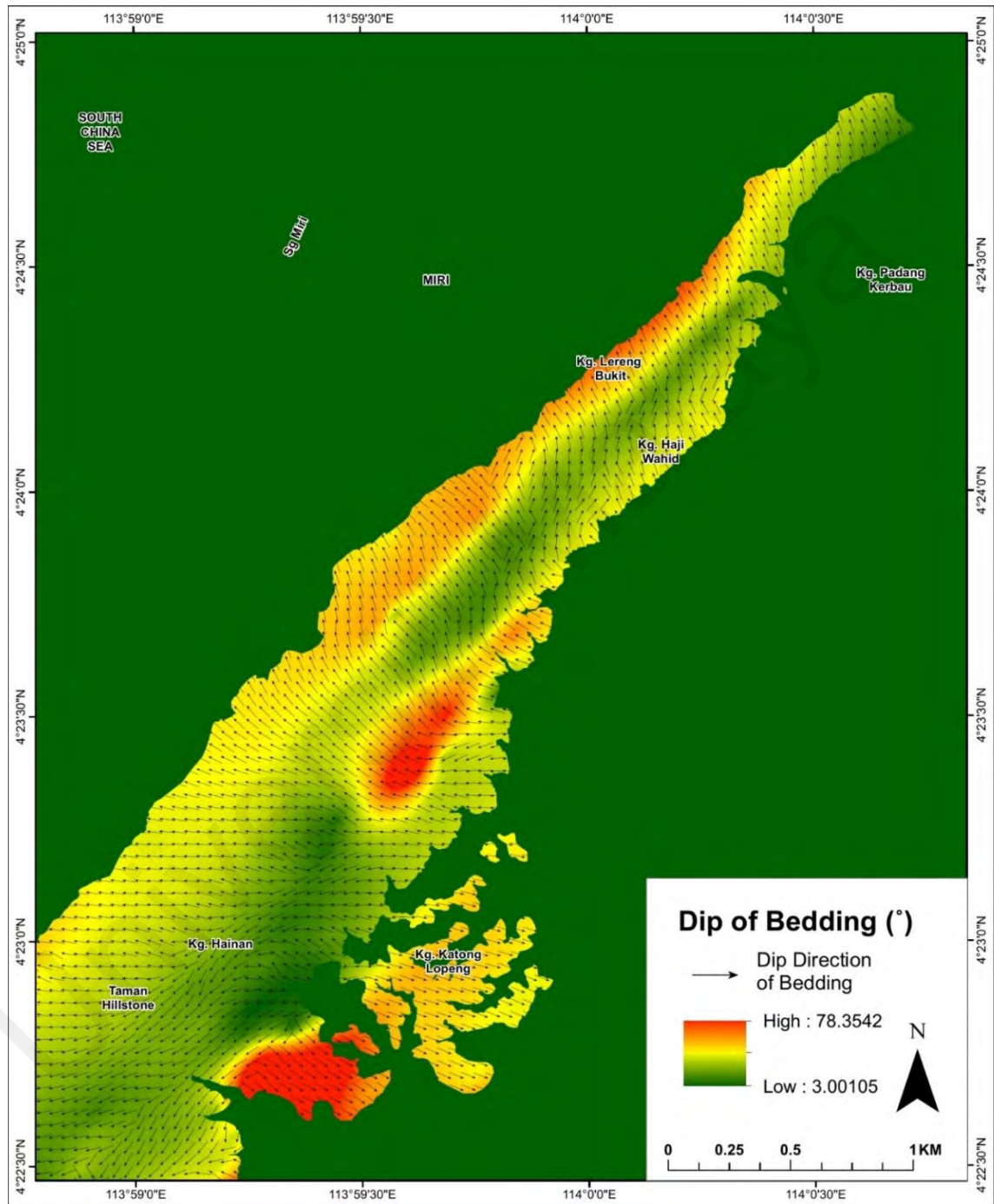


**Figure 5.22:** Interpolated dip direction of bedding overlain on dip angle map.

The next step is to extract the value of slope aspect and slope gradient to the single shapefile that now contains the attributes of  $\cos \alpha$ , and  $\cos \beta$ ,  $\cos \gamma$ , azimuth, dip direction and dip. Extraction of the cells of the slope aspect and slope gradient raster files are based on the coordinate points of the shapefile containing the former mentioned attributes. It can be run in ArcGIS using the Spatial Analyst tool. With these values embedded in the same shapefile, the calculation for the relationship between slope aspect and dip direction and relationship between slope gradient and dip can be done using the Field Calculator Tool. Decision criteria were established to assign ratings to the subclasses for the maps produced by the calculation of these relationships. This will be described further in the following subchapters, along with the final steps of this assessment. The workflow of the initial planar failure susceptibility assessment is illustrated in Figure 5.23.

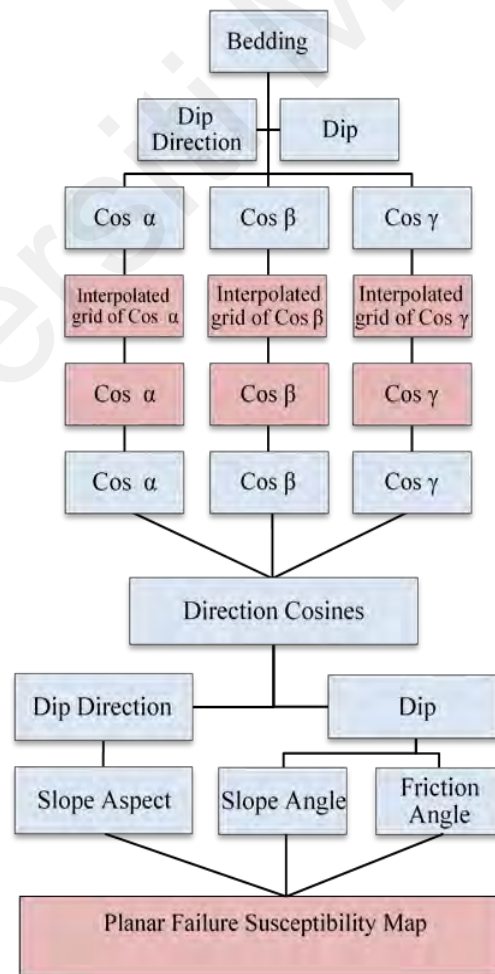


**Figure 5.23:** Workflow for the initial planar failure susceptibility assessment. The red-colored boxes indicate raster files and the blue-colored boxes indicate shapefiles.

### 5.3.2 Relationship Between Direction of Slope Face and Dip Direction of Bedding Plane

The stability of a rock slope is partly influenced by the dip direction of the discontinuity sets. Plane sliding is not possible if the dip direction of the discontinuity differs from the dip direction of the face by more than about  $20^\circ$  (Wyllie & Mah, 2004) because there will be an increasing thickness of intact rock at the end of the block which will have sufficient strength to resist failure, though a difference of  $30^\circ$  is chosen in this study. The idea behind this relationship establishment is to identify the degree of parallelism between slope aspect and dip direction of bedding plane in order to be used for the analysis in the next subchapter.

4 different relationships (Table 5.2) based on the smallest angle difference between azimuth of slope face and dip direction were established to aid in assigning different ratings of the varying relationship of discontinuity sets. The difference is obtained by subtracting the azimuth of slope face with the dip direction of the bedding plane. The scenarios for these relationships are illustrated in Table 5.3 and the stability map is shown in Figure 5.24.

**Table 5.2:** Relationship between direction of slope face and dip direction of bedding plane.

No	Smallest angle difference between aspect of the slope face and dip direction of the bedding plane	Rating	Slope stability in relation to planar failure
1	$0^\circ \leq \delta \leq 30^\circ$	4	Not favorable
2	$30^\circ \leq \delta \leq 60^\circ$	3	Less favorable
3	$60^\circ \leq \delta \leq 90^\circ$	2	Moderately favorable
4	$90^\circ \leq \delta \leq 180^\circ$	1	Most favorable

**Table 5.3:** 3D scenarios of four different relationships in Table 5.2.

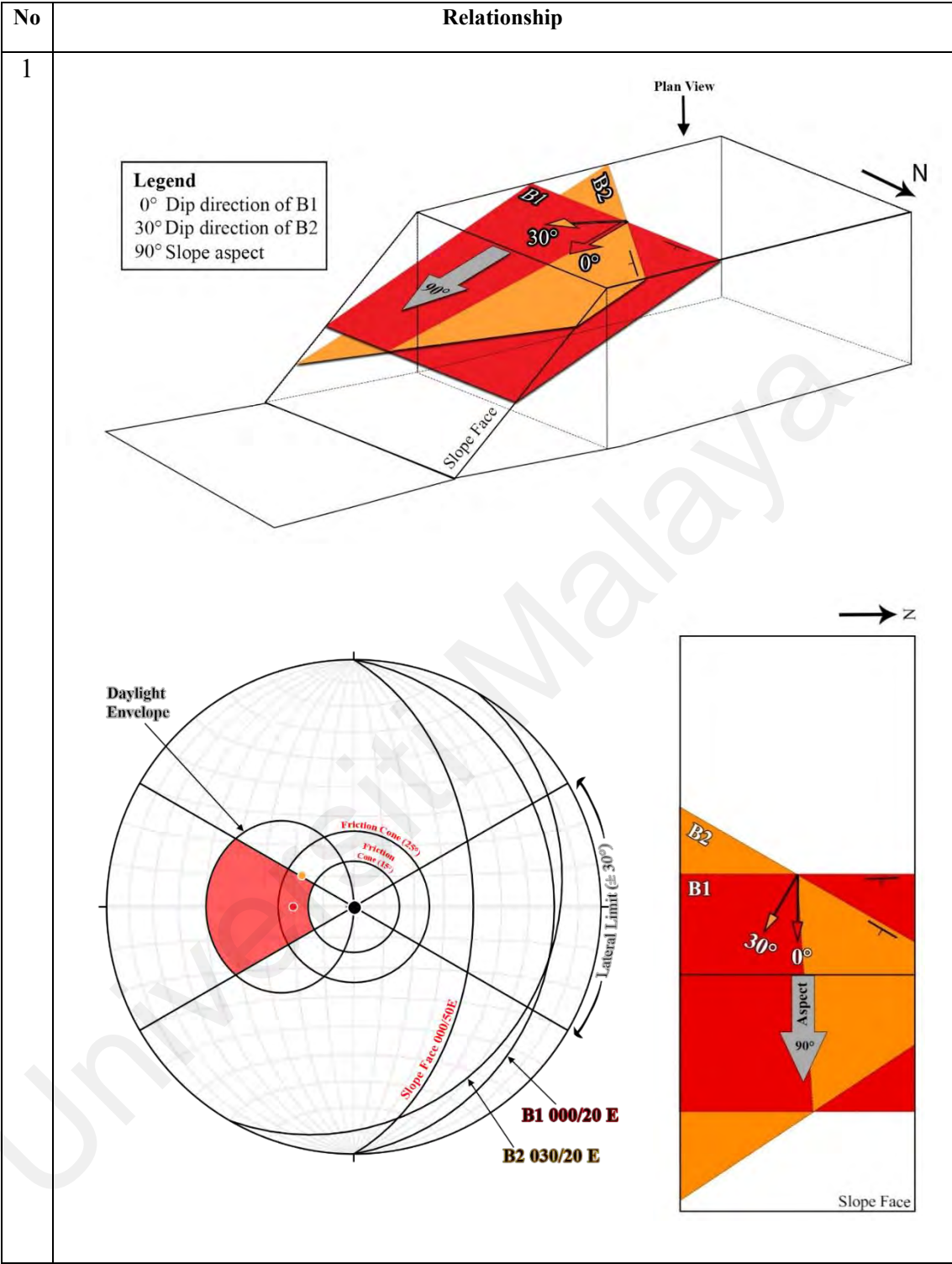


Table 5.3, continued.

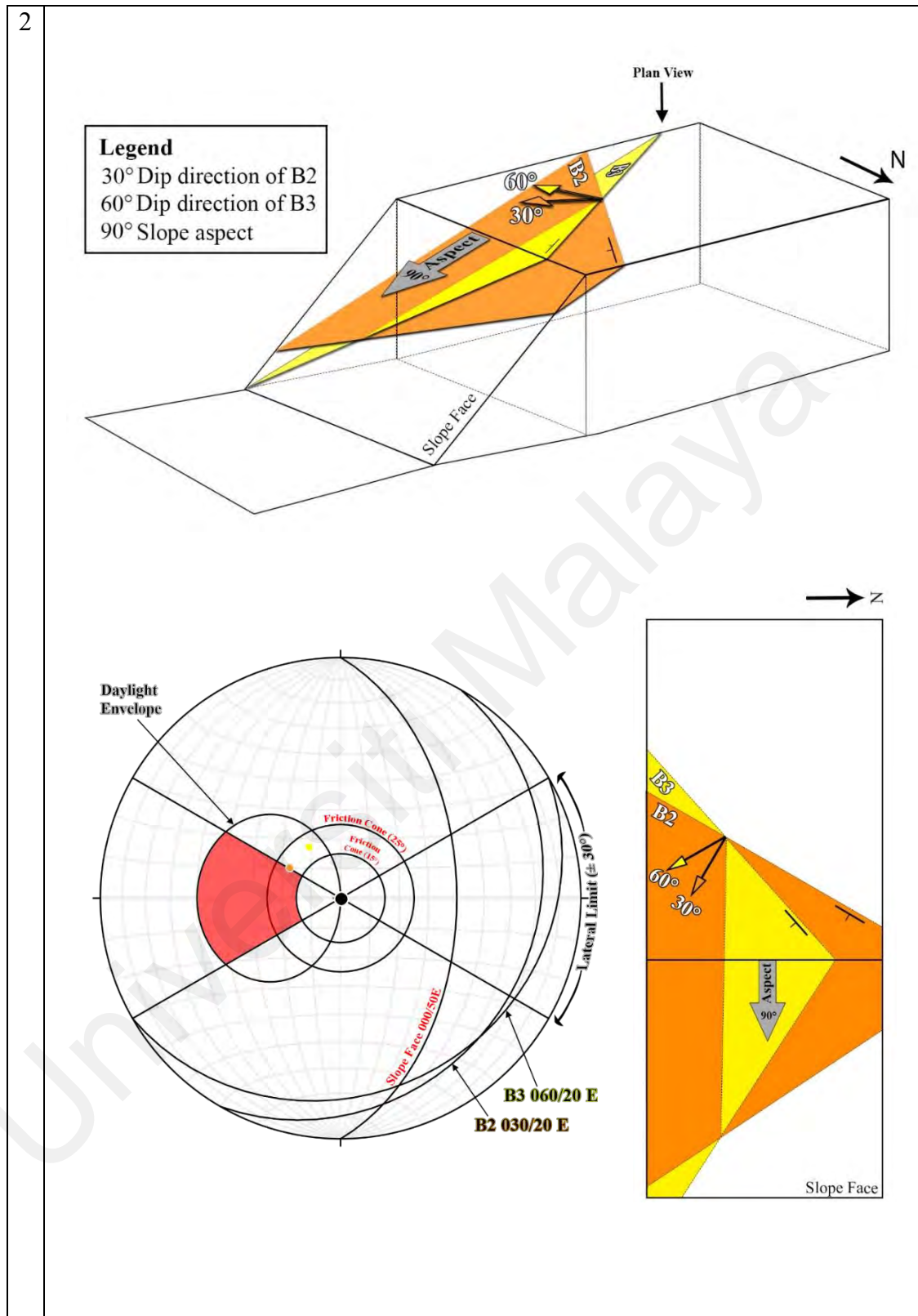




Table 5.3, continued.

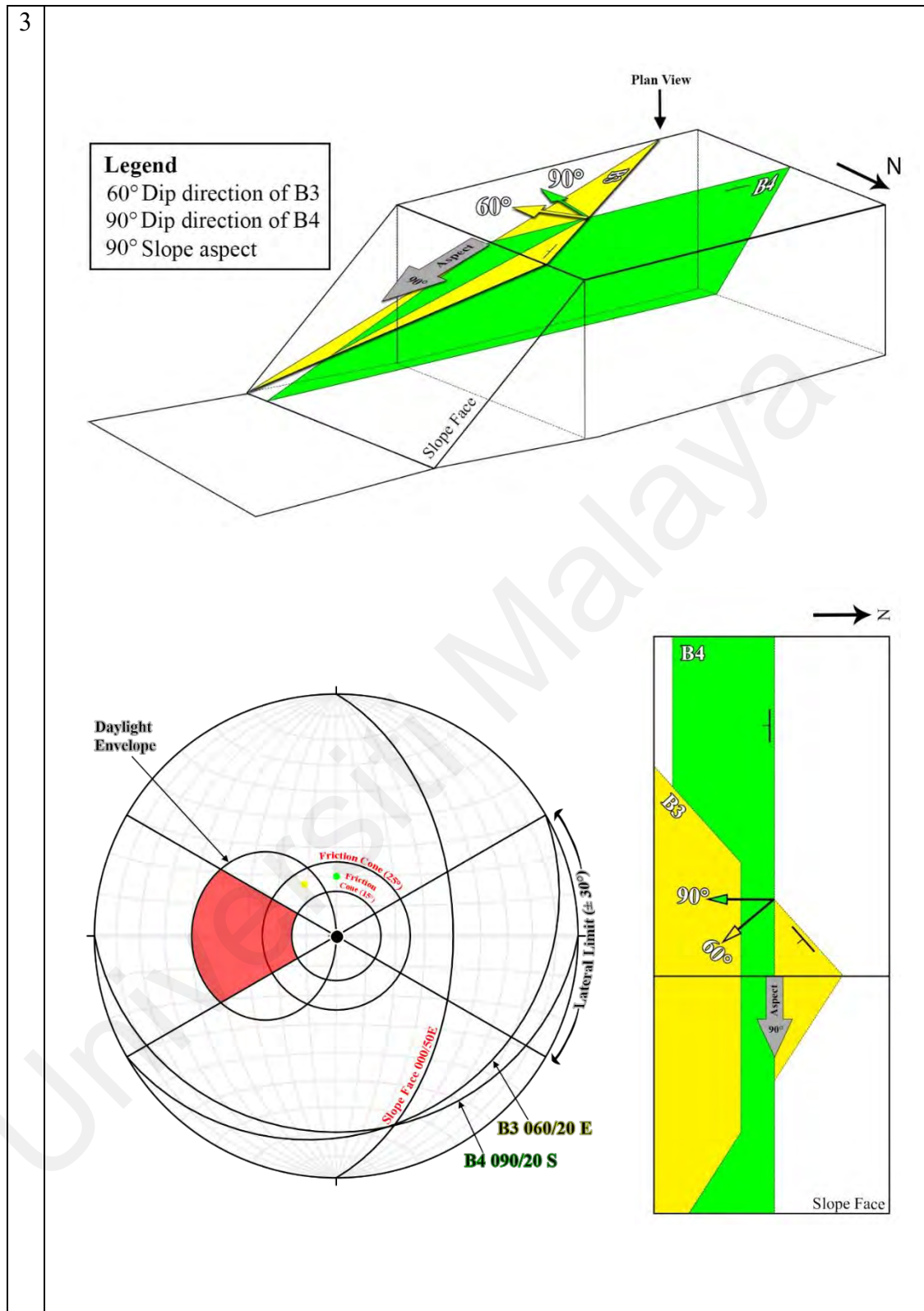
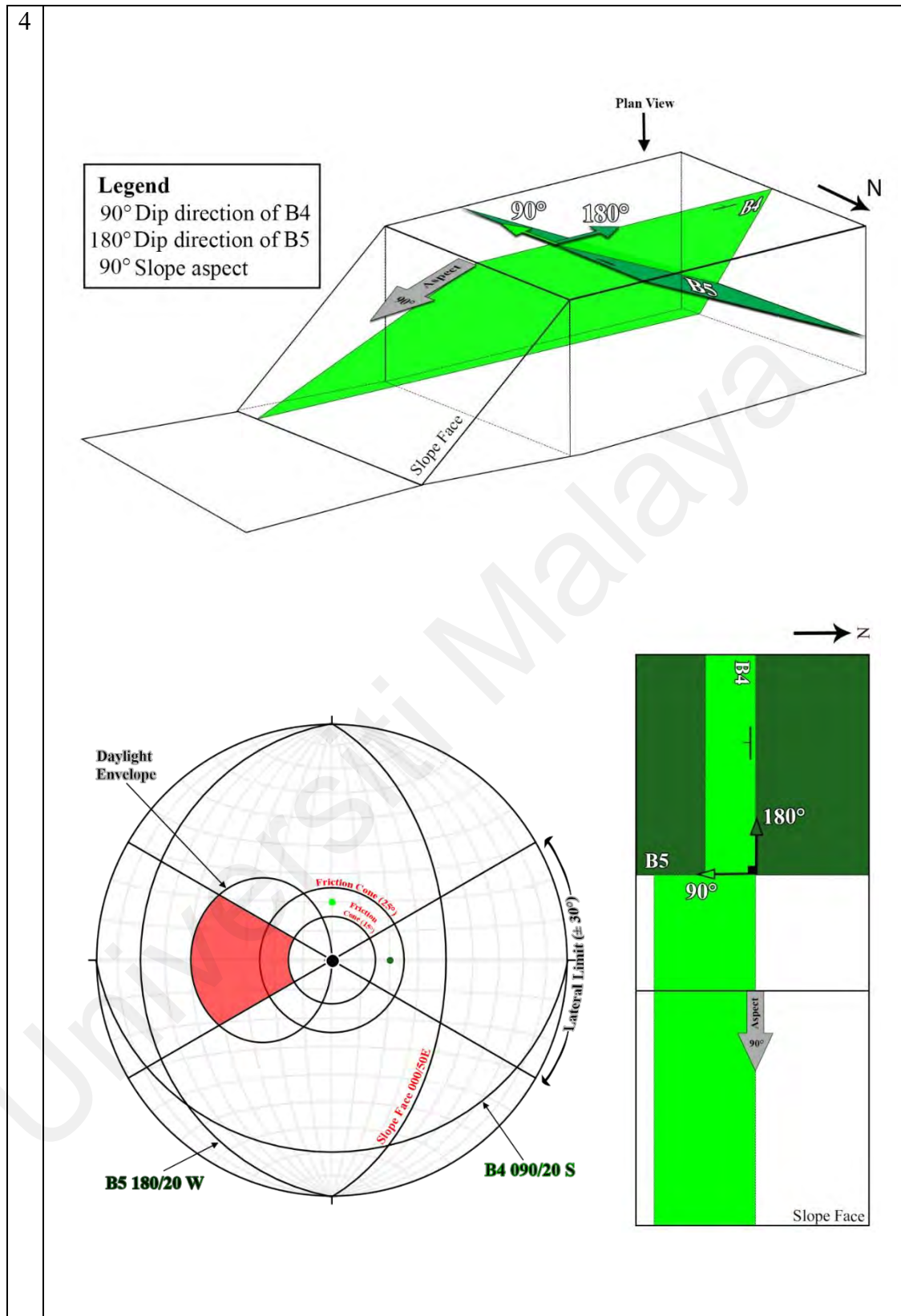
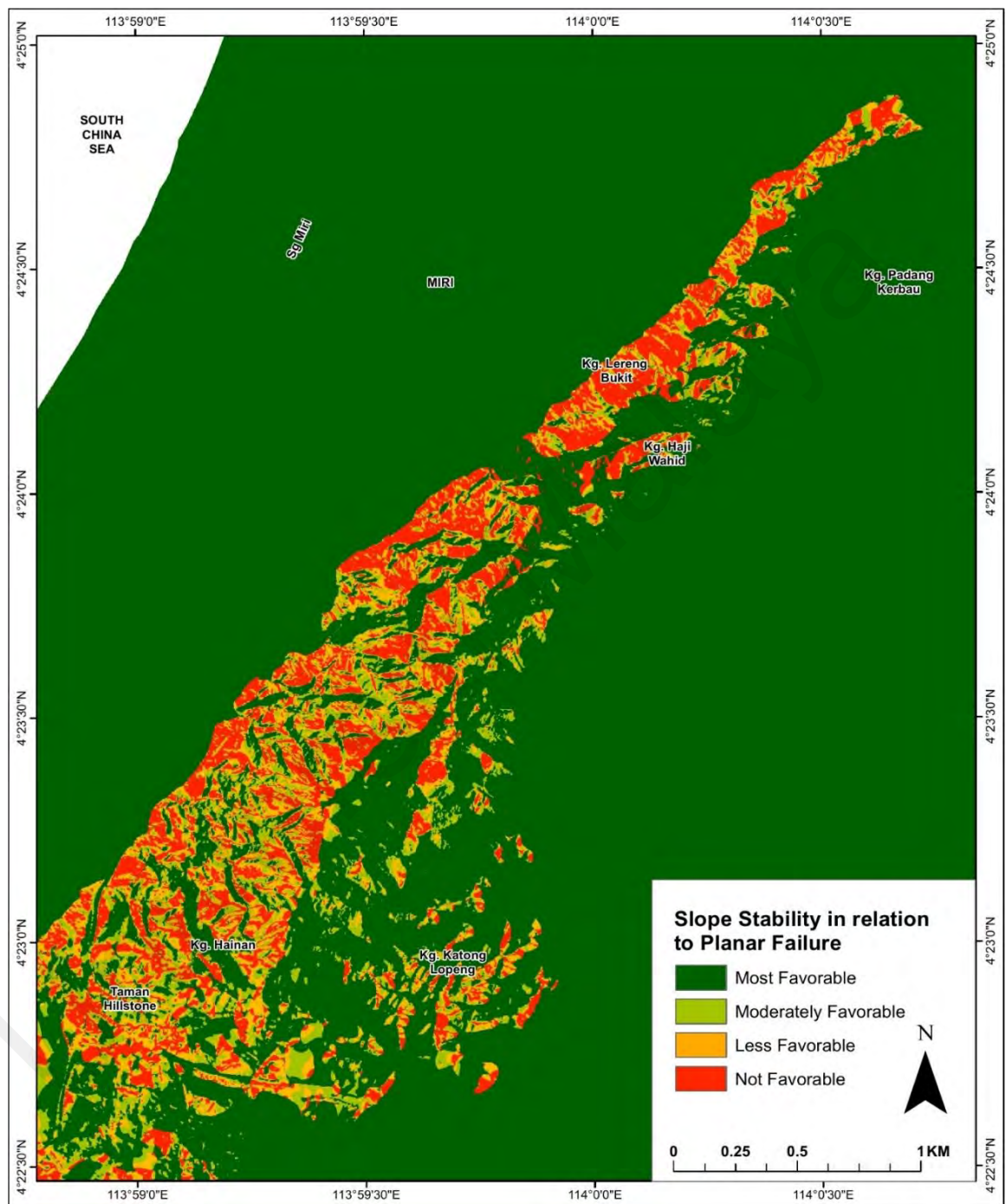


Table 5.3, continued.





**Figure 5.24:** Map of the relationship between direction of slope face and dip direction of bedding plane.

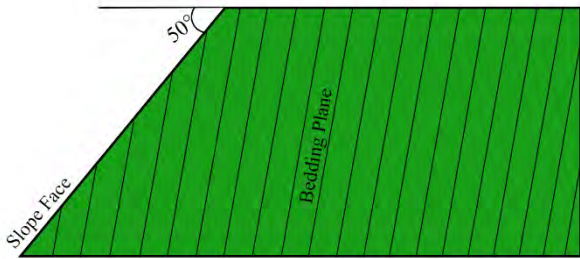
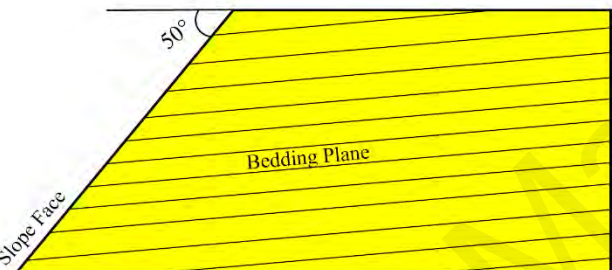
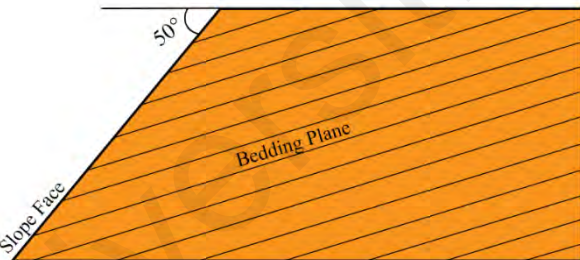
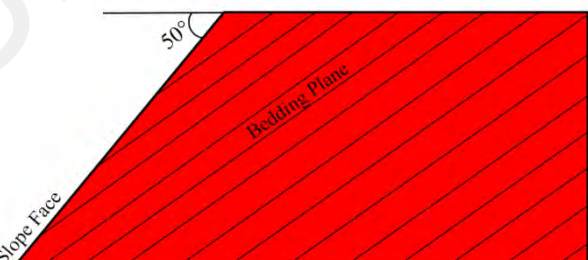


### 5.3.3 Relationship Between Slope Gradient and Dip Angle of Bedding Plane

The downward-acting gravitational force of a rock resting on a tilted discontinuity is created by a down-slope component which acts as one of the driving forces that initiates movement of a rock during failure. The stability of a rock slope depends on whether the driving forces could be outweighed by the present resisting forces which arises from the friction on the discontinuity that operates as the potential plane of sliding (Lisle & Leyshon, 2004). One of the geometrical criteria that meets the requirement of a plane failure is when a sliding plane “daylights” in the slope face which means that the dip of the plane must be less than the dip of the slope face and the dip of the sliding plane must be greater than the angle of friction of this plane (Wyllie & Mah, 2004).

This friction depends on the nature of the rock material above and below the discontinuity and the nature of the discontinuity. The component of the weight of the rock acting normal to the discontinuity surface also affects the frictional forces. Therefore, the steeper the slope, the lesser the frictional resistance on the slide mass as the gravity increases. This can be quantified by the angle of sliding friction,  $\phi$ . In this study, a range value of  $15^\circ$  to  $25^\circ$  was used to distinguish between the stable and unstable planes. Four different relationships (Table 5.4) between the dip angle of slope and bedding plane were established to determine the probability to failure of a rock slope. The stability map generated based on this relationship is shown in Figure 5.25.

**Table 5.4:** Relationship between the dip of slope face and the bedding plane.

No	Relationship between dip of slope face and bedding plane	Rating	Slope stability in relation to planar failure
1	 <p>Dip of Slope Face &lt; Dip of Bedding Plane</p>	1	Most favorable
2	 <p>Dip of Slope Face &gt; Dip of Bedding Plane, Dip of Bedding Plane<sup>o</sup> &lt;&lt; 15°</p>	2	Moderately favorable
3	 <p>Dip of Slope Face &gt; Dip of Bedding Plane, 15° ≤ Dip of Bedding Plane ≤ 25°</p>	3	Less favorable
4	 <p>Dip of Slope Face &gt; Dip of Bedding Plane, Dip of Bedding Plane ≥ 25°</p>	4	Not favorable

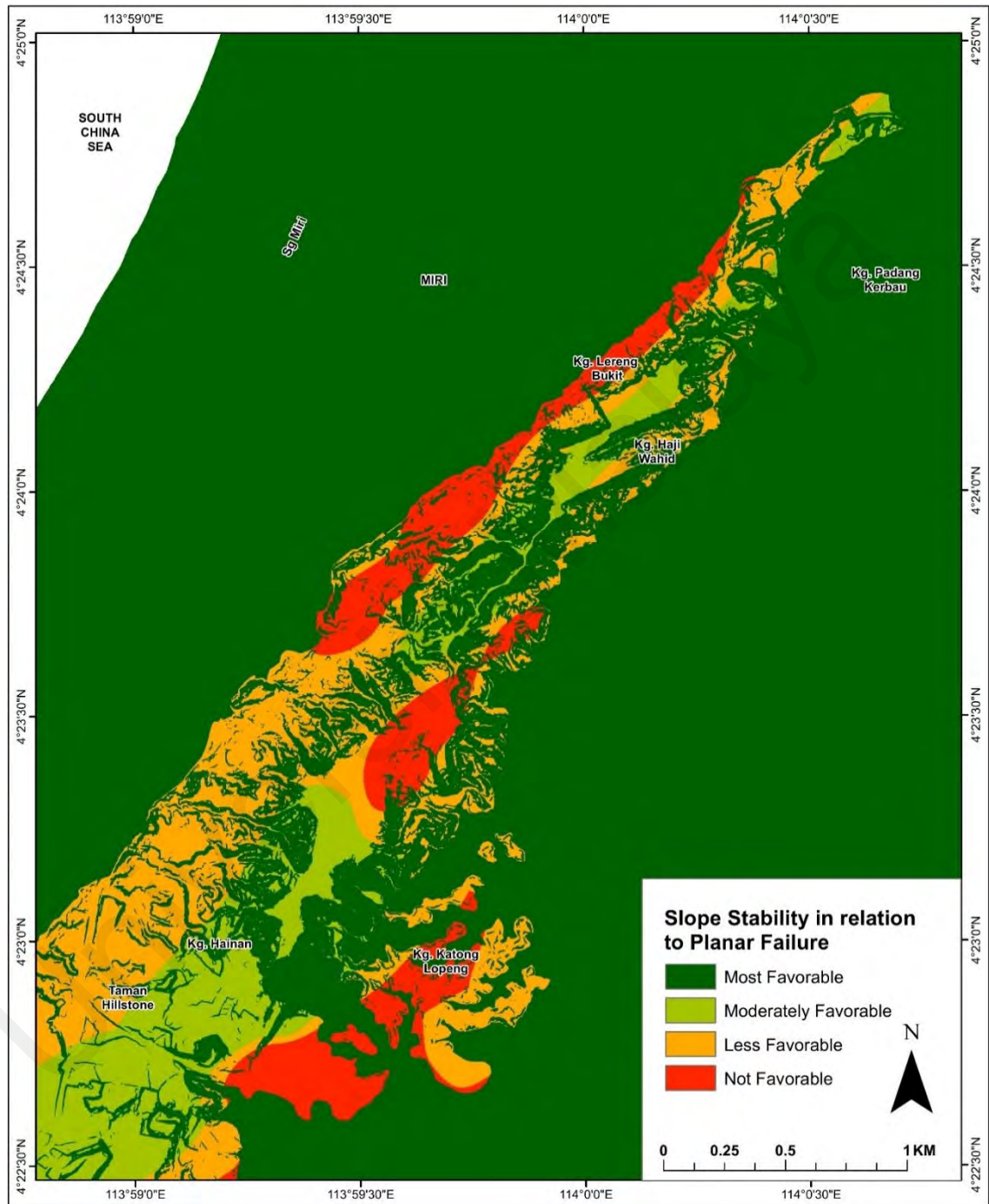


**Figure 5.25:** Map of the relationship between dip of slope and dip of bedding plane.

### 5.3.4 Result

The planar failure susceptibility map is the combination of the relationships present between; slope aspect and dip direction; slope gradient and dip; friction angle of slope and dip. All these relationships are established to determine the degree of parallelism of two surfaces, the daylighting and sliding potential. The production of this map highlights the planar failure susceptibility of the slopes as a factor on its own, among other landslide-controlling parameters.

**Table 5.5:** Planar failure susceptibility classification matrices.

Dip Direction vs Slope Aspect	Dip vs Slope Gradient				
	Rating	1	2	3	4
	1				
	2				
	3				
	4				

**Table 5.6:** Planar failure susceptibility descriptors.

Class	Name	Description
	Most Favorable	Daylighting slope is not present. Planar failures very unlikely to occur in the area but consideration to potential problems of the adjacent areas must be considered.
	Moderately Favorable	Daylighting slope is unlikely to be present. Planar failures are not likely to happen but consideration to potential problems of the adjacent areas must be considered.
	Slightly Favorable	Possibility of presence of daylighting slope is low. Planar failure problems of small to moderate scale may exist or possible to happen after major changes in ground conditions and triggering factors are present.
	Less Favorable	Possibility of presence of daylighting slope is moderate. Planar failure in moderate to large scale probably exist in the past and could reoccur if the combination of contributing factors exists in the adverse event of an intense or continuous rainfall period.
	Not Favorable	Possibility of presence of daylighting slope is high. Planar failure in moderate to large scale have occurred in the past and may be active if the combination of contributing factors exists in the adverse event of an intense or continuous rainfall period.

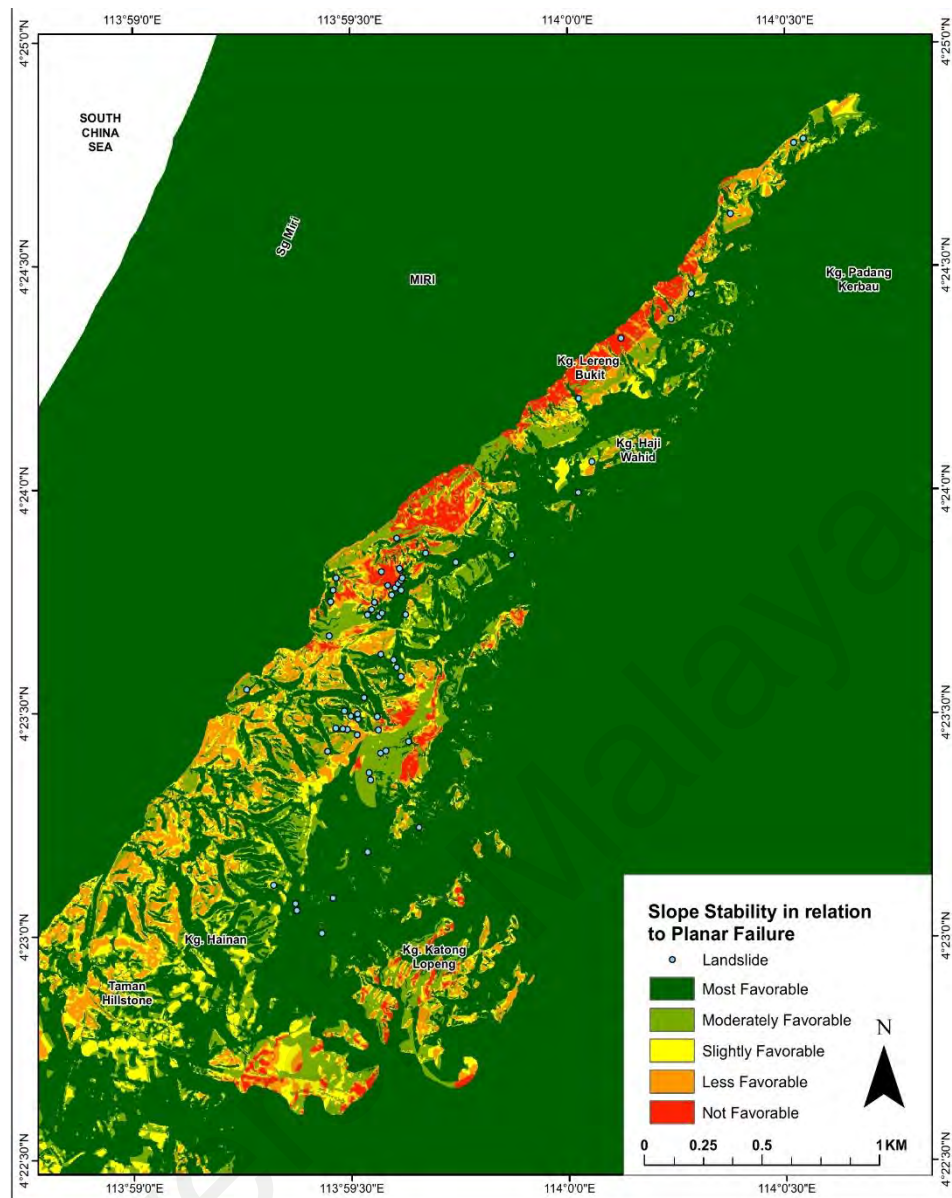


**Figure 5.26:** Planar failure susceptibility map of Canada Hill.

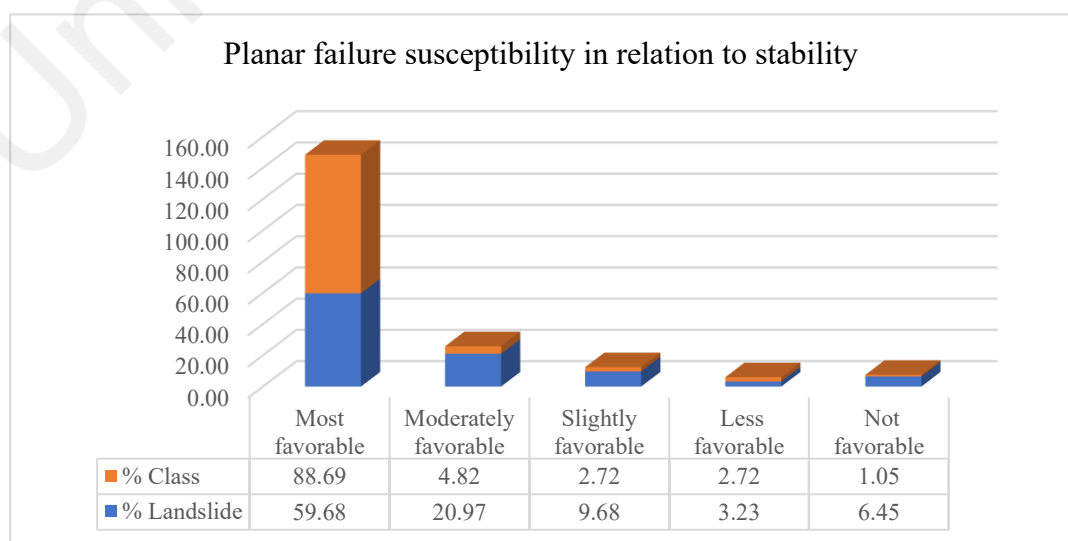


**Figure 5.27:** Histogram of landslide occurrence and areal extent of the subclasses on the planar failure susceptibility map.

The generation of the planar failure susceptibility map is done by combining the weighted maps produced in subchapter 5.3.2 and subchapter 5.3.3. The degree of influence (%) is similar for both weight maps. The classification of the planar failure susceptibility is divided into 5 classes based on the matrix accomplished in Table 5.5 and described in Table 5.6. The planar failure susceptibility map was reclassified based on the decision rules and was overlain with the landslide map to obtain the number of landslide occurrences in each cell of the map (Figure 5.26). The analysis of landslide occurrence will aid in assigning the contribution ratio of the planar failure susceptibility map. Following paragraph will use the term “stability” to explain the effect on potential planar failures only.

The histogram of landslide occurrence overlain on the planar failure susceptibility map as shown in Figure 5.27 indicated that most of the landslides occurred in the area of most favourable stability, which accounts for 59.68% of the landslide occurrence while the non-favourable stability area accounts for 6.45%. Probable explanation of this number is because most of the landslides that were recorded in the inventory are shallow minor landslides that failed rotationally as opposed to having planar failure mechanism in addition to the total area covered by the non-favourable areas are only 1%. However, the most destructive landslide events that were recorded in the Canada Hill area, which includes LS1 and LS2 which plots in the non-favourable stability area has a planar failure mechanism. It is inferred that the planar failure occurrence in the study area is not frequent, but the effects are extensive and devastating. Hence, the subclass representing unfavourable stability was given the highest rating for the subsequent landslide susceptibility assessment.

#### **5.4 Slope Gradient**

Slope gradient is considered as a very important parameter in landslide susceptibility assessment. In a study done by Reichenbach *et al.* (2018), slope gradient made up 10.5%

of the inputs used in landslide susceptibility models from 565 works done from 1983 to 2016, proving the importance of slope gradient as a landslide-controlling parameter.

This study utilized the slope gradient parameter to understand the morphological character, rate of soil erosion and mass wasting. Generally, steeper slopes are relatively unstable compared to gentle slopes thus, landslide frequency will increase with slope gradient. This parameter was divided into 6 classes (Figure 5.28). Figure 5.29 showed that the slope gradient with a reading of  $15^{\circ}$  to  $25^{\circ}$  recorded the highest number of landslides (35.48%) as opposed to the higher slope gradient. This may indicate that the direct control of slope gradient on the slope failure is low. There are also no landslide occurrences in the steepest slopes ( $60^{\circ}$ - $90^{\circ}$ ) because this class has a very small areal extent (0.03%), while the  $15^{\circ}$ - $25^{\circ}$  slopes have a larger areal extent (6%). Slope gradients ranging from  $5^{\circ}$  to  $15^{\circ}$ ,  $25^{\circ}$  to  $35^{\circ}$  and  $35^{\circ}$  to  $60^{\circ}$  each recorded moderate amount on landslides ranging from 11 to 15 landslides. Precaution should still be taken on areas with higher slope gradient depending on the strength of slope-forming materials. The heavily jointed, young rocks of Miri Formation may impose some weakness in strength of the formation as steepness increases, especially when subjected to a triggering factor such as rainfall. The weak rocks in this formation were considered during the assignation of the highest degree of influence in the heuristic approach.

## **5.5 Geology**

Canada Hill is divided into 5 classes of geology namely the Fill Material, Miri Formation, Quaternary Deposits, Seria Formation and Terrace Deposits (Figure 5.30). 96.7% of the observed landslides are in the Miri Formation while the remaining 3.3% occurred in the Terrace Deposits (Figure 5.31). Miri Formation occupies the whole stretch of Canada Hill with an areal extent of 18.42% across the study area while Seria Formation outcrops at the SE of the hill making up 2.47%. The nature of the interbedded sandstone and shale which formed this hill are highly sensitive to extrinsic factors, leading to the



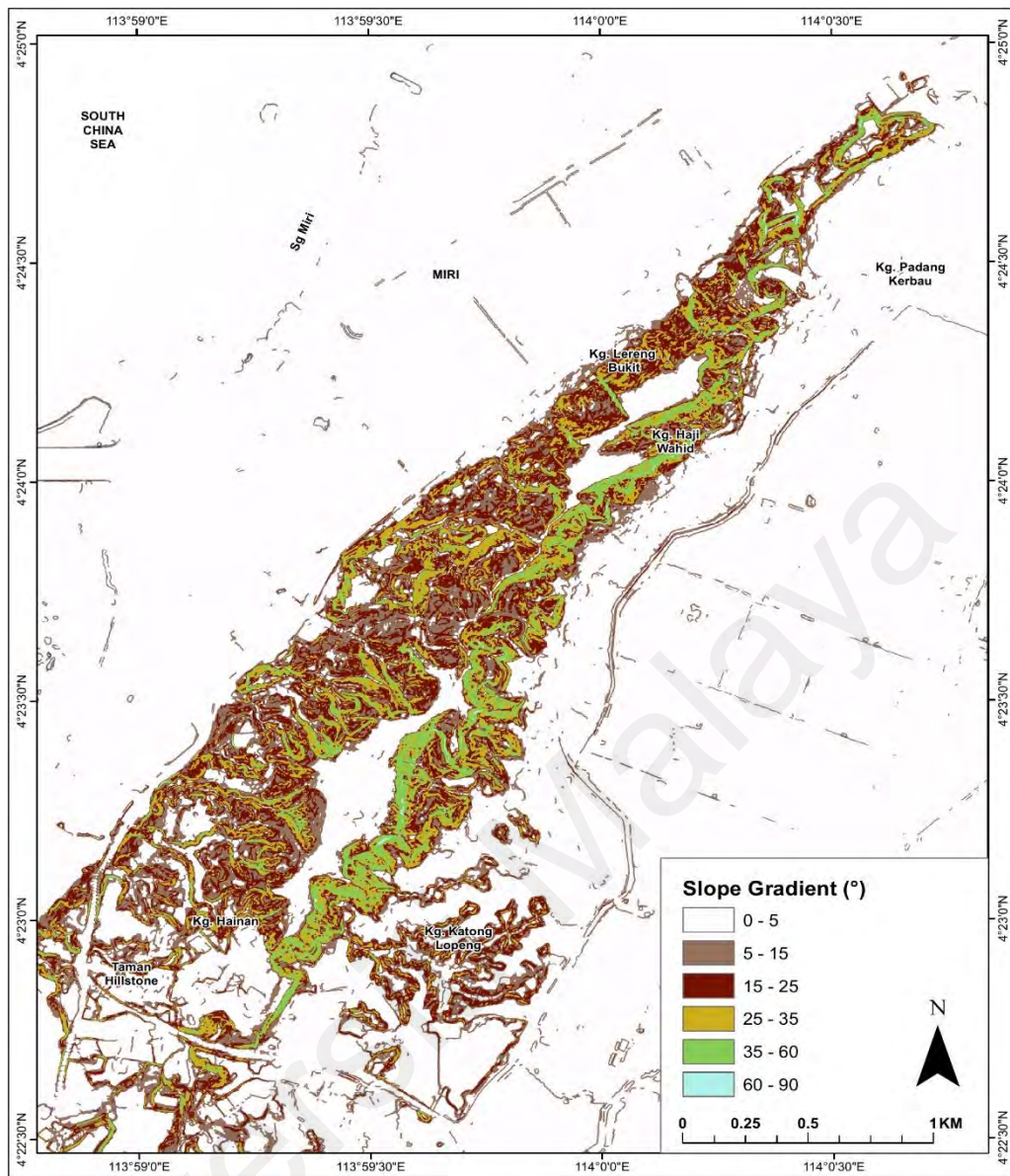


**Figure 5.28:** Slope gradient map of Canada Hill.

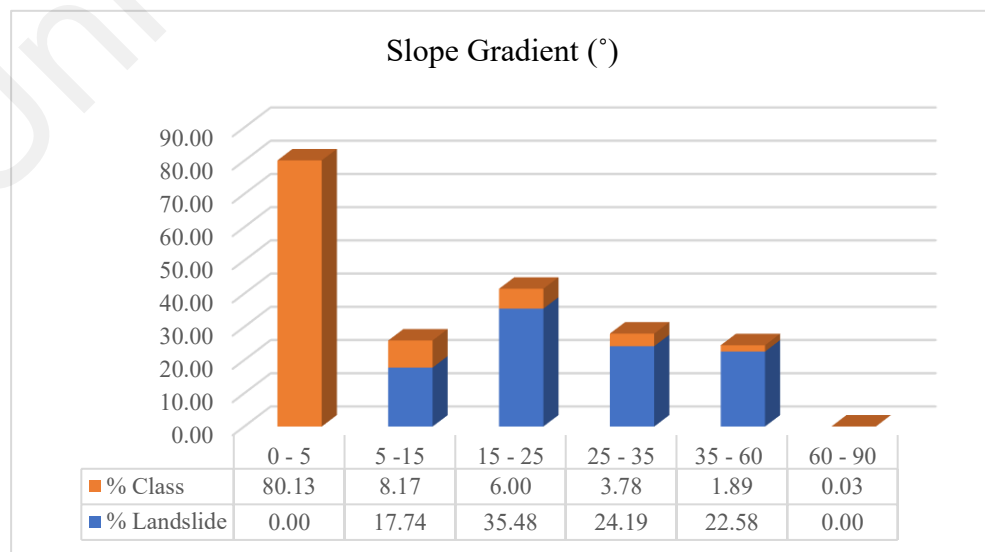


**Figure 5.29:** Histogram of landslide occurrences and areal extent of the subclasses on the slope gradient map.



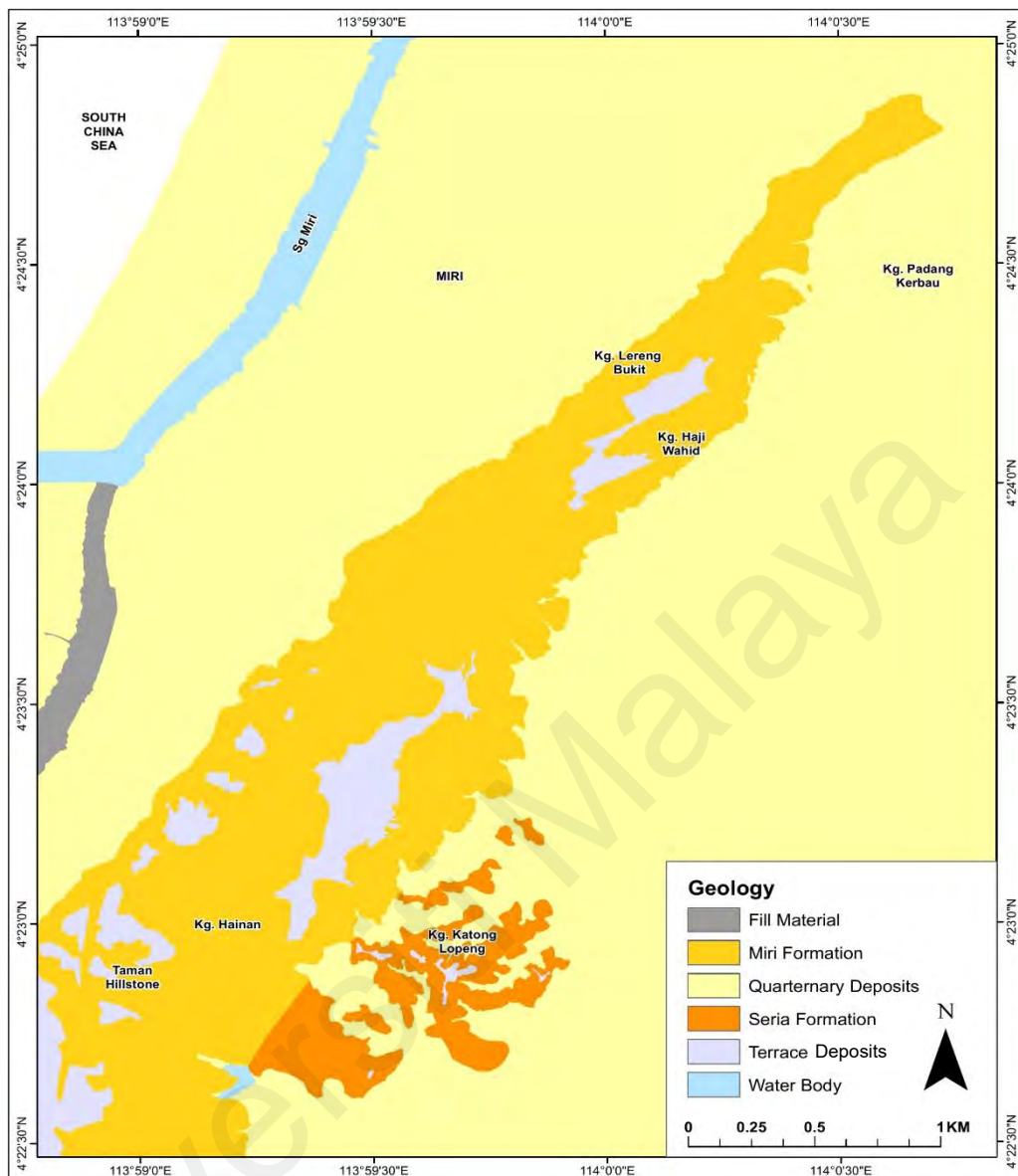


**Figure 5.30:** Geology map of Canada Hill.

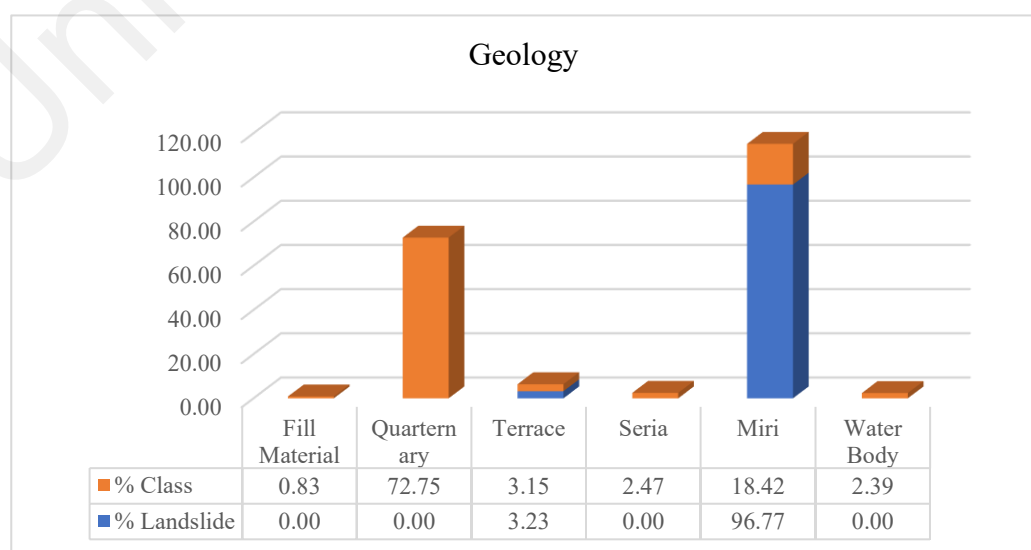


**Figure 5.31:** Histogram of landslide occurrences and areal extent of the subclasses on the geology map.

acceleration of physical and chemical weathering, owing to a relatively young age of deposition and uplift. The suitable condition for podzolization process which leads to decrease in cohesion, profound mineral alteration in shale increasing the rate of shale slaking, the low plasticity index of the shale and the highly porous sandstone are also the main factors in assignment of the contribution ratio of this parameter.

## **5.6 Distance to Lineament**

Geological structures have a profound role in the landslide susceptibility. Joints and major faults present around the hill, which may have formed more complex fault system with branch thrusts, introduces tectonic stress the bedrocks within the zone. Therefore, bedrocks become highly unstable, in line with the observation of the release planes which caused landslides to occur. The distance to lineament was assigned to 5 buffer regions (Figure 5.32) and a higher number of landslides occur as the zones close in into the zone of lineament (Figure 5.33).

## **5.7 Normalized Difference Vegetation Index**

Normalized Difference Vegetation Index (NDVI) indicates the vegetation cover of an area. The higher the NDVI value, the higher the vegetation cover. The potential for soil and terrain erosion increases with decreasing vegetation density (He *et al.*, 2019). Vegetation density greatly affects soil hydrology through the increase of rainfall interception, infiltration and evapo-transpiration, which decreases the chance of oversaturation. Roots reinforcement from the vegetation cover can increase soil strength, considerably reducing the rate of landslide occurrence (Yalcin *et al.*, 2011).

The study area was divided into 4 classes of NDVI (Figure 5.34). The barren/built up areas are developed areas adjacent to Canada Hill while dense vegetation covers most of Canada Hill with occasional areas being covered with sparse and moderate vegetation where human settlement is present. Most of the landslide occurrence occupy the areas with moderate and dense vegetation cover (Figure 5.35) which may indicate the effects

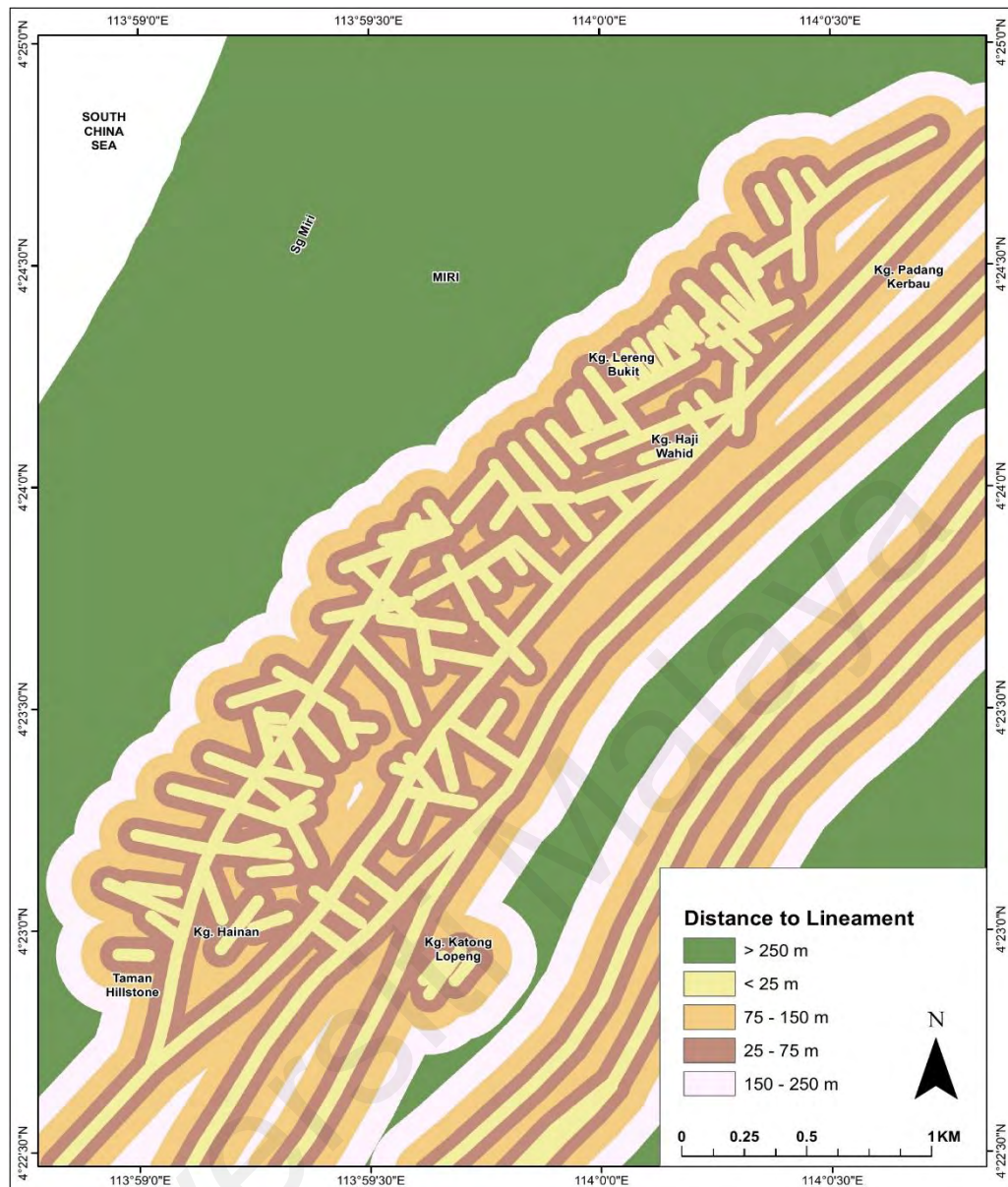


**Figure 5.32:** Distance to lineament map of Canada Hill.

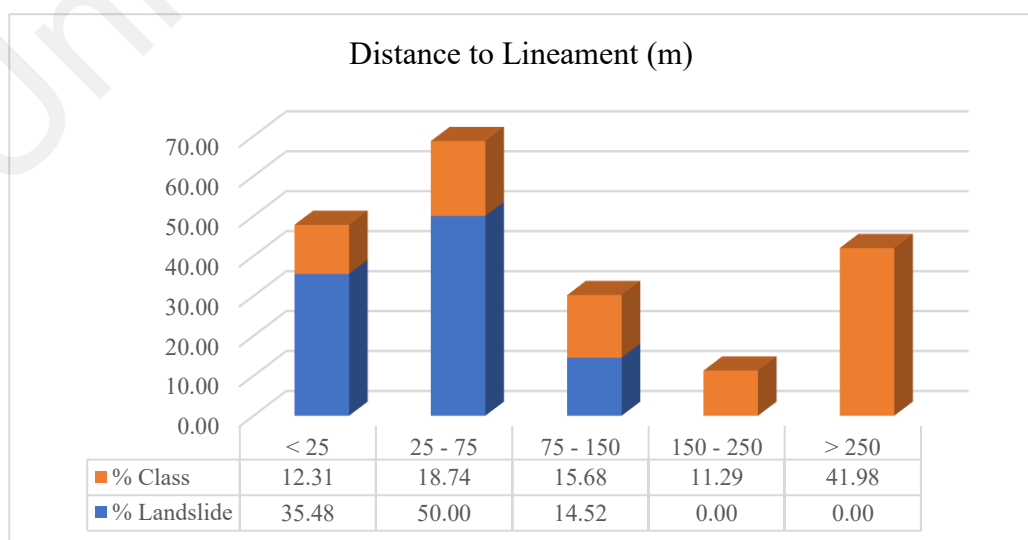


**Figure 5.33:** Histogram of landslide occurrences and areal extent of the subclasses in the distance to lineament map.

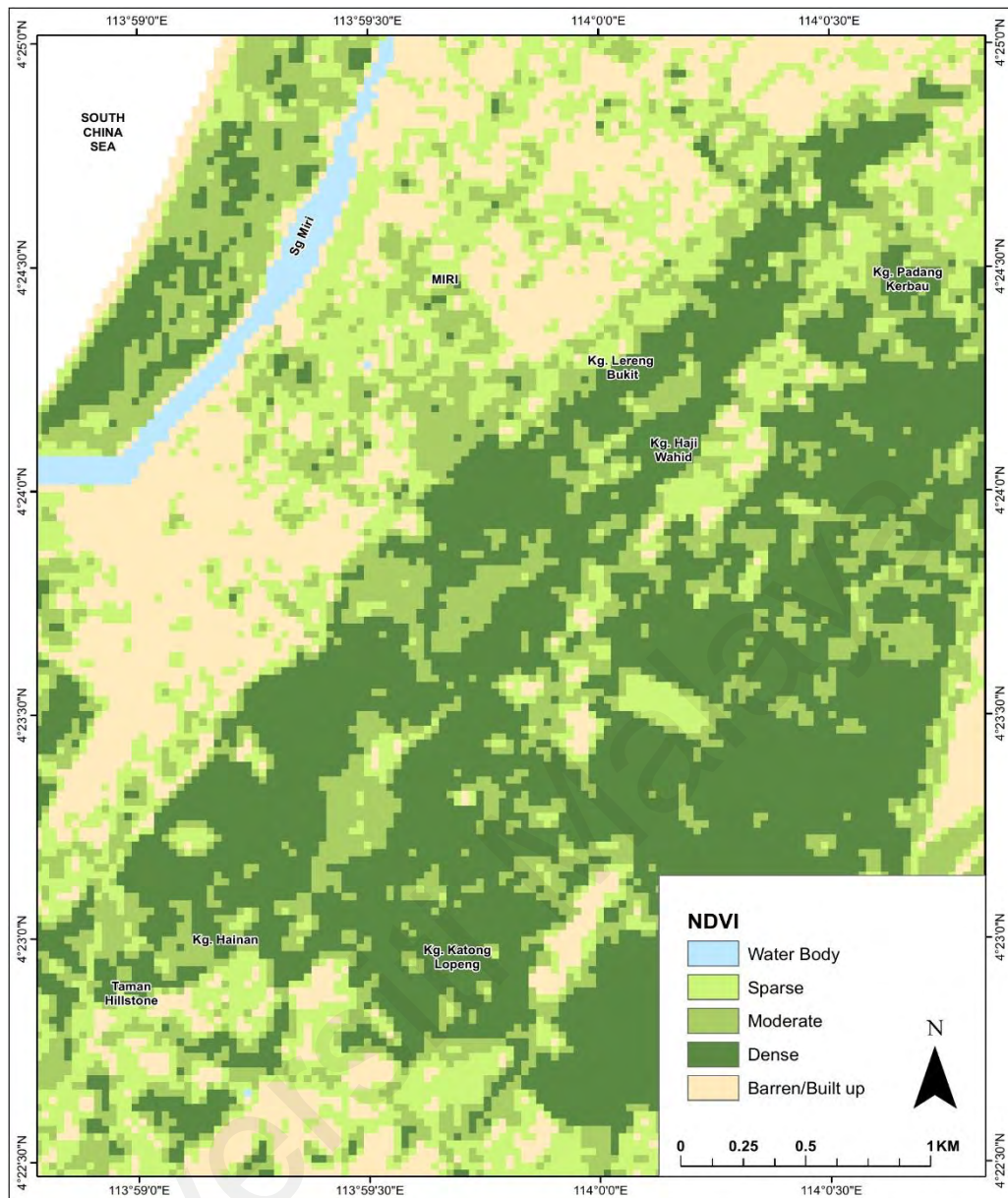


**Figure 5.34:** NDVI map of Canada Hill.

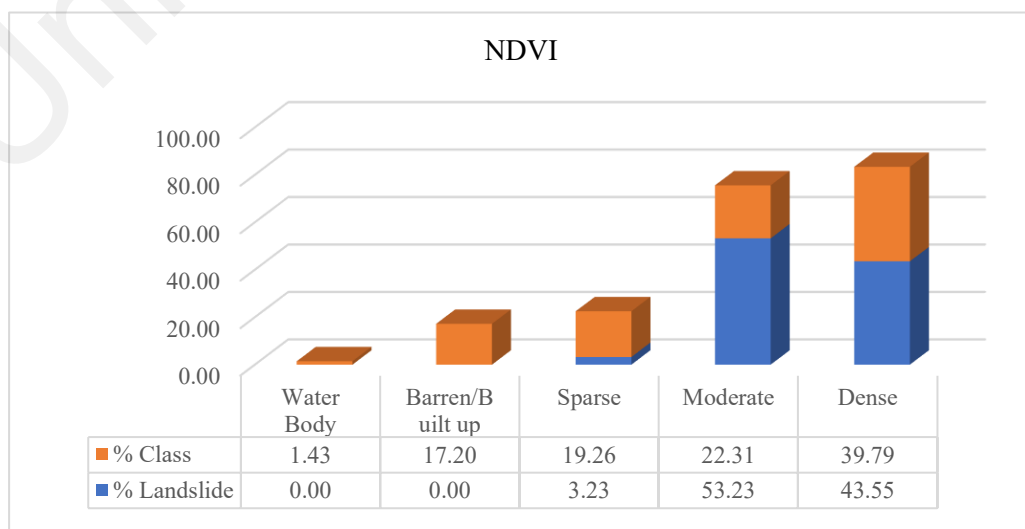


**Figure 5.35:** Histogram of landslide occurrences and areal extent of the subclasses in the NDVI map.

of cultivation activities seen along the slopes of the hill. The effect of converting a forested slope into a cropland will be permanent and landslides will still be common because as vegetation removal occurs cyclically, the window-of-susceptibility is open until the roots re-establish for about 5-7 years in humid tropical weather (Forbes & Broadhead, 2011).

## **5.8 Elevation**

The elevation of the study area was divided into five classes (Figure 5.36). The effects of elevation on the landslide occurrences depend to the lithological character of the units. Higher elevations may also promote the development of first order streams, resulting in slope steepening (Mandal & Mandal, 2017). The occurrence landslides in the study area indicates a higher instability with increasing elevation (Figure 5.37). However, this is limited to its' relationship with the strength of the lithology and steepness. The highest elevation areas are underlain by a relatively thin layer Terrace Deposit which limits its' effect to the slope.

## **5.9 Slope Curvature**

Slope curves as either convex or concave and each has different responses to stability, based on their moisture retention capabilities. The surface of concave slopes can retain moisture for a long time and indirectly may become a catchment for sediments to accumulate from overland flow. On the other hand, convex slopes act oppositely by draining out moisture immediately upon receipt of moisture. Landslides are more prone in concave slopes than convex slopes.

The slope curvature is divided into 4 classes (Figure 5.38). Flat areas are divided into Flat (A) and Flat (B) to differentiate the flat areas at two varying elevations which has different influences on the overall susceptibility. Figure 5.39 shows that 64.5% of the landslides occurred in convex slopes.



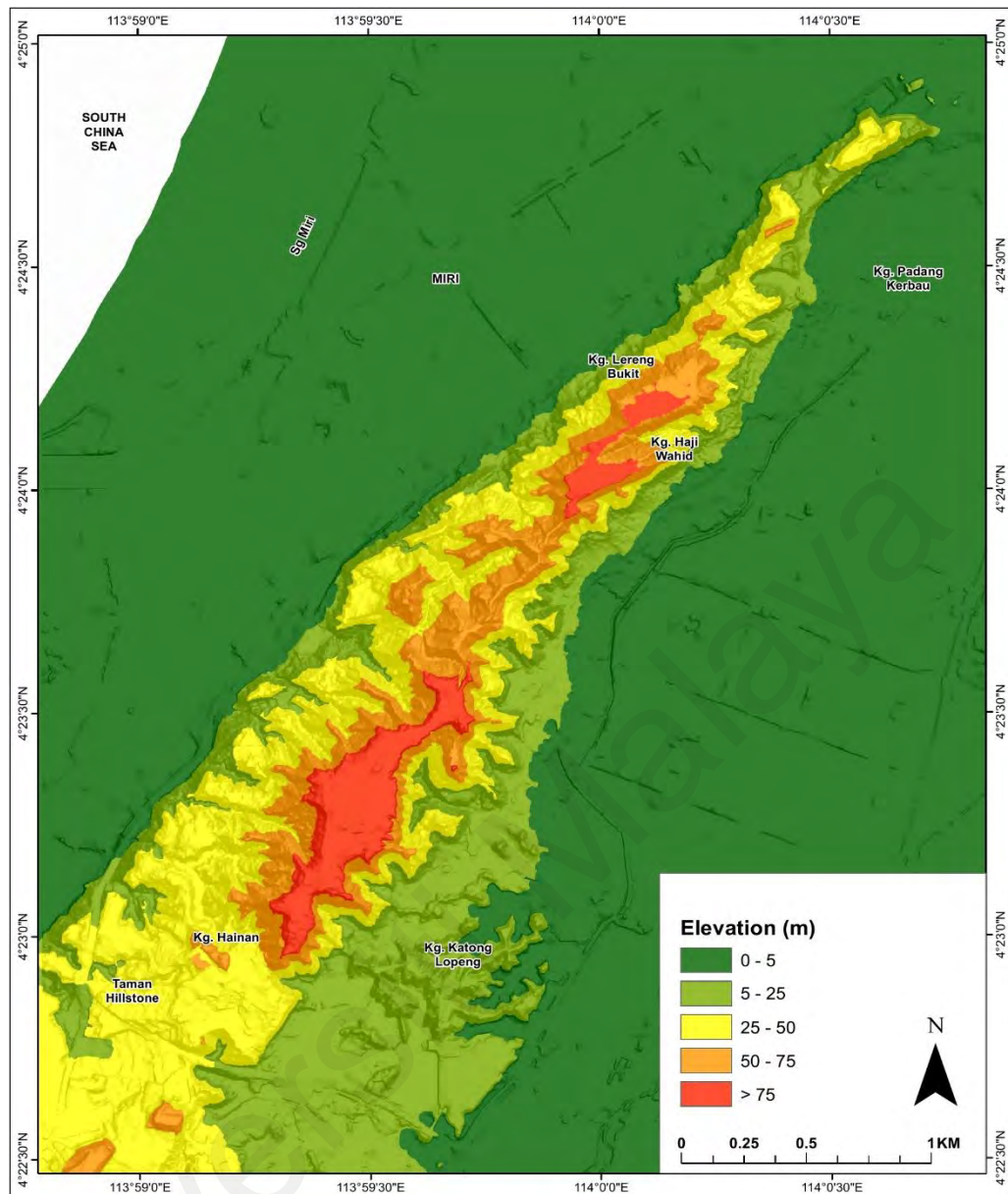


**Figure 5.36:** Elevation map of Canada Hill.

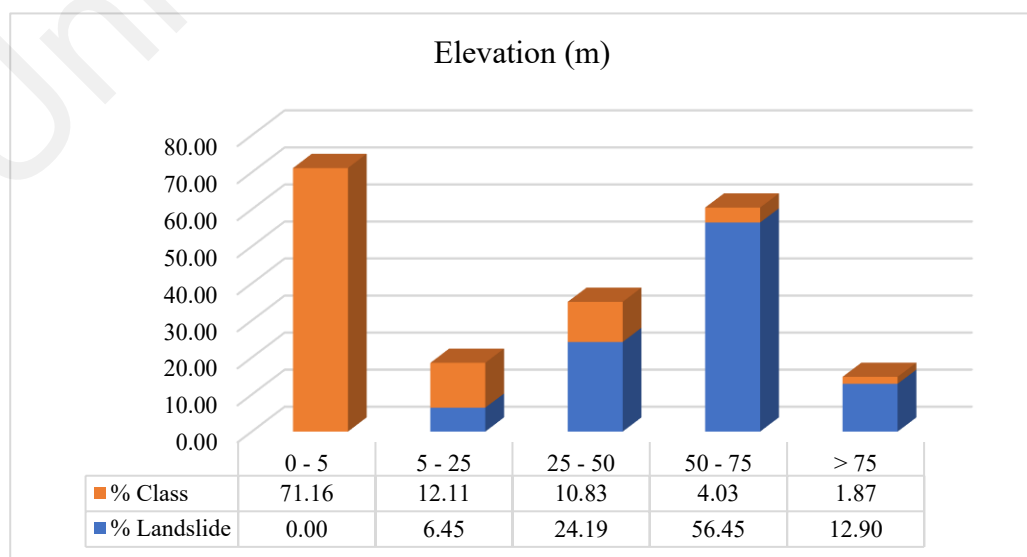


**Figure 5.37:** Histogram of landslide occurrences and areal extent of the subclasses in the elevation map.

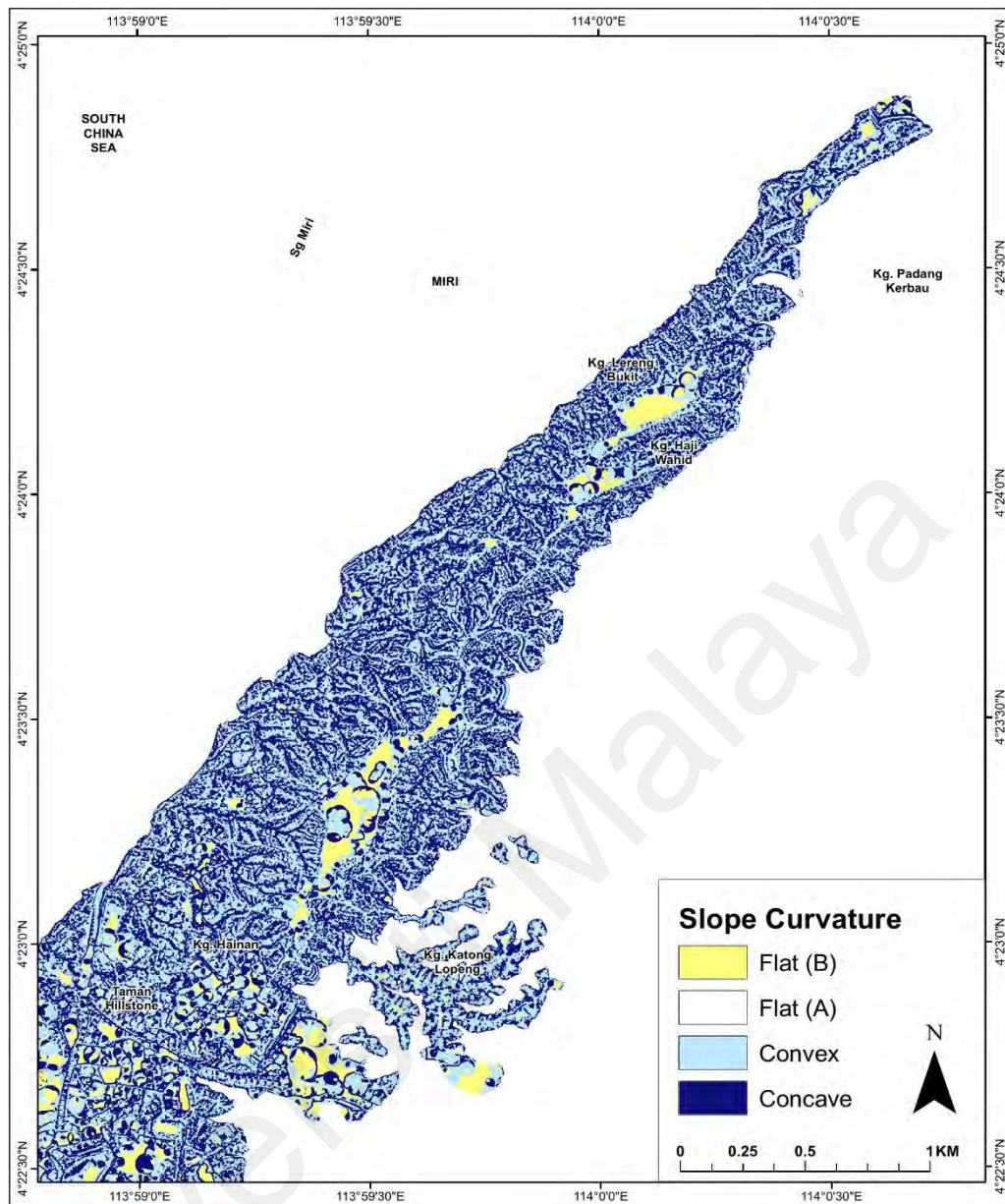


**Figure 5.38:** Slope curvature map of Canada Hill.

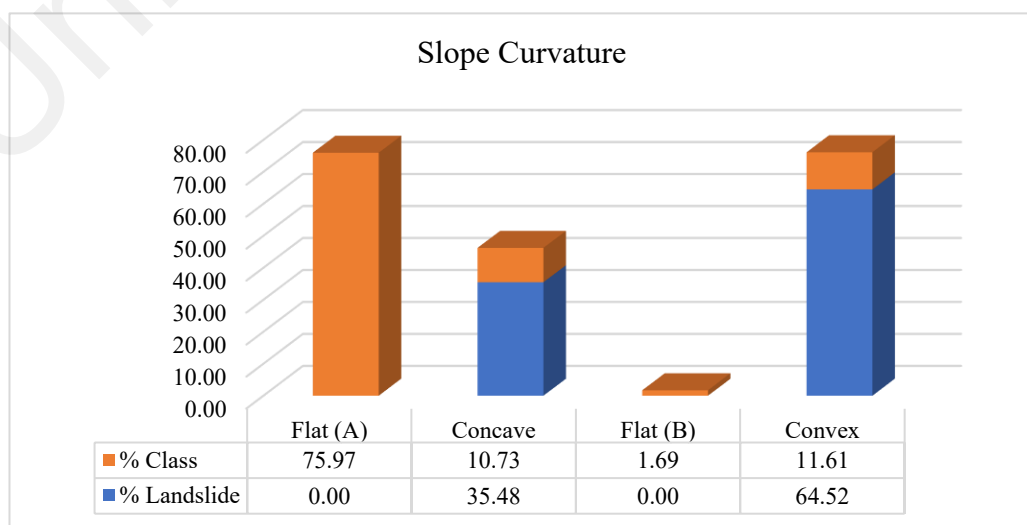


**Figure 5.39:** Histogram of landslide occurrences and areal extent of the subclasses in the slope curvature map.



### 5.10 Slope Aspect

The slope aspect in this study is effectively used to identify slope segments that are most susceptible to landslides. Parameters that are assessed from slope aspect include exposure to sunlight, drying winds, rainfall and discontinuities (Yalcin *et al.*, 2011). Visual representation of slope aspect in a map also enables the representation of the direction of flow based on the orientation of ridges, spurs and valleys which in turn, can delineate places of potential water surplus region (Mandal & Mandal, 2017).

Slope aspect is divided into 9 classes as shown in Figure 5.40. Surface tools in ArcGIS was utilized for the generation of the slope aspect from a DEM. Landslide occurrences are common in the slopes facing E, SW, W, NW (Figure 5.41), with the highest recorded in NW slopes (19.35%).

### 5.11 Cut and Fill

Cut and fill areas are utilized as a parameter in this study to determine the effects of anthropogenic factors to landslide susceptibility. Prolonged exposure of bedrocks on cut slope to weathering may pose instability problems during extreme weather events. Cut slopes and embankments that are not regulated may also lead to instability, often affecting main roads or service facilities. The cut and fill parameter was divided into 3 classes (Figure 5.42). 96.8% of the landslide occurrences were located at undisturbed areas (Figure 5.43) which denotes a higher influence of natural slopes to landslides. This is also due to majority of the study area is occupied by the undisturbed areas with an 83.50% areal extent compared to the cut areas with only a 6.02% areal extent.

### 5.12 Summary

Analysis of the relationship between landslide distribution and the landslide-controlling parameters indicated its' degree of influence to the occurrence of landslides in Canada Hill. The degree of impact of the parameter and its' subclasses was inferred

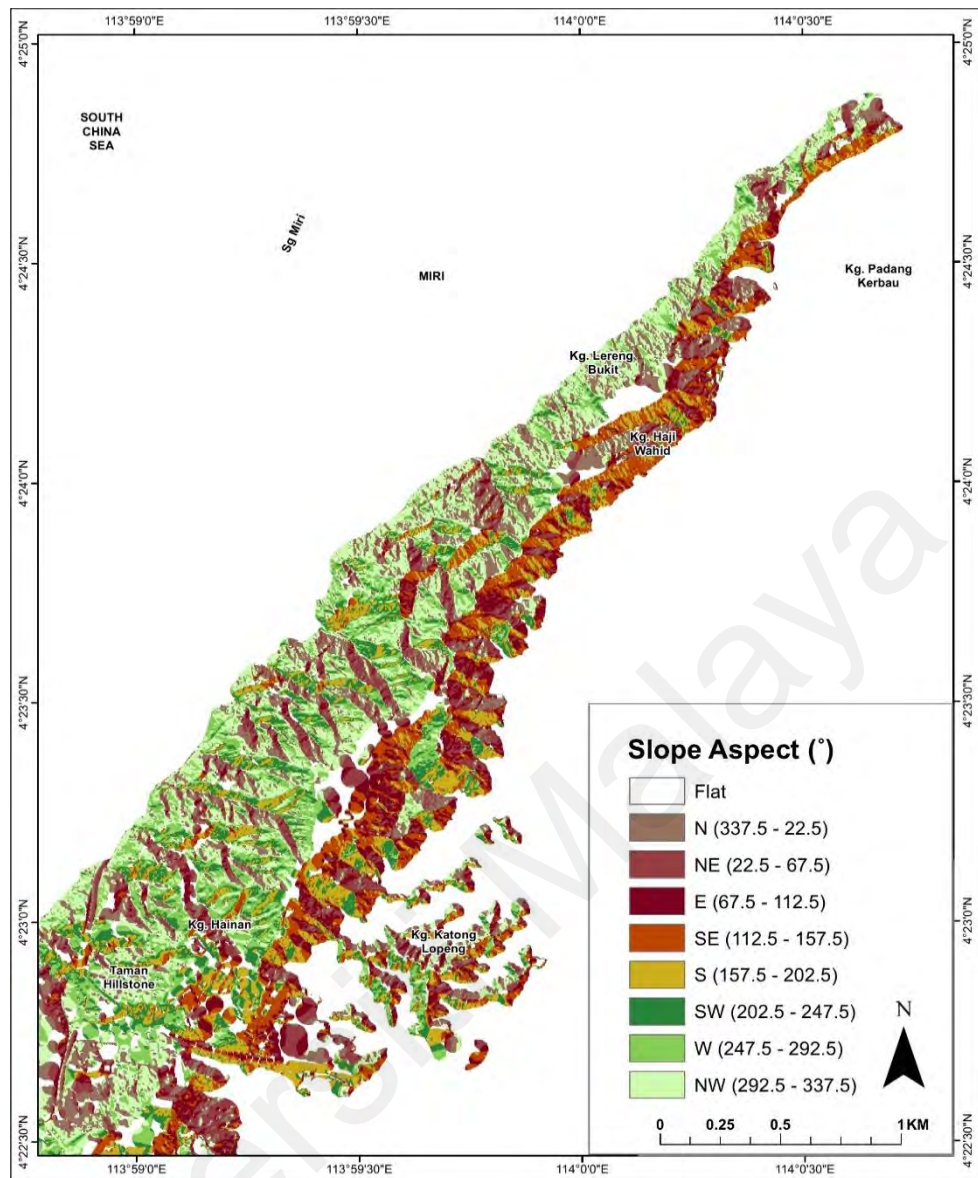


**Figure 5.40:** Slope aspect map of Canada Hill.

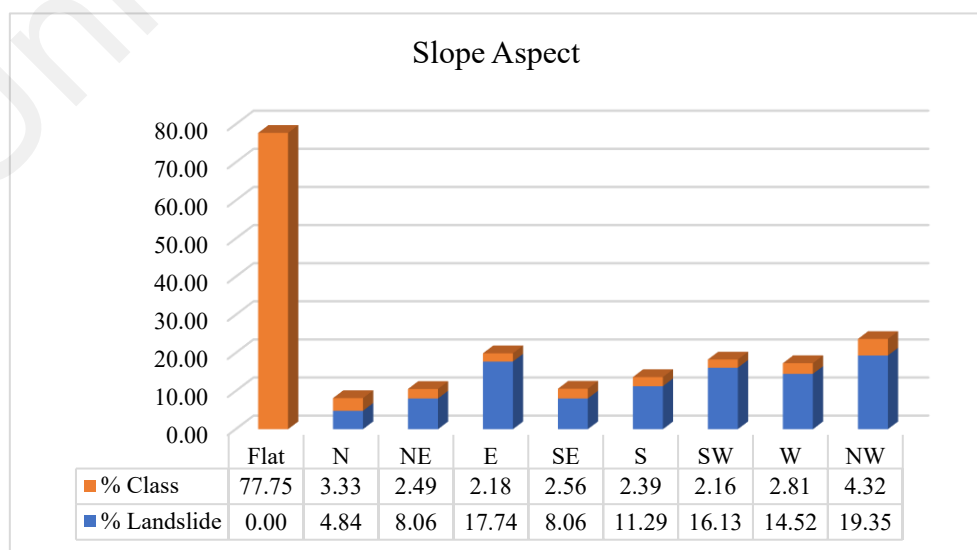


**Figure 5.41:** Histogram of landslide occurrences and areal extent of the subclasses in the slope aspect map.

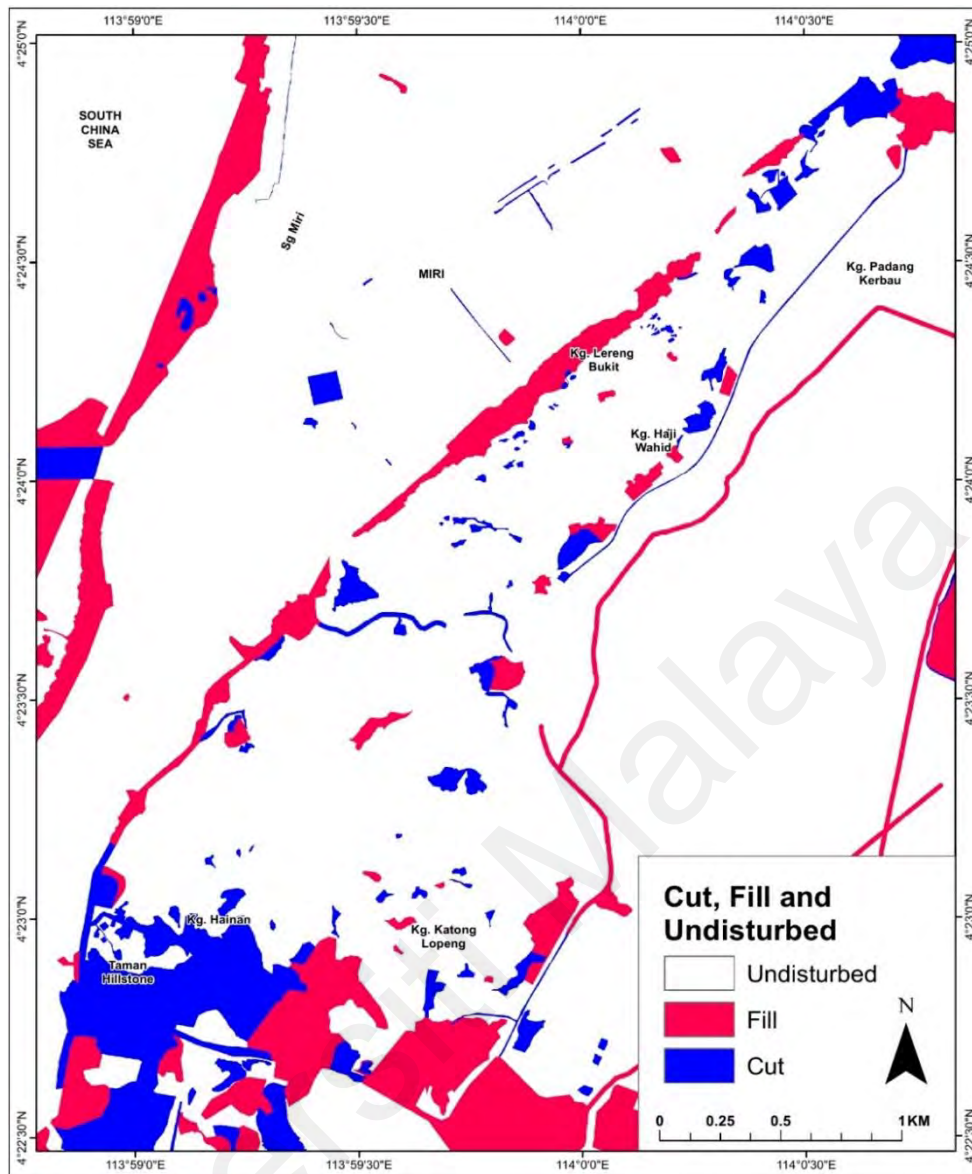


**Figure 5.42:** Cut and fill map of Canada Hill.

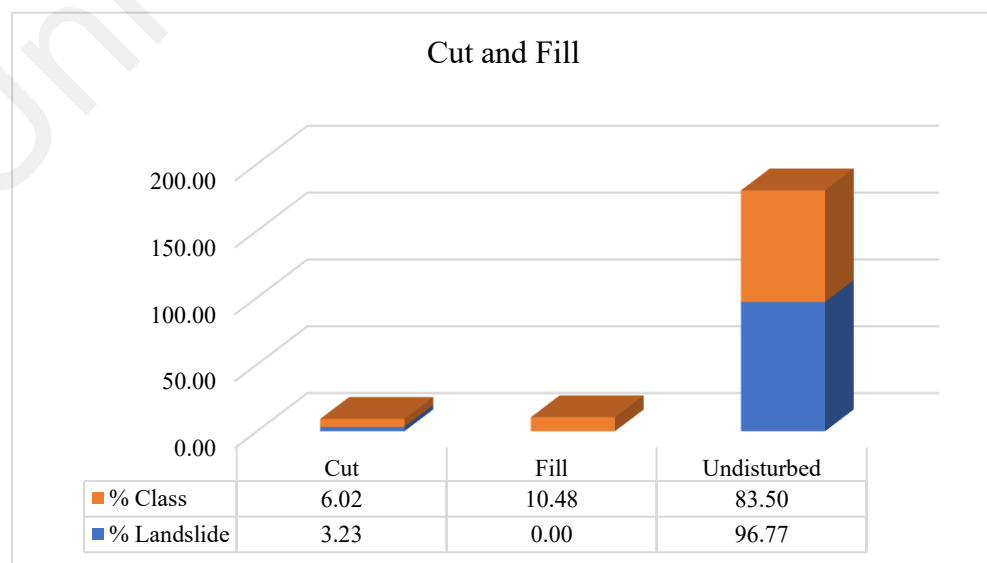


**Figure 5.43:** Histogram on landslide occurrences and areal extent of the subclasses in cut and fill map.

for assignation of weightages in order to produce the final landslide susceptibility map. The heuristic and bivariate statistics approach calculate the weightages differently which will be described in the next chapter. The known theoretical or hypothetical relationship between the classes with landslides have been taken into consideration for the ranking of the subclasses in the heuristic approach while the bivariate statistics approach calculates the weightage based on the distribution of landslides and areal extent of the subclasses.

The selected landslide-controlling parameters that will be used for the analysis of the landslide susceptibility map differs along the two approaches. The slope aspect factor was eliminated from the overlay analysis for the generation of the final susceptibility map in the heuristics approach because the planar failure assessment parameter has included the slope aspect parameter in its' initial analysis and therefore, incorporating the slope aspect parameter would be redundant. In the bivariate statistics approach, the NDVI parameter and the cut and fill parameter were eliminated as the calculation of weightages showed a low significant degree of impact to the landslide distribution. Table 5.7 shows the summary of the list of parameters and subclasses along with which will be applied in the overlay analysis in the two different approaches.

**Table 5.7:** List of landslide-controlling parameters applied in the heuristic and the bivariate statistics approach.

Parameter	Heuristic	Bivariate Statistics	Parameter Subclass
Slope Gradient	✓	✓	0° – 5° 5° -15° 15° - 25° 25° - 35° 35° - 60° 60° - 90°
Geology	✓	✓	Fill Material Quaternary Deposit Terrace Deposit Seria Formation Miri Formation

**Table 5.7, continued.**

Distance to Lineament	✓	✓	< 25m 25m – 75m 75m – 150m 150m – 250m > 250m
Elevation	✓	✓	0m – 5m 5m – 25m 25m – 50m 50m – 75m > 75m
Cut and Fill	✓	✗	Cut Fill Undisturbed
Slope Curvature	✓	✓	Flat (A) Concave Flat (B) Convex
Normalized Difference Vegetation Index (NDVI)	✓	✗	Water Body Barren/Built up Sparse Moderate Dense
Planar Failure Assessment	✓	✗	Not Favourable Less Favourable Slightly Favourable Moderately Favourable Very Favourable
Slope Aspect	✗	✓	Flat N NE E SE S SW W NW

## **CHAPTER 6 : LANDSLIDE SUSCEPTIBILITY ASSESSMENT**

### **6.1 Introduction**

This chapter will describe the findings for the landslide susceptibility assessment for Canada Hill. It will be separated into two subchapters; one subchapter will describe the application of a heuristic approach and one subchapter will describe the application of the bivariate statistics approach. The analysis of the relationship of the landslides and the landslide susceptibility maps will also be discussed in this chapter followed by discussion.

### **6.2 Landslide Susceptibility Assessment Using the Heuristic Approach**

The heuristic or index-based approach involves the combination of parameter maps that were selected and weighted by the experts based on the theoretical relationship of the parameter with the contribution to landslide occurrence. One of the major advantages of the application of this approach to the study area is that the planar failure susceptibility parameter was considered which will generate a landslide susceptibility map which will show the potential occurrences of major planar failure alongside smaller failures. The parameters that were used in the overlay analysis for the generation of the landslide susceptibility map are; planar failure susceptibility, slope gradient, geology, distance to lineament, NDVI, elevation, slope curvature, and cut and fill. Table 6.1 shows the relationship of the landslide distribution and landslide-controlling parameters which is reflected in the rank, contribution ratio and weightages. The rank indicates the degree of influence the class have on the probability of landslide occurrence. A rank of 5 denotes the highest impact rank of 1 denotes the lowest impact and rank of 0 denotes no impact. The contribution ratio indicates the effect of the whole parameter to the probability of landslide occurrence. A higher contribution ratio means a higher impact on the occurrence probability and the total contribution ratio of all the parameters total to 100%. The ranks and contribution ratio were assigned based on the known theoretical or hypothetical relationship between the classes with landslides. The obtained weightages of the classes



**Table 6.1:** The rank, contribution ratio and weightage of the parameters used in the overlay analysis of landslide susceptibility map. Weightages were calculated using Eq 3.1.

No	Parameter & Subclasses	Landslide (%)	Class (%)	Rank	Contributing Ratio (%)	Weightage
1	<b>Planar Failure Susceptibility</b>					
	Most favourable	59.68	88.69	1	10	10
	Moderately favourable	20.97	4.82	2		20
	Slightly favourable	9.68	2.72	3		30
	Less favourable	3.23	2.72	4		40
	Not favourable	6.45	1.05	5		50
2	<b>Slope Gradient (°)</b>					
	0 – 5	0.00	80.13	1	25	25
	5 – 15	17.74	8.17	2		50
	15 – 25	35.48	6.00	3		75
	25 – 35	24.19	3.78	4		100
	35 – 60	22.58	1.89	5		125
	60 - 90	0.00	0.03	5		125
3	<b>Geology</b>					
	Fill Material	0.00	0.83	3	20	60
	Quaternary Deposits	0.00	72.75	5		100
	Terrace Deposits	3.23	3.15	5		100
	Seria Formation	0.00	2.47	1		20
	Miri	96.77	18.42	4		80
	Water Body	0.00	2.39	0		0
4	<b>Distance to Lineament (m)</b>					
	< 25	35.48	12.31	5	10	50
	25 – 75	50.00	18.74	4		40
	75 – 150	14.52	15.68	3		30
	150 – 250	0.00	11.29	2		20
	> 250	0.00	41.98	1		10
5	<b>Normalized Difference Vegetation Index (NDVI)</b>					
	Water Body	0.00	1.43	0	5	0
	Barren/Built up	0.00	17.20	5		50
	Sparse	3.23	19.26	4		40
	Moderate	53.23	22.31	3		30
	Dense	43.55	39.79	2		20
6	<b>Elevation (m)</b>					
	0 – 5	0.00	71.16	1	20	20
	5 – 25	6.45	12.11	2		40
	25 – 50	24.19	10.83	3		600
	50 – 75	56.45	4.03	4		80
	> 75	12.90	1.87	5		100

**Table 6.1, continued.**

<b>7</b>	<b>Slope Curvature</b>					
	Flat (A)	0.00	75.97	1	5	5
	Concave	35.48	10.73	3		15
	Flat (B)	0.00	1.69	1		5
	Convex	64.52	11.61	2		10
<b>8</b>	<b>Cut and Fill</b>					
	Cut	3.23	6.02	3	5	15
	Fill	0.00	10.48	2		10
	Undisturbed	96.77	83.50	1		5

were calculated based on Eq 3.1 of which were used to reclassify the landslide-controlling parameter maps. These reclassified maps were analysed using the Overlay tools and applied the Eq 3.2 in ArcGIS to generate the landslide susceptibility map.

The values of the obtained landslide susceptibility map from the overlay analysis was normalized to a value of 0 to 1, which was then divided and reclassified into classes with an interval of 0.1 to be able to classify the susceptibility classes manually according to Fell *et al.* (2008). The landslide susceptibility map was divided into 5 classes of susceptibility; very high, high, moderate, low and very low (Figure 6.1). Figure 6.2 shows that the very high susceptibility class covered 4.25% of the total study area and 48.39% of the landslide occurred in the very high susceptibility class. 27.42% of the total landslides occurred in the high susceptibility area which makes up 4.62% of the study area. Slopes with very high and high susceptibility are mostly seen in the slopes at the NW flank of Canada Hill in the vicinity of *Kampung Lereng Bukit* and at the SE flank near *Kampung Hainan* and *Kampung Katong Lopeng*. The very high and high susceptibility areas show a positive correlation with areas of steep slopes, slopes at higher elevations and areas that are susceptible to planar failure occurrences. This resonates well with the fact that instabilities in slope increase with steepness along with elevation, in addition to the weak sandstone shale of Miri Formation. The major LS1 and LS2 incidence location fall into the high susceptibility areas which also indicate a positive relationship between landslide susceptibility and planar failure susceptibility. Proximity

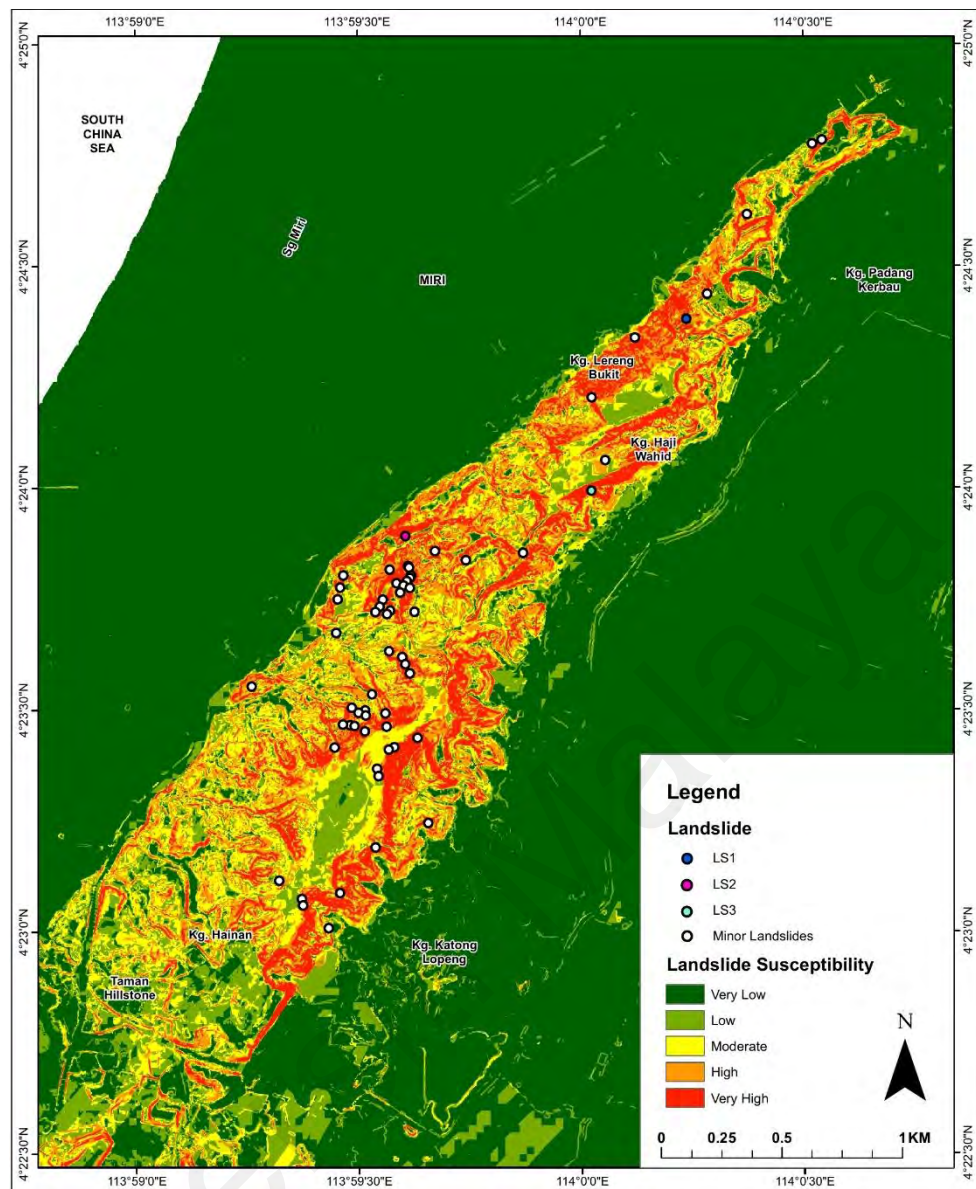


**Figure 6.1:** Landslide susceptibility map of Canada Hill produced through the heuristic approach.

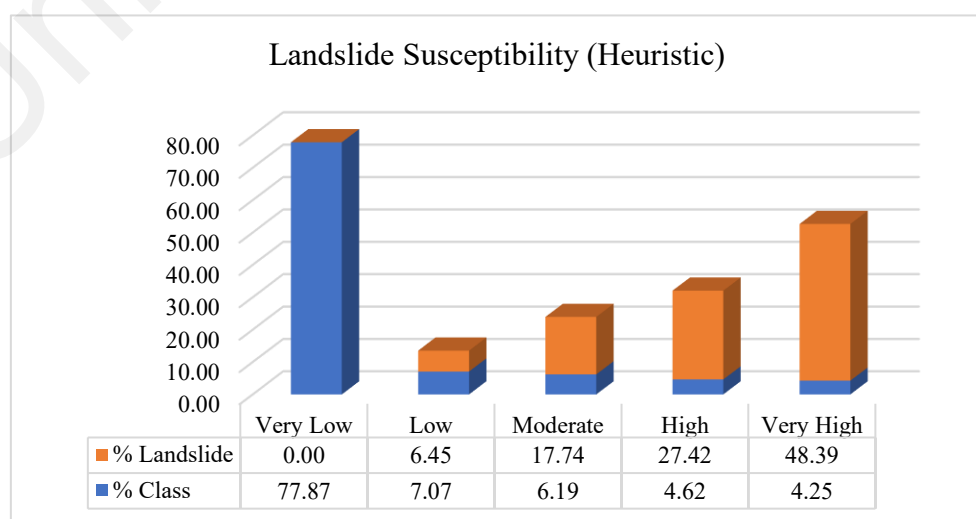


**Figure 6.2:** Histogram of landslide distribution and areal extent of subclasses of landslide susceptibility in Canada Hill using the heuristic approach.

to lineaments as seen in the sites of major landslides also contributes to the increased susceptibility of landslide susceptibility especially in the zones where lineaments are closely spaced, and different sets of lineaments are intersected. The moderate susceptibility areas cover 6.19% of the study area and mostly extend over gentler slopes ( $15^{\circ}$  -  $25^{\circ}$ ) and accounts for 17.74% of the landslides in the area. The area adjacent to slopes at the plateau top of Canada Hill are delineated as area of moderate susceptibility as well which agrees with the instabilities that may be posed by the incohesive terrace deposits which develops on top of the hill. 7.07% of the study area has a low susceptibility and dominated by zones of gentle slopes ( $5^{\circ}$  -  $15^{\circ}$ ) and the flat peak of Canada Hill. 6.45% of the landslides occur in this zone of susceptibility as some minor shallow landslide occur in soils at low and gentle slopes. Majority of the very low susceptibility areas are underlain by the flat Quaternary deposits around Canada Hill which makes up 77.87% of the study area.

### **6.3 Landslide Susceptibility Assessment Using the Bivariate Statistical Approach**

The landslide parameters that were analysed for assignation of weightages in the bivariate statistical approach are geology, distance to lineament, slope gradient, NDVI, elevation, slope aspect, slope curvature and cut and fill. However, the NDVI parameter and cut and fill parameter were not included in the overlay analysis due to the possibly incorrect assessment stemmed from the relationship between the landslide distribution and the areal extent. For example, there were no landslide occurrences on the barren or built up areas as these areas are concentrated on the flatter part of the area around Canada Hill where development is located and does not extend much on the slopes. The landslides occur on the slopes where vegetation is relatively dense which will introduce a weightage that goes against the accepted theory of the increasing stability of slope by root actions of vegetation. This is also the case for cut and fill parameter as most of landslides occur in the undisturbed areas where vegetation is dense. Areas that are being exposed to cut and

**Table 6.2:** The relationship of landslide-controlling parameters and landslide distribution. Weightages were calculated using Eq 3.3.

Landslide Parameter	Class	Landslide		Class		LS Density/km <sup>2</sup>	Weightage
		Pixel	%	Pixel	%		
<b>Geology</b>	Fill Material	0	0.00	142589	0.83	0.00	0
	Quaternary Deposit	0	0.00	12528329	72.75	0.00	0
	Terrace Deposit	2	3.23	542039	3.15	3.69	2
	Seria Formation	0	0.00	424700	2.47	0.00	0
	Miri Formation	60	96.77	3171898	18.42	18.92	166
<b>Distance to Lineament (m)</b>	< 25	22	35.48	2120302	12.31	10.38	106
	25 - 75	31	50.00	3228133	18.74	9.60	98
	75 - 150	9	14.52	2699911	15.68	3.33	-8
	150 - 250	0	0.00	1944255	11.29	0.00	0
	> 250	0	0.00	7228933	41.98	0.00	0
<b>Slope Gradient (°)</b>	0 - 5	0	0.00	13799323	80.13	0.00	0
	5 - 15	11	17.74	1406292	8.17	7.82	78
	15 - 25	22	35.48	1033156	6.00	21.29	178
	25 - 35	15	24.19	651266	3.78	23.03	186
	35 - 60	14	22.58	326035	1.89	42.94	248
	60 - 90	0	0.00	5462	0.03	0.00	0
<b>Normalized Difference Vegetation Index (NDVI)</b>	Barren/Built up	0	0.00	2975400	1.43	0.00	0
	Sparse	2	0.00	3332700	17.20	0.60	-179
	Moderate	33	3.23	3860100	19.26	8.55	87
	Dense	27	53.23	6884100	22.31	3.92	9
<b>Elevation (m)</b>	0 - 5	0	0.00	12254336	71.16	0.00	0
	5 - 25	4	6.45	2085528	12.11	1.92	-63
	25 - 50	15	24.19	1865807	10.83	8.04	80
	50 - 75	35	56.45	693227	4.03	50.49	264
	> 75	8	12.90	322636	1.87	24.80	193
<b>Slope Aspect</b>	Flat	0	0.00	13389750	1.78	0.00	0
	N	3	4.84	574296	3.33	5.22	37
	NE	5	8.06	428651	2.49	11.66	118
	E	11	17.74	375233	2.18	29.32	210
	SE	5	8.06	440783	2.56	11.34	115
	S	7	11.29	411659	2.39	17.00	155
	SW	10	16.13	372696	2.16	26.83	201
	W	9	14.52	484553	2.81	18.57	164
	NW	12	19.35	743913	4.32	16.13	150
<b>Slope Curvature</b>	Flat (A)	0	0.00	13082897	75.97	0.00	0
	Concave	22	35.48	1848221	10.73	11.90	120
	Flat (B)	0	0.00	290937	1.69	0.00	0
	Convex	40	64.52	1999479	11.61	20.01	172
<b>Cut &amp; Fill</b>	Cut	2	3.23	1036368	6.02	1.93	-62
	Fill	0	0.00	1805137	10.48	0.00	0
	Undisturbed	60	96.77	14380027	83.50	4.17	15

fill activities centre only at development areas where slopes are lacking. The bivariate statistics approach calculates the weightage based on the distribution of landslides and areal extent of the subclasses. The resulting weightages are shown in Table 6.2. Negative weights indicate that the landslide density is lower than normal, positive weights will be obtained if the landslide density is higher than normal and a zero weight will be obtained if there are no landslide occurrences in a certain parameter class or the class may or may not contribute to landslide occurrences (van Westen, 1997). The weightages were then used to reclassify the chosen landslide-controlling parameters to be used in the overlay analysis for the generation of landslide susceptibility map (Figure 6.3).

The landslide susceptibility map created from the overlay analysis of the reclassified landslide-controlling parameter maps yields a continuous value and was normalized to a value ranging from 0 to 1 for subsequent reclassification for classification into 5 susceptibility classes based on the application of the same classification method as the heuristic approach. The landslide susceptibility map was divided manually according to Fell *et al.* (2008) into five classes to denote areas of very low, low, moderate, high and very high susceptibility to landslide occurrences.

The very high and high landslide susceptibility area extends 2.78% and 4.70% over the study area, respectively. 53.23% of landslides occur in the very high susceptibility areas while 27.42% of landslide occur in the high susceptibility areas (Figure 6.4). Areas that have a very high and high landslide susceptibility are concentrated on the higher elevations of Miri Formation at 50 to 75m and at areas with moderately steep to very steep slopes ( $35^{\circ}$  to  $60^{\circ}$ ). This relationship indicates that the landslide susceptibility is controlled by the geology of Miri Formation comprising of interbedded sandstone and shale. As the slopes get steeper, the soils that form from the weathered sandstone and shale may become more unstable. This is then aggravated by the high relief. The concavity of the slope may also be another factor that aggravates the instability as very



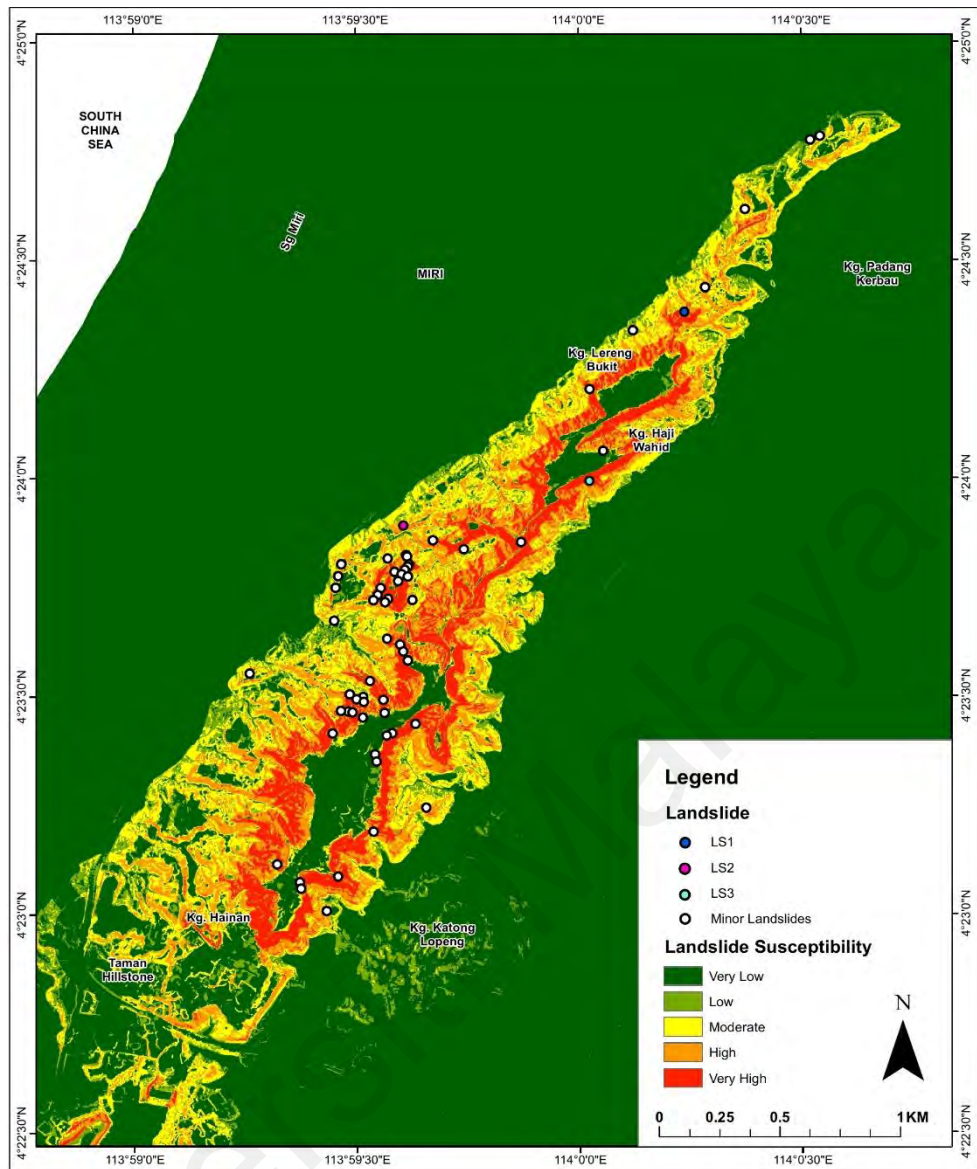


**Figure 6.3:** Landslide susceptibility map of Canada Hill produced through the bivariate statistics approach.

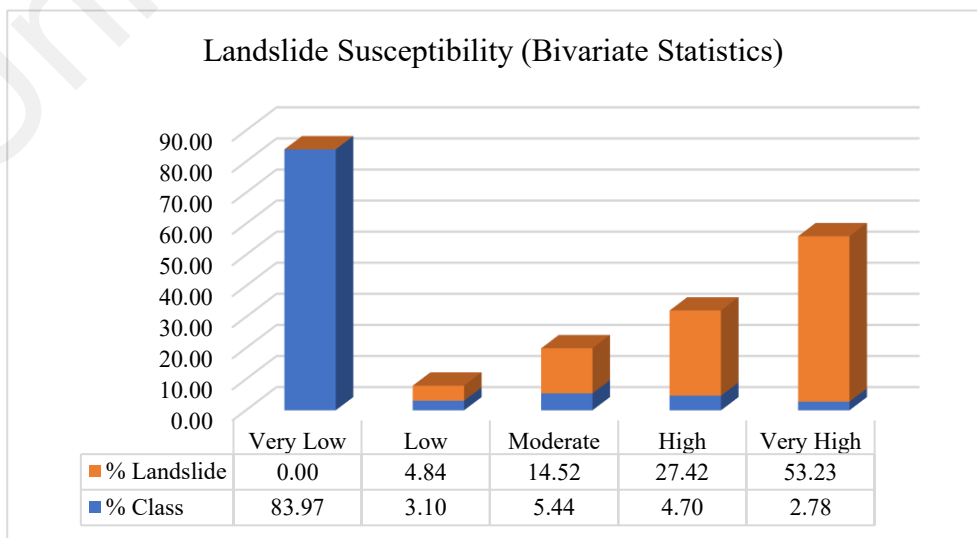


**Figure 6.4:** Histogram of landslide distribution and areal extent of subclasses of landslide susceptibility in Canada Hill using the bivariate statistics approach.

high and high landslide susceptibility extends over these areas as well. The soils gradually receive water through percolation and the concave slopes act like a catchment which may increase the rate of saturation of soils or the shale between sandstone layers. Areas that are proximal to lineaments also accounts for a high susceptibility, in addition to coinciding some gentle slopes ( $15^{\circ}$  to  $25^{\circ}$ ). The moderate susceptibility area accounts for 14.52% of the landslide occurrence in Canada Hill over an areal extent of 5.44%. This class extends over majority of the lower part of Canada Hill which has an elevation of 25 to 50 m and at the slopes that faces NW. The low susceptibility class occupies 3.10% study area and accounts for 4.84% of the landslide occurrence. This susceptibility class also occur in accordance with gentle slopes ( $15^{\circ}$  to  $25^{\circ}$ ) but at a much lower elevation at 5m to 20m. Most of the area is of very low susceptibility which makes up a total of 83.97% which accounts to no landslide occurrence since the very low susceptibility class lie in the flatter area underlain by Quaternary Deposits around Canada Hill and at the top of Canada Hill.

#### **6.4 Discussion**

The quality of these landslide susceptibility models based on the goodness of fit relative to the landslide occurrences was tested. The landslide susceptibility classes were reclassified into 10 classes from 0 – 100 with the interval of 10 for the sensitivity analysis purpose. Based on the success rate curves of the models as shown in Figure 6.5, the model resulted from the bivariate statistics approach performed better and is more precise. The model produced using the bivariate statistics approach has an AUC of 80.8% compared to the heuristic approach which has an AUC of 74%. It is also shown that 50% of the landslide occurrences occurred in 17.5% of the most susceptible class in the model produced using the bivariate statistic approach compared to 25.7% in the model produced using the heuristic approach.

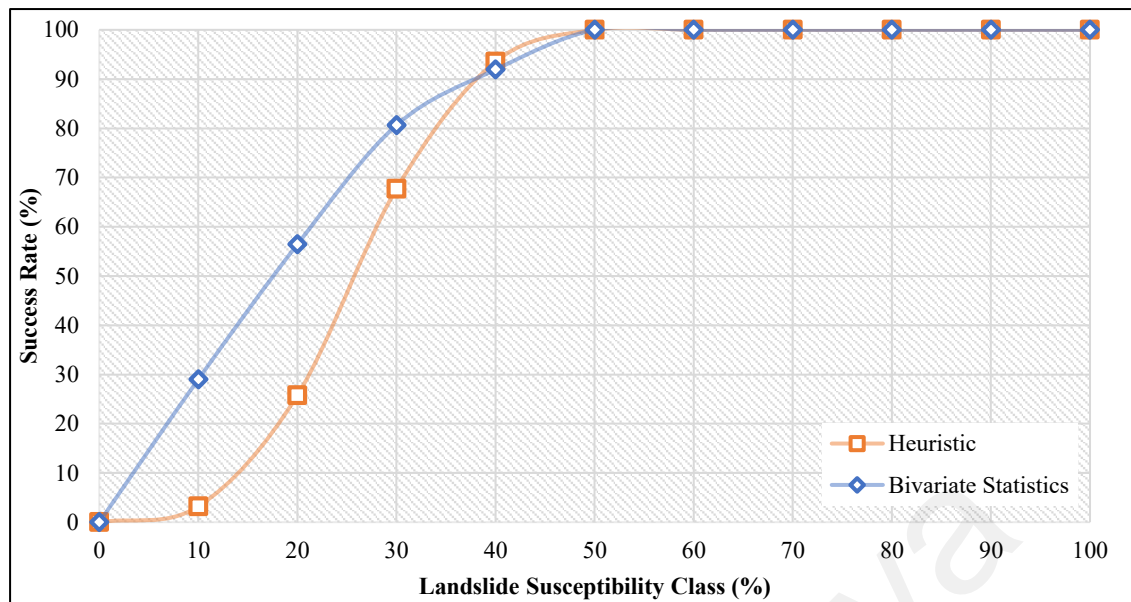


**Figure 6.5:** Comparison of the success rates obtained using the heuristic and bivariate statistics method.

The reliability and completeness of a landslide susceptibility map depends wholly on the quality of the input parameters used in the assessment of landslide susceptibility. The understanding of the process that induce landslide occurrences gives an idea of landscape evolution, with regards of whether it being site-specific or homogenous across different areas. This also provides a platform for subsequent susceptibility assessment works which may be refined by newer data and findings with time.

The most important parameter that lays a foundation for the landslide susceptibility is the landslide inventory map which will be linked to all the parameters used for the final analysis of the landslide susceptibility. An unreliable landslide inventory data would cause the final landslide susceptibility to be unreliable as well. The landslide inventory map of Canada Hill was prepared through reviews of newspaper reports, unpublished reports from government bodies and historical records from previous literatures. However, this was only limited to the landslides that are large enough and caused damage to infrastructure and lives, so data was still very limited. Hence, the interpretation of LiDAR, sequential analysis of satellite imageries, fieldwork was applied to map out the spatial distribution of landslides. Although this aided for the identification of landslide

zones through the morphology changes of the study area, especially LiDAR as the vegetation cover have mostly been filtered out, difficulties were still faced at some extent, especially when mapping past minor shallow failure where rapid increase of vegetation growth took place which impeded the identification of relict landslide features, as is a usual attribute of tropical climate areas. However, data collected can still be used for analysis. The quality and scale of the topographic maps and satellite imageries, the degree of experience of the person and the complexity of the study area geologically (Magliulo *et al.*, 2009) also effects the landslide inventory maps as well as the rest of the landslide-controlling parameters.

The landslide susceptibility was approached by two assessment methods, a qualitative measure known as the heuristic approach and a quantitative approach known as the bivariate statistics approach. The utilization of both approaches was done in ArcGIS 10.5 which served as an advantage in terms of the ease of storing and updating data in a single database and the ability to perform processing actions and automatically in the same database. The heuristic approach was more direct in ranking the parameters by expert opinions, which incorporated the theoretical knowledge of the effects each parameter has on landslide occurrence while a bivariate statistics approach relies heavily on a field-surveyed datum to deduce the relationships of selected landslide-controlling parameters with the landslide occurrences.

The possible shortcoming of a heuristic approach over a statistical approach, would be the subjectivity of the rankings but this was then verified with the field-surveyed landslide inventory map which showed an increasing trend of the percentage of landslide occurrence with the decrease of percentage of classes of susceptibility. Conversely, the advantage of the heuristic approach enables the input of an important parameter for the planar failures occurrences in which cases are common for the Canada Hill area following prolonged heavy rain. The incorporation of a planar failure assessment parameter in the

final landslide susceptibility map placed the major LS1 and LS2 in the very high susceptibility zone, as expected.

Bivariate statistical method approached the calculation of the weightages of the parameter differently by considering the true condition of the relationship of the parameter with the landslide occurrences. The comparison of a field-surveyed landslide inventory with the planar failure susceptibility assessment was not possible for bivariate statistics analysis in this study without introducing an element of subjectivity to the statistical analysis. This led to the major LS1 and LS2 failure to be plotted in the moderate to low susceptibility zones. Nevertheless, the landslide susceptibility map produced from the bivariate statistical method resulted in a higher percentage of landslide occurrence within a smaller percentage of very high susceptibility zone as opposed to the landslide susceptibility map produced by the heuristic approach.

The landslide susceptibility maps showed a good correlation of landslide occurrences with the increasing susceptibility of the area. The bivariate statistical approach did not consider the planar failure assessment and therefore, failed to place the major LS1 and LS2 in the very high and high susceptibility zones but it is a good approach for translational and smaller circular failure in soil. The heuristic approach considered the planar failure assessment which made this approach better for the assessment of planar failure in rocks, translational and shallow rotational landslides in soil. Future work may include additional inventory of the landslides to perform a more detailed validation through the application of training data and prediction data. The consideration of the adjacent undisturbed morphological conditions to make up for features exhausted by previous landslide occurrences may also refine the analysis which can be done by adding a buffer in GIS to the plotted landslide scar (van Westen, 1993).

## CHAPTER 7 : CONCLUSION

Landslide is an important natural hazard attributed by natural or anthropogenic factors. The fundamental understanding of the processes involved is required for subsequent hazard management in order to keep safety of the population at risk in check. Landslide susceptibility assessment has been successfully performed throughout the world using various methods depending on the scale of study and the available data for analysis of the susceptibility assessment.

Devastating landslide occurrences in Canada Hill, Miri are common especially after prolonged heavy rainfall period. The danger of landslides should be addressed especially as it has brought damage on the infrastructure and loss of lives. This study was done as an effort to understand the processes that lead to the occurrence of landslide and to produce the landslide susceptibility map of Canada Hill, Miri which can aid the local planners and policy makers to ensure proper landslide mitigation measures.

The main findings from this study are as follows:

1. The geology of the study area was examined to infer the possible factors of contribution to landslides. Canada Hill, comprising of the Miri Formation and Seria Formation is a geologically young sandstone shale formation, susceptible to physical and sulphate weathering, shown by the steep, deeply incised terrains, encrustations on the rock surface and presence of podzol layers overlying the Fe-rich impermeable layer (“iron pan”) within the interbedded sandstone and shale. The study of the mechanism of the major planar failures in Miri is inferred to also be contributed by the “iron pan”, situated below the failed plane. Weathered soils comprising of highly erodible sand and clay with low plasticity may introduce more susceptibility with a slight increase of water. This may be further aggravated by the prolonged rain season during the monsoon, attributed to the tropical climate and may have been a root cause of the other translational and smaller rotational



failures. Following this investigation, spatial identification of past landslides from the field and various sources was done to set up a landslide inventory in the GIS database which included the shallow failures and details of the location and type of failures.

2. There are varying factors that contribute to landslide occurrence and are often complex and unknown. This study allows the effort to perform the landslide susceptibility analysis by analysing a selection of nine parameters using the heuristic and bivariate statistical approach, which included slope gradient, geology, elevation, planar failure susceptibility, distance to lineament, slope curvature, slope aspect, NDVI and cut and fill. The geological, topographical and environmental parameters were the focus on this initial assessment study as the tendency of failing after precipitation indicated unfavourable topography and lithology materials.
3. The application of Geographical Information System (GIS) was manifested in this study from the integrating, storing, editing, and analysing processes. The use of GIS for landslide susceptibility assessment has brought ease to working with any spatial-related data, in addition to time and cost-saving. Visually enhanced maps created in the GIS translates the ground condition information in a simpler language which may set the motion for seamless knowledge transfer between related agencies.
4. This study has allowed the assessment of landslide susceptibility at Canada Hill, Miri using a qualitative and quantitative method. A good correlation of the landslide occurrences with the landslide-controlling parameters were deduced from the landslide susceptibility maps depending on the type of landslides investigated. The generated landslide susceptibility map using the heuristic approach is useful for the determination of potential planar failure in rocks,

translational failures and shallow rotational failures in soil while the landslide susceptibility map produced using the bivariate statistical approach is more useful for the sole determination of the potential circular and translational failures in soil.

The initial findings in this study area hopes to lay a foundation for the landslide susceptibility assessment of Canada Hill which may be helpful for the local authorities to provide mitigation measures to ensure safety of the population residing below or near the slopes of the hill. This study has also determined a few data gaps that should be addressed as suggestions for future research.

In order to refine the relationship of the landslide occurrence with landslide-controlling parameters, additional and more detailed landslide inventory which encompasses the whole study area is required. This is also necessary to perform a more detailed validation of the landslide susceptibility map through the application of training data and prediction data. Hence, a continual process of updating the landslide inventory is indispensable.

The determination of how the landslide data points in the map will be utilized may also be approached differently by adding a landslide scar buffer polygon which will also include into the analysis the undisturbed geomorphological conditions prior to exhaustion of material due to a previous landslide event.

This study also suggests the continual refining of the landslide susceptibility through the incorporation of more possible combination of landslide-controlling factors. Other available methods could also be applied to the landslide susceptibility assessment for a better comparison between methods which will improve the landslide susceptibility assessment in time.

## REFERENCES

- Abieda, H., Zahir, Z., Harith, Z., Hadi, A., & Abd Rahman, A. H. (2005). Depositional controls on petrophysical properties and reservoir characteristics of Middle Miocene Miri Formation sandstones, Sarawak. *Bulletin of the Geological Society of Malaysia*, 51, 63-75.
- Aleotti, P., & Chowdhury, R. (1999). Landslide hazard assessment: summary review and new perspectives. *Bulletin of Engineering Geology and the Environment*, 58(1), 21 - 44.
- Amadesi, E., & Vianello, G. (1978). Nuova guida alla realizzazione di una carta di stabilità dei versanti. *Memorie della Società Geologica Italiana*, 19, 53-60.
- Armas, I., Vartolomei, F., Stroia, F., & Brasoveanu, L. (2013). Landslide susceptibility deterministic approach using geographic information systems: application to Breaza town, Romania. *Natural Hazards*, 70(2), 995 - 1017.
- Avenza Systems Incorporated. (2017). Best Practices for Processing and Importing Maps into the Avenza Maps App. Retrieved on 15 November 2019 from <https://www.avenza.com/resources/blog/2017/02/09/best-practices-processing-and-importing-maps-avenza-maps-app/>
- Ayalew, L., & Yamagishi, H. (2005). The application of GIS-based logistic regression for landslide susceptibility mapping in the Kakuda-Yahiko Mountains, Central Japan. *Geomorphology*, 65, 15 - 31.
- Ayalew, L., Yamagishi, H., & Ugawa, N. (2004). Landslide susceptibility mapping using GIS-based weighted linear combination, the case in Tsugawa area of Agano River, Niigata Prefecture, Japan. *Landslides*, 1, 73 - 81.
- Banda, R., Zakaria, M., & Kamaludin, H. (2009, June). *Geological Significance of landslide occurrences in Canada Hill, Miri, Sarawak*. Paper presented at the GEOSEA 2009: Eleventh Regional Congress on Geology, Mineral and Energy Resources of Southeast Asia, Hotel Istana, Kuala Lumpur, Malaysia.
- Barredo, J. I., Benavides, A., Hervás, J., & van Westen, C. J. (2000). Comparing Heuristic Landslide Hazard Assessment Techniques using GIS in the Tirajana Basin, Gran Canaria Island, Spain. *International Journal of Applied Earth Observation and Geoinformation*, 2(1), 9 - 23.
- Bell, F. G., Culshaw, M. G., Forster, A., & Nathanail, C. P. (2009). The engineering geology of the Nottingham area, UK. In M. Culshaw, H. Reeves, I. Jefferson, & T. W. Spink (Eds.), *Engineering Geology for Tomorrow's Cities* (pp. 1 - 24). London, UK: The Geological Society, London.

- Brabb, E. E. (1985). Innovative approaches to landslide hazard and risk mapping. In *Proceedings of 4th International Symposium on Landslides, Toronto, Canada* (pp. 307 - 324). Tokyo, Japan: Japan Landslide Society.
- Brabb, E. E. (1991). The World Landslide Problem. *Episodes*, 14(1), 52 - 61.
- Carrara, A. (1983). A multivariate model for landslide hazard evaluation. *Mathematical Geology*, 15, 403 - 426.
- Chung, C.-J. F., & Fabbri, A. G. (2003). Validation of Spatial Prediction Models for Landslide Hazard Mapping. *Natural Hazards*, 30, 451 - 472.
- Corominas, J., van Westen, C., Frattini, P., Cascini, L., Malet, J. P., Fotopoulou, S., . . . Smith, J. T. (2013). Recommendations for the quantitative analysis of landslide risk. *Bulletin of Engineering Geology and the Environment*, 73, 209 - 263.
- Crozier, M. J. (1986). *Landslides: Causes, Consequences and Environment*. London: Croom Helm.
- Crozier, M. J., & Glade, T. (2005). Landslide hazard and risk: issues, concepts, and approach. In T. Glade, M. Anderson, & M. J. Crozier (Eds.), *Landslide hazard and risk* (pp. 1 - 40). New York: Wiley.
- De Kemp, E. A. (1998). Three-Dimensional Projection of Curvilinear Geological Features Through Direction Cosine Interpolation of Structural Field Observations. *Computers & Geosciences*, 24(3), 269 - 284.
- Dietrich, E. W., Reiss, R., Hsu, M. L., & Montgomery, D. R. (1995). A process-based model for colluvial soil depth and shallow landsliding using digital elevation data. *Hydrological Process*, 9, 383 - 400.
- Dikau, R., Brunsden, D., Schrott, L., & Ibsen, M. L. (1996). *Landslide Recognition. Identification, Movements and Causes*. Chichester, England: Wiley.
- Dundang, A. G. (1983). *Stratigraphy and Sedimentology of the Miri Formation in the Miri Area, Sarawak, East Malaysia*. (Unpublished academic exercise). Universiti Malaya, Kuala Lumpur, Malaysia.
- Fell, R., Corominas, J., Bonnard, C., Cascini, L., Leroi, E., & Savage, W. Z. (2008). Guidelines for Landslide Susceptibility, Hazard and Risk Zoning for Land Use Planning. *Engineering Geology*, 102, 85 - 98.

- Forbes, K., & Broadhead, J. (2011). *Forests and Landslides: The role of trees and forests in the prevention of landslides and rehabilitation of landslide-affected areas in Asia*. Bangkok: Food and Agriculture Organization of the United Nations.
- Froude, M. J., & Petley, D. N. (2018). Global Fatal Landslide Occurrence from 2004 to 2016. *Natural Hazards Earth System Science*, 18, 2161 - 2181.
- Geotechnical Control Office (GCO). (2017). *Guide to Rock and Soil Descriptions (Geoguide 3)*. Hong Kong: Geotechnical Control Office.
- Goodchild, M. F. (2015). Geographic Information Systems. In J. Wright (Ed.), *International Encyclopedia of the Social & Behavioral Sciences* (pp. 58 - 63). Elsevier.
- Google Earth. (2001a). *LS1 site in year 2001*. Retrieved on 15 July 2014 from [earth.google.com/web/](http://earth.google.com/web/)
- Google Earth. (2001b). *LS2 site in year 2001*. Retrieved on 15 July 2014 from [earth.google.com/web/](http://earth.google.com/web/)
- Google Earth. (2001c). *LS3 site in year 2001*. Retrieved on 15 July 2014 from [earth.google.com/web/](http://earth.google.com/web/)
- Google Earth. (2008a). *LS1 site in year 2008*. Retrieved on 15 July 2014 from [earth.google.com/web/](http://earth.google.com/web/)
- Google Earth. (2008b). *LS3 site in year 2008*. Retrieved on 15 July 2014 from [earth.google.com/web/](http://earth.google.com/web/)
- Google Earth. (2011). *LS2 site in year 2011*. Retrieved on 15 July 2014 from [earth.google.com/web/](http://earth.google.com/web/)
- Google Earth. (2013a). *3D view of LS1*. Retrieved on 15 July 2014 from [earth.google.com/web/](http://earth.google.com/web/)
- Google Earth. (2013b). *3D view of LS2*. Retrieved on 15 July 2014 from [earth.google.com/web/](http://earth.google.com/web/)
- Google Earth. (2013c). *LS1 site in year 2013*. Retrieved on 15 July 2014 from [earth.google.com/web/](http://earth.google.com/web/)
- Google Earth. (2013d). *LS2 site in year 2013*. Retrieved on 15 July 2014 from [earth.google.com/web/](http://earth.google.com/web/)

- Google Earth. (2014). *2014 imagery of the LS3 area*. Retrieved on 15 July 2014 from earth.google.com/web/
- Google Earth. (n. d.). *Location of Miri and Canada Hill*. Retrieved on 20 July 2014 from earth.google.com/web/
- Groshong, R. H. (2006). Direction Cosines and Vector Geometry. In *3-D Structural Geology* (373 - 382). Berlin, Heidelberg: Springer.
- Guzzetti, F., Carrara, A., Cardinali, M., & Reichenbach, P. (1999). Landslide hazard evaluation: a review of current techniques and their application in a multi-scale study, Central Italy. *Geomorphology*, 31, 181 - 216.
- Guzzetti, F., Galli, M., Reichenbach, P., Ardizzone, F., & Cardinali, M. (2006). Landslide Hazard Assessment in the Collazzone Area, Umbria, Central Italy. *Natural Hazards and Earth System Sciences*, 6, 115 - 131.
- Haile, N. S. (1974). Borneo. In A. M. Spencer (Ed.), *Mesozoic-Cenozoic Orogenic Belts: Data for Orogenic Studies* (pp. 333 - 347). Edinburgh: Scottish Academic Press Ltd for the Geological Society, London.
- Haliza, A. R., & Jabil, M. (2017). Landslide Disaster in Malaysia: an Overview. *Health and the Environment Journal*, 8(1), 58 - 71.
- Hansen, A. (1984). Landslide Hazard Analysis. In D. Brunsden & D. B. Prior (Eds.), *Slope Instability* (pp. 523 - 602). New York: Wiley.
- He, H., Hu, D., Sun, Q., Zhu, L., & Liu, Y. (2019). A Landslide Susceptibility Assessment Method Based on GIS Technology and an AHP-Weighted Information Content Method: A Case Study of Southern Anhui, China. *ISPRS International Journal of Geo-Information*, 8, 266.
- Highland, L. M., & Bobrowsky, P. (2008). *The Landslide Handbook - A Guide to Understanding Landslides* (Vol. 1325). Reston, Virginia: U. S. Geological Survey.
- Hutchinson, J. N. (1988, July). *General Report: Morphological and Geotechnical Parameters of Landslides in Relation to Geology and Hydrology*. Paper presented at the 5th International Symposium on Landslides, Rotterdam, Balkema.
- Hutchison, C. S. (1989). *Geological Evolution of South East-Asia*. England: Oxford University Press.

- Hutchison, C. S. (2005). *Geology of north-west Borneo: Sarawak, Brunei and Sabah*. Amsterdam: Elsevier.
- International Association of Engineering Geology (IAEG). (1976). *Engineering Geological Maps: A Guide to Their Preparation*. Paris: UNESCO Press.
- International Association of Engineering Geology (IAEG). (1981). Soil description and classification for engineering geological mapping report by the IAEG Commission on Engineering Geological Mapping. *Bulletin of the International Association of Engineering Geology - Bulletin de l'Association Internationale de Géologie de l'Ingénieur*, 24(1), 235-274.
- International Society for Rock Mechanics (ISRM). (2007). *The complete ISRM suggested methods for rock characterization, testing and monitoring: 1974 - 2006*. Turkey: International Society for Rock Mechanics, Commission on Testing Methods.
- Joeckel, R. M., Ang Clement, B. J., & VanFleet Bates, L. R. (2005). Sulfate-mineral crusts from pyrite weathering and acid rock drainage in the Dakota Formation and Graneros Shale, Jefferson County, Nebraska. *Chemical Geology*, 215, 433 - 452.
- Kessler, F. L., & Jong, J. (2014). The origin of Canada Hill — A result of strike-slip deformation and hydraulically powered uplift at the Pleistocene/Holocene border? *Bulletin of the Geological Society of Malaysia*, 60, 35 - 44.
- Liechti, P., Roe, F. W., & Haile, N. S. (1960). *The Geology of Sarawak, Brunei and the Western Part of North Borneo: Compiled from Work of the Royal Dutch Shell Group of Companies in the British Territories in Borneo and from Various Published Accounts*. Kuching, Sarawak, Malaysia: Geological Survey Department British Territories in Borneo.
- Lisle, R. J., & Leyshon, P. R. (2004). *Stereographic Projection Techniques for Geologists and Civil Engineers* (2nd ed.). Cambridge: Cambridge University Press.
- Luqman, K. (2009). *Laporan Tanah Runtuh di Lot 506, Jalan Miri Pujut, Bukit Kanada, Miri, Sarawak*. (JMG.SWK(GBN) 3/2009). Kuching, Sarawak: Mineral and Geoscience Department Malaysia.
- Madon, M. H. (1999). Geological Setting of Sarawak. In *The Petroleum geology and resources of Malaysia* (pp. 275 - 290). Kuala Lumpur, Malaysia: Petronas.
- Magliulo, P., Lisio, A. D., & Russo, F. (2009). Comparison of GIS-based methodologies for the landslide susceptibility assessment. *Geoinformatica*, 13, 253 - 265.



- Malaysian Meteorological Department. (2017). Daily Rainfall Miri (96449) & Mulu (96448) for year 2007 - 2017. [Data file]. Retrieved 1st November 2017 from Malaysian Meteorological Department
- Malczweski, J. (1999). *GIS and Multicriteria Decision Analysis*. New York: Wiley.
- Mandal, B., & Mandal, S. (2017). Landslide susceptibility mapping using modified information value model in the Lish river basin of Darjiling Himalaya. *Spatial Information Research*, 25, 205 - 218.
- Mandal, S., & Mondal, S. (2019). Frequency Ratio (FR) Model and Modified Information Value (MIV) Model in Landslide Susceptibility Assessment and Prediction. In *Statistical Approaches for Landslide Susceptibility Assessment and Prediction*. Cham: Springer
- Mason, P. J. (2013). Remote Sensing | GIS. In *Reference Module in Earth Systems and Environmental Sciences*. London, UK: Elsevier.
- Mohd, F. A. K. (2014). *Siasatan Tanah Runtuh di Kampung Padang Kerbau, Miri, Bahagian Miri, Sarawak*. (JMG.SWK(GBN)1/2014). Kuching, Sarawak: Mineral and Geoscience Department Malaysia
- Montana, L. (2008). Geographic Information Systems. In *International Encyclopedia of Public Health* (pp. 56 - 59). USA: Elsevier.
- Montgomery, D. R., & Dietrich, E. W. (1994). A Physically Based Model for the Topographic Control on Shallow Landsliding. *Water Resources Research*, 30(4), 1153 - 1171.
- Morley, C. K., Back, S., Van Rensbergen, P., Crevello, P., & Lambiase, J. J. (2003). Characteristics of repeated, detached, Miocene–Pliocene tectonic inversion events, in a large delta province on an active margin, Brunei Darussalam, Borneo. *Journal of Structural Geology*, 25(7), 1147-1169.
- Muol, E. (2009). *Laporan Tanah Runtuh di Kg. Lereng Bukit, Bukit Kanada, Miri, Sarawak*. (JMG.SWK(GBN) 1/2009). Kuching, Sarawak: Mineral and Geoscience Department Malaysia
- Naranjo, J. L., van Westen, C. J., & Soeters, R. (1994). Evaluating the use of training areas in bivariate statistical landslide hazard analysis: a case study in Colombia. *ITC Journal*, 3, 292 - 300.

- National Research Council (U.S.) Transportation Research, B., Schuster, R. L., & Krizek, R. J. (1978). *Landslides, Analysis and Control* (R. L. Schuster & R. J. Krizek Eds.). Washington: National Academy of Sciences.
- Oliveira, S. C., Zêzere, J. L., Catalão, J., & Nico, G. (2015). The contribution of PSInSAR interferometry to landslide hazard in weak rock-dominated areas. *Landslides*, 12(4), 703-719.
- Paramanathan, S. (2008). Tropical Lowland Peats: To Conserve or Develop Them? In *Selected Papers on Soil Science: Problem Soils* (pp. 15 - 49). Petaling Jaya, Selangor, Malaysia: Agricultural Crop Trust (ACT) & Param Agricultural Soil Surveys (PASS).
- Paramanathan, S. (2011). *Keys to the identification of Malaysian soils according to parent materials (Mimeo)*. Petaling Jaya, Selangor, Malaysia: Param Agricultural Soil Surveys (M) Sdn. Bhd.
- Paramanathan, S., Academy of Sciences Malaysia, & Param Agricultural Soil Surveys. (2000). *Soils of Malaysia: Their Characteristics and Identification*. Kuala Lumpur, Malaysia: Academy of Sciences Malaysia.
- Paramanathan, S., & Pupathy, U. T. (2012). Need for a Unified Classification of Acid Sulfate Soils of Malaysia. In *Selected Paper on Soil Science: Problem Soils* (pp. 67 - 83). Petaling Jaya, Selangor, Malaysia: Agricultural Crop Trust (ACT) & Param Agricultural Soil Surveys (PASS).
- Petley, D. (2012). Global patterns of loss of life from landslides. *Geology*, 40(10), 927-930.
- Ramachandra, T., Subash Chandran, M., Joshi, N., Julka, P., Kumar, U., Aithal, B. H., . . . Mukri, V. (2012). *Landslide Susceptible Zone Mapping in Uttara Kannada, Central Western Ghats*. Bangalore, India: Indian Institute of Science.
- Reichenbach, P., Galli, M., Cardinali, M., Guzzetti, F., & Ardizzone, F. (2005). Geomorphologic Mapping to Assess Landslide Risk: Concepts, Methods and Applications in the Umbria Region of Central Italy. In T. Glade, M. Anderson, & M. J. Crozier (Eds.), *Landslide Risk Assessment* (pp. 429 - 468). New Jersey, US: John Wiley.
- Reichenbach, P., Rossi, M., Malamud, B. D., Mihir, M., & Guzzetti, F. (2018). A review of statistically-based landslide susceptibility models. *Earth-Science Reviews*, 180, 60 - 91.
- Remondo, J., González, A., Terán, J. R. D. D., Cendrero, A., Fabbri, A., & Chung, C.-J. F. (2003). Validation of Landslide Susceptibility Maps; Examples and

Applications from a Case Study in Northern Spain. *Natural Hazards*, 30, 437 - 449.

Rib, H. T., & Liang, T. (1978). Recognition and Identification. In R. L. Schuster & R. J. Krizek (Eds.), *Landslide Analysis and Control*. Washington Transportation Research Board, Special Report 176 (pp. 34 - 80). Washington: National Academy of Sciences.

Rimstidt, J. D., & Vaughan, D. J. (2003). Pyrite oxidation: a state-of-the-art assessment of the reaction mechanism. *Geochimica et Cosmochimica Acta*, 67(5), 873–880.

Roslee, R., Simon, N., Tongkul, F., Norhisham, M. N., & Taharin, M. R. (2017). Landslide Susceptibility Analysis (LSA) using Deterministic Model (Infinite Slope) (DESSISM) in the Kota Kinabalu Area, Sabah, Malaysia. *Geological Behavior*, 1(1), 6 - 9.

Saaty, T. L. (1980). *The Analytic Hierarchy Process*. New York: McGraw-Hill.

Sameen, M. I., Pradhan, B., Bui, D. T., & Alamri, A. M. (2019). Systematic sample subdividing strategy for training landslide susceptibility models. *Catena*, 187, 104358.

Siedel, H., Pfefferkorn, S., Plehwe-Leisen, E. v., & Leisen, H. (2010). Sandstone weathering in tropical climate: Results of low-destructive investigations at the temple of Angkor Wat, Cambodia. *Engineering Geology*, 115, 182 - 192.

Soeters, R., & Van Westen, C. J. (1996). Slope Instability Recognition Analysis and Zonation. In K. T. Turner & R. L. Schuster (Eds.), *Landslides: Investigation and Mitigation (Transportation Research Board, National Research Council, Special Report; 247)* (pp. 129 - 177). Washington D.C., USA: National Academy Press.

Tan, D. N. K. (1979). *Lupar Valley, West Sarawak, Malaysia : explanation of sheets 1-111-14, 1-111-15, and part of 1-111-16*. Kuching: National Printing Department.

The Borneo Post. (2017). JKR To Resolve Road Erosion Along Canada Hill To Kpg Katong. *The Borneo Post*. Retrieved on 24 April 2019 from [https://www.sarawak.gov.my/web/home/news\\_view/119/9110](https://www.sarawak.gov.my/web/home/news_view/119/9110)

The Star. (2009a). Continuous rain can lead to landslides at Canada Hill. *The Star*. Retrieved on 24 April 2019 from <https://www.thestar.com.my/news/community/2009/12/21/continuous-rain-can-lead-to-landslides-at-canada-hill/>

- The Star. (2009b). Hilltop churches stop services after landslide. *The Star*. Retrieved on 24 April 2019 from <https://www.thestar.com.my/news/nation/2009/02/05/hilltop-churches-stop-services-after-landslip/>
- The Star. (2009c). Landslides threaten hillslope villages. *The Star*. Retrieved on 24 April 2019 from <https://www.thestar.com.my/news/nation/2009/02/02/landslides-threaten-hillslope-villages/>
- The Star. (2009d). Six houses buried, two damaged in Miri landslide. *The Star*. Retrieved on 24 April 2019 from <https://www.thestar.com.my/news/nation/2009/01/31/six-houses-buried-two-damaged-in-miri-landslide/>
- The Star. (2009e). Six houses destroyed in Miri landslide. *The Star*. Retrieved on 24 April 2019 from <https://www.thestar.com.my/news/nation/2009/01/30/six-houses-destroyed-in-miri-landslide/>
- The Star. (2009f). Two Indonesian workers killed in Miri landslide. *The Star*. Retrieved on 24 April 2019 from <https://www.thestar.com.my/news/nation/2009/01/16/two-indonesian-workers-killed-in-miri-landslide/>
- The Star. (2018a). Miri hit by sudden flash flood. *The Star*. Retrieved on 24 April 2019 from <https://www.thestar.com.my/news/nation/2018/12/07/miri-hit-by-sudden-flash-flood>
- The Star. (2018b). Repair roads fast to prevent further damage, says asst minister. *The Star*. Retrieved on 24 April 2019 from <https://www.thestar.com.my/metro/metro-news/2018/01/09/repair-roads-fast-to-prevent-further-damage-says-asst-minister/>
- Then, S. (2010). Sarawak's Canada Hill on fire. *The Star*. Retrieved on 24 April 2019 from <https://www.thestar.com.my/news/nation/2010/03/28/sarawaks-canada-hill-on-fire/>
- Then, S. (2011). Canada Hill fire causes haze in Miri City. *The Star*. Retrieved on 24 April 2019 from <https://www.thestar.com.my/news/community/2011/07/10/canada-hill-fire-causes-haze-in-miri-city>
- Then, S. (2014). Northern region folk, especially those staying on hillslopes, fearful of more landslides. *The Star*. Retrieved on 24 April 2019 from <https://www.thestar.com.my/news/community/2014/01/23/heavy-rain-makes-residents-edgy-northern-region-folk-especially-those-staying-on-hillslopes-fearfu>

- Then, S. (2017a). Rain causes collapse of Canada Hill slope in Miri. *The Star*. Retrieved on 24 April 2019 from <https://www.thestar.com.my/news/nation/2017/11/15/rain-causes-collapse-of-canada-hill-slope-in-miri/>
- Then, S. (2017b). Several houses in Miri under threat of collapsing following heavy rain. *The Star*. Retrieved on 24 April 2019 from <https://www.thestar.com.my/news/nation/2017/11/13/miri-houses-damaged-landslides-flood/>
- Then, S. (2018). Two villages in Miri hit by floods and mudflows. *The Star*. Retrieved on 24 April 2019 from <https://www.thestar.com.my/news/nation/2018/01/07/two-villages-in-miri-city-hit-by-floods-and-mudflows/#ExwAZPVtd5DEkb26.99>
- Thomas, M. F. (1995). *Geomorphology in the tropics: A study of weathering and denudation in low latitudes*. Chichester: John Wiley & Sons.
- Tongkul, F. (1996, June). *Sedimentation and tectonics of Paleogene sediments in central Sarawak*. Paper presented at the Annual Geological Conference, Kota Kinabalu, Sabah.
- Toyat, J. (2018). Heavy rain in Miri causes flooding and congestion. *The Borneo Post*. Retrieved on 24 April 2019 from <https://www.theborneopost.com/2018/12/07/heavy-rain-in-miri-causes-flooding-and-congestion/>
- United Nations Office for Disaster Risk Reduction (UNDRR) (n.d.). *PreventionWeb - Knowledge platform for disaster risk reduction*. Retrieved on 10 August 2019 from <https://www.preventionweb.net/english/>
- United States Geological Survey (USGS) (n.d.). *Earth Explorer*. Retrieved on 5 July 2019 from <https://earthexplorer.usgs.gov/>
- Van Asch, T. W. J., Buma, J., & Van Beek, L. P. H. (1999). A view on some hydrological triggering systems in landslides. *Geomorphology*, 30, 25 - 32.
- van der Zee, W., & Urai, J. L. (2005). Processes of normal fault evolution in a siliciclastic sequence: a case study from Miri, Sarawak, Malaysia. *Journal of Structural Geology*, 27(12), 2281-2300.
- van Westen, C. J. (1993). *Application of geographic information systems to landslide hazard zonation*. (Doctoral Dissertation, International Institute for Geo-Information Science and Earth Observation, Enschede). Retrieved on 13 March 2019 from

- van Westen, C. J. (1997). Statistical landslide hazard analysis. *ILWIS*, 2, 73-84.
- van Westen, C. J. (2004). Geo-Information Tools for Landslide Risk Assessment: An Overview of Recent Developments. In W. Lacerda, M. Erlich, S. A. B. Fontoura, & A. S. F. Sayao (Eds.), *Landslides : evaluation and stabilization - glissement de terrain: Evaluation et Stabilisation : Proceedings of the 9th International Symposium on Landslides, June 28 - July 2, 2004 Rio de Janeiro, Brazil* (pp. 39 - 56). London, UK: Balkema.
- van Westen, C. J., Castellanos, E., & Kuriakose, S. L. (2008). Spatial data for landslide susceptibility, hazard, and vulnerability assessment: An overview. *Engineering Geology*, 102(3-4), 112-131.
- van Westen, C. J., Rengers, N., Terlien, M. T. J., & Soeters, R. (1997). Prediction of the occurrence of slope instability phenomena through GIS-based hazard zonation. *Geologische Rundschau*, 86, 404 - 414.
- van Westen, C. J., & Terlien, M. T. J. (1996). An Approach Towards Deterministic Landslide Hazard Analysis in GIS. A Case Study from Manizales (Colombia). *Earth Surface Processes and Landforms*, 21, 853 - 868.
- van Westen, C. J., van Asch, T. W. J., & Soeters, R. (2005). Landslide hazard and risk zonation—why is it still so difficult? *Bulletin of Engineering Geology and the Environment*, 65(2), 167-184.
- Varnes, D. J. (1978). Slope movements, Type and Processes. In R. L. Schuster & R. J. Krizek (Eds.), *Landslide Analysis and Control. Transportation Research Board, Special Report 176* (pp. 11 - 33). Washington, DC: National Academy of Sciences.
- Varnes, D. J. (1984). *Landslide Hazard Zonation: A Review of Principles and Practice*. Paris, France: United Nations Educational, Scientific and Cultural Organization (UNESCO).
- von Schumacher, P. (1941). *The Miri Field, Exploration Report No. 306, Sarawak Oilfield Ltd.* Unpublished manuscript.
- Waltham, A. C. (1994). *Foundations of Engineering Geology*. London: Blackie Academic and Professional.

- Wannier, M., Lesslar, P., Lee, C., Raven, H., Sorkhabi, R., & Ibrahim, A. (2011). *Geological Excursions Around Miri, Sarawak*. Miri, Sarawak, Malaysia: EcoMedia Software.
- Wu, & Chen, S. C. (2009). Determining Landslide Susceptibility in Central Taiwan from rainfall and six site factors using the analytical hierarchy process method. *Geomorphology*, 112(3), 190 - 204.
- Wu, & Chen, S. C. (2013). Integrating spatial, temporal, and size probabilities for the annual landslide hazard maps in the Shihmen watershed, Taiwan. *Natural Hazards and Earth System Sciences*, 13, 2353 - 2367.
- Wyllie, D. C., & Mah, C. W. (2004). *Rock Slope Engineering: Civil and Mining* (4th ed.). New York, NY: Spon Press.
- Yalcin, A. (2008). GIS-based landslide susceptibility mapping using analytical hierarchy process and bivariate statistics in Ardesen (Turkey): Comparisons of results and confirmations. *Catena*, 72(1), 1-12.
- Yalcin, A., Reis, S., Aydinoglu, A. C., & Yomralioglu, T. (2011). A GIS-based comparative study of frequency ratio, analytical hierarchy process, bivariate statistics and logistics regression methods for landslide susceptibility mapping in Trabzon, NE Turkey. *Catena*, 85(3), 274-287.
- Yeo, H. (2011). Erosion threatens the lives of foothill residents. *The Star*. Retrieved on 24 April 2019 from <https://www.thestar.com.my/news/community/2011/01/21/erosion-threatens-the-lives-of-foothill-residents/>
- Zaid, D. (2009). *Laporan Geologi Kejuruteraan Kg. Lereng Bukit, Bukit Kanada, Miri, Sarawak*. (JMG.SWK(GBN) 2/2009). Kuching, Sarawak: Mineral and Geoscience Department Malaysia.